Stochastic Approaches for Estimating the Performance of Low Impact Development Practices

By

Rui Guo

Faculty of Engineering
Department of Civil Engineering

A Thesis
Submitted to the School of Graduate Studies
In Partial Fulfillment of the Requirements
For the Degree

Doctor of Philosophy

McMaster University
Hamilton, Ontario, Canada
December 2017

DOCTOR OF PHILOSOPHY (2017) McMaster University
(Civil Engineering) Hamilton, Ontario

TITLE:	**Stochastic Approaches for Estimating the Performance of Low Impact Development Practices**
AUTHOR:	**Rui Guo**
SUPERVISOR:	**Dr. Yiping Guo**
NUMBER OF PAGES:	**XI, 187**

Dedications

To my parents and sister

Abstract

To reduce the impacts of urbanization on the natural hydrologic cycle, low impact development (LID) practices have been increasingly implemented worldwide. This thesis aims at improving the existing analytical models and developing new sets of analytical equations to quantify the performance statistics of structural LID practices. As a starting point, the previously developed analytical probabilistic approach is extended for developing an event-based probabilistic model of infiltration facilities, which is based on the exponential probability distributions of rainfall characteristics and the mathematical representation of the hydrologic processes involved in the operation of infiltration facilities. Analytical equations for the determination of their overflow frequency and stormwater capture efficiency are obtained.

To better understand the antecedent condition and avoid using any simplifying assumptions about it, an analytical stochastic approach is then proposed for the analysis of rainwater harvesting (RWH) systems and permeable pavement systems (PPSs). Using this approach, the forward stochastic differential equations that relate the probabilities of the moisture state involved in the operation of RWH systems and PPSs are established. The steady-state probability distributions of moisture contents are then analytically solved from these stochastic differential equations. Based on these steady-state probability distributions, the stormwater

capture and water saving efficiencies of RWH systems are analytically derived. Applying the stochastic approach together with the analytical probabilistic approach to study the operation of PPSs, analytical equations that can be used for evaluating the stormwater capture efficiency of PPSs are also obtained.

Verifications of all the analytical solutions are made for a wide range of cases located in different climate regions by comparison with continuous simulations. It is demonstrated that the analytical equations presented in this thesis provide an easy-to-use tool with higher accuracy and wider application range for the planning and design of LIDs, which is much needed given the increasing implementations of LIDs.

Acknowledgement

I would like to express my appreciation to my supervisor Dr. Y. Guo for his guidance, support and mentoring over the past years. I will forever be grateful for his guidance and encouragement.

I would also like to thank the other members of my supervisory committee Dr. P. Coulibaly and Dr. S. E. Dickson for their helpful suggestions on my research.

I gratefully acknowledge the funding that I received from the China Scholarship Council, the Natural Sciences and Engineering Research Council of Canada, and the School of Graduate Studies and the Department of Civil Engineering at McMaster University.

Last and foremost, I would like to thank my family and friends for their support and understanding.

Publication List

This thesis consists of the following papers:

Paper I

Guo, R., and Guo, Y. (2017). Analytical Equations for Use in the Planning of Infiltration Facilities. *Journal of Sustainable Water in the Built Environment*, Accepted for publication, August 2017.

Paper II

Guo, R., and Guo, Y. (2017). Stochastic Modelling of the Hydrologic Operation of Rainwater Harvesting Systems. Submitted to *Journal of Hydrology* in December, 2017.

Paper III

Guo, R., Guo, Y., and Wang, J. (2017). Stormwater Capture and Antecedent Moisture Characteristics of Permeable Pavements. Submitted to *Hydrological Processes* in December, 2017.

Thesis related Paper (Appendix A)

Guo, R., and Guo, Y. (2017). Discussion of "Green Infrastructure Recovery: Analysis of the Influence of Back-to-Back Rainfall Events" by Bridget M. Wadzuk, Conor Lewellyn, Ryan Lee, and Robert G. Traver. *Journal of Sustainable Water in the Built Environment*, Accepted for publication, September, 2017.

Co-Authorship

This thesis has been prepared in accordance with the regulations for a 'Sandwich' thesis format or as a compilation of papers stipulated by the Faculty of Graduate Studies at McMaster University and has been co-authored.

For the papers presented in Chapter 2 and Chapter 3, the mathematical derivation, continuous simulations, and comparison analysis were conducted by R. Guo in consultation with Dr. Y. Guo, the papers were written by R. Guo and edited by Dr. Y. Guo.

For the paper presented in Chapter 4, the mathematical derivation and comparison analysis were conducted by Rui Guo in consultation with Dr. Y. Guo, the continuous simulations were conducted by R. Guo and J. Wang, the paper was written by Rui Guo and edited by Dr. Y. Guo.

For the Appendix A, the mathematical derivation and comparison analysis were conducted by R. Guo in consultation with Dr. Y. Guo, the paper was written by R. Guo and edited by Dr. Y. Guo.

Table of Contents

Chapter 1

Background and Objectives

1.1 Urban Stormwater Management

A natural catchment mostly consists of pervious land surfaces and is covered by vegetation; when rainfall falls on the land, some portion evaporates, some seeps into the ground, and the remainder becomes surface runoff that eventually flows to oceans and lakes through local waterways (rivers and streams). With an increasing proportion of people living in cities, natural landscapes are replaced by built urban areas, buildings, roads, and parking lots are constructed on the original farmland, grassland, and forests. Such urban development generally turns green areas into impervious surfaces and these changes greatly affect the natural hydrologic cycle. Hydrologic abstractions such as canopy interception, evapotranspiration, and soil infiltration tend to decrease, while direct surface runoff and stormwater entering into streams tend to increase (Coffman 2000; Hammer 1972; Leopold 1968). Additionally, urban development increases the concentrations of contaminants in runoff, nutrients, heavy metals, insecticides, and polycyclic aromatic hydrocarbons are examples of contaminants carried by urban runoff (USEPA 2003). Urban runoff also carries sediments into downstream waterways, erodes channels and negatively affects human and aquatic lives.

To reduce the risk of urban flooding, drains and catch basins are installed to collect stormwater, sewer pipes are used to convey stormwater and deliver it to the nearby receiving water bodies; some structural stormwater management facilities (e.g. detention ponds) are usually constructed downstream to store the conveyed off-site volumes (Dietz 2007). Thus, storm sewers located upstream can rapidly convey runoff to downstream areas, whereas downstream storage or infiltration facilities can reduce peak discharge and improve the quality of the water entering local streams (USEPA 2000).

1.2 Low Impact Development Practices

To preserve the natural hydrology as much as possible and improve existing urban stormwater management, Low Impact Development (LID) practices were recently developed and promoted (USEPA 2000). LIDs emphasize site specific, small-scale control of stormwater at its sources (Elliott and Trowsdale 2007). In this thesis, example LID practices such as infiltration facilities (infiltration trenches as a representative), rainwater harvesting (RWH) systems and permeable pavement systems (PPSs) are studied.

Infiltration trenches are installed to collect runoff from relatively small drainage areas such as parking lots and roof tops, provide temporary storage, and facilitate the infiltration of stormwater into surrounding soils. The ratio between

the drainage area and the footprint area of an infiltration trench is usually restricted within 5:1 and 20:1. Site soils with relatively high permeabilities (e.g. greater than 13 mm/h) are recommended (WEF and ASCE 2012, CVC 2010). Infiltration trenches are usually excavated as they are relatively long, moderately wide, and shallow in dimensions (Pitt et al. 1999). The storage layer of a trench is filled with gravel aggregates, plastic lattice structures or other void forming materials. Overflow pipes are usually installed at or near the top of the storage layer and are connected to nearby storm sewers. Underdrains are usually installed in the storage layer if the local soils are not very permeable. The storage layer may or may not be covered by a top soil layer. Non-woven filter fabrics are installed at the interface of the storage layer and the surrounding soils. Sedimentation pretreatment or other types of pretreatment are usually implemented upstream of an infiltration trench to remove larger suspended solids (Duchene and McBean 1992). Surface runoff from the source area after going through pretreatment and rainfall falling directly onto the surface of the trench can both flow through the surface layer and then through the storage layer of the trench, before finally infiltrating into the surrounding native soils. The gravel in the storage layer can effectively remove smaller sediments and other suspended pollutants through filtration and sorption. Non-woven filter fabrics can prevent pollutants from entering the soils. When an infiltration trench's storage space is filled, the additional water would be conveyed by overflow pipes to a downstream storm sewer system (OMOE 2003).

RWH systems are implemented for the collection of on-site rainwater (Kim et al. 2012; Sample et al. 2012) and reuse of the captured stormwater (Fewkes and Wam 2000; Guo and Baetz 2007; Matos et al. 2013; Sturm et al. 2009). They are usually storage units with various shapes and sizes, and constructed of different materials. For example, rain barrels are usually installed to collect rooftop runoff and have small sizes, whereas water tanks and cisterns are to collect runoff from an impervious catchment area and usually have large sizes. Some forms of pretreatment (e.g. filtration or first-flush diversion) are implemented before stormwater is conveyed into a RWH (Mun and Han 2012) and when the storage capacity of the system is fully utilized, overflow would be discharged to the nearby sewer system.

PPSs are implemented as replacement of traditional impervious pavements servicing places such as low traffic parking lots, driveways, pedestrian plazas, and walkways. A PPS usually consists of a permeable pavement layer underlined with a storage filled with uniformly graded coarse aggregate/stones. There are several types of permeable pavement layers, such as porous asphalt pavers, permeable concrete pavers, permeable interlocking concrete pavers with topsoils, pea gravel aggregates or grass filling in the openings, and segmental interlocking plastic pavers filled with grass. Similar to infiltration trenches, rainfall falling onto the surface of a PPS and runoff from nearby drainage areas can flow into the storage

layer directly through the surface of the PPS, and temporarily remain there until infiltrating into the native soils (Ball and Rankin 2010; Bean et al. 2007; Collins et al. 2008; Fassman and Blackbourn 2010). Sediments and other suspended pollutants can also be filtered out by the aggregate in the storage layer.

As described above, these LID practices can be considered as on-site storage units with or without underlying permeable soils, provided with the purpose of collecting on-site runoff, temporarily storing it and allowing it to infiltrate into the ground or be used for water supply purposes (Fewkes and Butler 2000; Guo and Baetz 2007; Hanson et al. 2009; Kim and Yoo 2009; Vaes and Berlamont 2001). They assist in reducing surface runoff volume and peak discharge (Ahiablame et al. 2013; Dietz 2007; Farahbakhsh et al. 2009) and improving water quality (Fach and Dierkes 2011; Warnaars et al. 1999). Their use can help lower the negative effects on streambanks and aquatic ecosystems.

The LIDs' primary performance indicators are usually considered as the main sizing criterion in many jurisdictions for the proper design of these facilities. Specifically, the fraction of runoff volume from the drainage areas that can be captured and infiltrated by a facility on a long-term basis, which is referred to as the stormwater capture efficiency or runoff reduction rate, is usually considered as the sizing criterion in the planning and design of an infiltration facility and a PPS (WEF and ASCE/EWRI 2012); while the system's water supply reliability is used

as a criterion for sizing a RWH system (Guo and Baetz 2007; Hajani and Rahman 2014; Mun and Han 2012; Palla et al. 2011; Santos and Taveira-Pinto 2013; Zhang et al. 2009).

1.3 Hydrologic Models of LID Practices

For planning and design purposes, assessing the stormwater management performances of LID practices and evaluating their important performance indicators are often required. Field tests and hydrologic models are usually used. Field tests are conducted to collect in-situ performance data from a LID facility for a period of several years and analyze their performance based on the monitored data (De Souza et al. 2002; Silva et al. 2009). However, monitoring studies are constrained to limited time periods and conditions and therefore do not provide sufficient hydrologic information of LID practices over all temporal and spatial scales and under all possible climatic conditions.

Many hydrological models using a specified design storm or continuous rainfall sequences have been developed and utilized. Single-event hydrological models are used to evaluate the performances of LID facilities in response to one individual rainfall event (Akan 2002a; Aron and Kibler 1990; Siriwardene et al. 2007). Although they can be easily set up, effects of the rainfall events preceding the specified rainfall event on a LID facility are usually not considered and the

accuracy is thus limited; more importantly, single-event models can not provide the required long-term average performance estimation.

Continuous hydrologic models simulating the responses of a LID facility to consecutive rain events over a long period are also commonly used (Ahiablame et al. 2012; Akan 2002a; Aron and Kibler 1990; Elliott and Trowsdale 2007; Fewkes 2000; Hajani and Rahman 2014; Lopes et al. 2017; Mun and Han 2012). The US EPA Storm Water Management Model (SWMM) (Rossman 2015) is one commonly-used continuous hydrologic model for LID practices (Akan 2002b; Elliott and Trowsdale 2007; Freni and Oliveri 2005; Sun et al. 2014). In SWMM models, LIDs are set up as equivalent catchments or the SWMM's LID module is directly used, and this was found to provide accurate estimations of their water quality and quantity control performances. With the input of continuous rainfall data, parameters of drainage areas, and the sizes of LID facilities, SWMM can output the total amount of the hydrologic measures over all the input years. By analyzing these outputs, the long-term based performance indicators can thus be calculated.

When continuous simulation methods are adopted for planning and design purposes, a trial and error procedure has to be used in order to obtain the required sizes. A possibly adequate configuration/size is selected first based on some guiding principles and a continuous simulation model is then established. If the

quantified performance determined by the continuous simulation is within the sizing criterion, the selected configuration is chosen; otherwise, a different configuration needs to be selected and the trial procedure is repeated. Above all, continuous simulations using long-term rainfall data can provide accurate performance statistics, but it requires more effort for setting up and is too time-consuming for use in individual design cases.

1.4 The Analytical Probabilistic Approach

The analytical probabilistic approach was proposed as an easy-to-use and computationally efficient alternative to continuous simulations. In essence, the approach uses as input the statistics of known random independent/input variables, expresses in closed-form mathematical equations the relationships between the unknown random dependent variables and the known independent/input variables, and then analytically derives the statistics of dependent variables based on the derived probability distribution theory. Employing this approach to deal with some urban stormwater management problems, the characteristics of random rainfall events are considered as independent variables and the hydrologic performance measures are usually treated as the dependent variables. Some event-based probabilistic stormwater models for modelling the general hydrologic processes have already been established (Adams and Papa 2000).

Continuous rainfall data can be separated into statistically independent rainfall events with an appropriately selected minimum inter-event time (MIET) (Bonta and Rao 1988; Guo and Adams 1998). MIET is the minimum number of dry hours between two separate rainfall events. Two consecutive rainfall episodes are considered as belonging to the same event if the dry time between them is less than the adopted MIET; otherwise, they are considered as belonging to two different events. Each rainfall event is characterized by its rainfall volume/intensity, rainfall duration, and inter-event time. Many suitable theoretical probability distributions have been proposed to describe the frequency distributions of rainfall event characteristics for specific locations of the world. These distributions include Gamma (Woolhiser and Pegram 1979), Lognormal (Guo and Hughes 2001; Guo et al. 2013), the Generalized Logistic, Pearson Type III, Pareto and the Generalized Pareto, as well as the Kappa distributions (Papalexiou and Koutsoyiannis 2012). Meanwhile, several studies have tested that rainfall event characteristics often follow exponential distributions in many regions of North America (Adams et al. 1986; Eagleson 1978; Guo 2001; Guo and Adams 1998; Howard 1976).

The analytical probabilistic approach was first employed to determine the frequency of peak streamflows from a catchment (Eagleson 1972). The exponential distribution models were used to describe the rainfall intensity, duration, and inter-event time and the mathematical expressions of peak streamflow were obtained as

a function of rainfall event characteristics using the kinematic wave relationships. Based on the derived probability distribution theory, the probability distribution of the peak streamflow was derived. Similar models were also applied to streams in different regions of Canada (Howard and Associates 1977, 1986; Howard and Smith 1977; Sanchez 1986). Following the work of Eagleson (1972), analytical probabilistic models for flood frequencies were developed adopting the same exponential distribution models of rainfall event characteristics and also assuming that rainfall intensity and duration are independent random variables, but using the mathematical expressions of flood flows based on the unit hydrograph theory (Díaz-Granados et al. 1984; Hebson and Wood 1982).

This analytical approach was also employed for stormwater control facilities. Howard (1976) adopted exponential distributions to describe the frequencies of rainfall volume and inter-event time and treated these two variables as independent random variables. He mathematically expressed the spill volume from a reservoir, and derived the probability distribution of spill volumes based on the derived probability distribution theory. The Howard's model was modified and extended for estimating other stormwater quantity control performance measures (Adams and Bontje 1984; Bontje et al. 1984; Guo and Adams 1999a, b) and for use for a system of a series of catchments in cascades (Sanchez and Adams 1990; Schwarz 1980). Such models were also extended to consider the pollutants in the runoff and

estimate the water quality control performances of storage-treatment systems (Díaz-Granados et al. 1984; Flatt and Howard 1978; Loganathan and Delleur 1984; Zukovs 1983). Models with other probabilistic models of rainfall event characteristics, such as the Weibull probability distribution (Bacchi et al. 2008; Balistrocchi et al. 2009) and gamma distribution (Di Toro and Small 1979), were also considered. Seto (1984) and Adams and Papa (2000) compared analytical results considering rainfall event characteristics as independent variables and also treating them as being dependent, where cases considering dependent input rainfall characteristics showed better performances.

Recently, the analytical probabilistic approach has also been applied to evaluate the stormwater management performances of LID practices (Zhang 2014). The analytical probabilistic models for RWH systems (Guo and Baetz 2007), green roofs (Guo et al. 2014; Zhang and Guo 2012a), rain gardens (Zhang and Guo 2012b), bioretentions (Zhang and Guo 2014b), and PPSs (Zhang and Guo 2014a) are established on the basis of exponential probability density functions (PDF) representing local rainfall characteristics, mathematical representations of the rainfall-overflow relationships, and the derived probability distribution theory.

1.5 Limitations of the Previously Developed Analytical Probabilistic Models

In applying the event-based analytical probabilistic approach to assess the hydrologic performances of stormwater storage facilities, an event-based water balance equation needs to be established at the outset. To obtain closed-form analytical results, the antecedent moisture condition or equivalently the storage water level of the storage unit at the start of a random rainfall event needs to be analytically expressed. Some previous studies directly assumed that the antecedent moisture content is equal to zero, i.e., the storage elements are assumed to be completely empty at the beginning of the analyzed random rainfall event (Bacchi et al. 2008; Balistrocchi et al. 2009). Some previous studies illustrated that the antecedent moisture condition is a random variable itself because it varies from one event to another, and it is dependent on the response of the storage elements to previous rainfall events and dry periods. For simplicity, previous studies made assumptions about the storage level at the end of the rainfall event immediately preceding the event under analysis with consideration of the fact that the earlier the event, the less its effect on the analyzed event, and analyzed the responses of the storage space through the dry period that precedes the analyzed random rainfall event. For example, assumptions that the storage reservoir is full (Howard 1976) or empty (Adams and Bontje 1984) at the end of the last rainfall event were made.

Howard's assumption was also employed in many studies of other types of stormwater management facilities (Loganathan and Delleur 1984).

In developing the analytical probabilistic models to quantify the hydrologic performances of LID practices, similar assumptions about the antecedent moisture content were adopted. Howard's assumption, which states that the storage space is filled at the end of a rainfall event, was applied in order to obtain the event-based antecedent moisture content of rain gardens (Zhang and Guo 2012b) and PPSs (Zhang and Guo 2014a). This assumption resulted in overestimations of overflows from rain gardens and PPSs and underestimations of their stormwater capture efficiencies. These two types of assumptions are acceptable for specific types of facilities operating under certain circumstances; however, the inaccuracy caused by this assumption may be aggravated when the storage capacity of the rain gardens and PPSs increases significantly and when the catchment area and the site soil's permeability are disproportionally small.

Some studies extended the analysis only to the rainfall event and the dry period that immediately precede the analyzed random rainfall event and considered the response of the storage unit to more than one dry period-rainfall event cycles. Such analysis was presented for bioretention systems where the storage capacity is assumed to be completely empty at the beginning of the rainfall event preceding the random rainfall event under analysis (Zhang and Guo 2014b) and for green

roofs where the storage space is assumed to be full at the end of the rainfall event preceding the previous rainfall event (Guo et al. 2014). Applying these assumptions, analyses of the response of the storage element to the previous rainfall event and dry period were conducted and the approximate expected value of the antecedent moisture content was thus obtained. Such derivations were proven to be advantageous over the use of the Howard's assumption, but systematic inaccuracies still exist due to the introduction of another assumption.

The above-described assumptions and derivations can provide an estimation of the initial condition of a storage space for a random event. However, the assumptions made are still not entirely realistic and may not be justified for extreme cases. Also, considering only one or two events preceding the random rainfall event under analysis is not enough to accurately describe the antecedent moisture conditions. Smith (1980) obtained the steady-state probability distribution of the reservoir contents at the end of the rainfall event preceding the analyzed random rainfall event. The work of Smith (1980) made the previously adopted assumptions unnecessary; however, it was found that the required numerical solution makes it complicated and limited its practical applications (Adams and Papa 2000).

1.6 The Analytical Stochastic Approach

It is desirable to develop a set of analytical models to model the hydrologic

performances of LID practices without adopting similar simplifying assumptions about the antecedent moisture conditions. It would be much better if the effects of the full rainfall event sequence preceding the analyzed rainfall event on the antecedent moisture conditions can be considered. An analytical stochastic approach is introduced in this thesis to express the antecedent moisture conditions' probability distribution or its long-term expected value, and thus improving the previously developed analytical probabilistic models.

The analytical stochastic approach originates from Takács virtual waiting time process, which can be described as follows: customers arrive to get serviced, arriving customers must queue and wait until all the customers ahead are served, when the arrivals occur in a Poisson process and the service time for each customer is independently and identically distributed, the process of the waiting time of a person arriving at the service can be reduced as a Markov process in continuous time having jump transitions of random amounts occurring at random times (Takács 1955). Cox and Isham (1986) found that for a storage unit, the storage content accumulates as water flow into it and depletes as water flows out of it. When the inflow occurs continuously in a Poisson process and the amounts of the inflow at random time points are independently and identically distributed, the process of the storage contents can also be treated as the above described Markov process, the same as the Takács virtual waiting time process. To quantitatively solve problems

involving such processes, the forward stochastic differential equations for the Markov process can be formulated and analytically solved.

In the above-referenced two studies, the waiting time was assumed to keep increasing as customers continually arrive and the storage water level keeps rising as water keeps flowing into it; therefore, there are no limitations on the values of these two variables (i.e., the waiting time and storage water level). Rodriguez-Iturbe et al. (1999) applied this stochastic approach to the study of the soil moisture dynamics at a point and took into account the upper bound that saturation imposes on the soil moisture. Rodriguez-Iturbe et al. (1999) treated the soil layer as a simple storage space with precipitation as its input and evaporation and leakage as losses, and established and solved the soil moisture balance equation at a point. In Rodriguez-Iturbe et al. (1999)'s work, rainfall events are assumed to occur instantaneously, the arrival of rainfall events is treated as a Poisson process, and the rainfall event volumes are assumed to be exponentially distributed.

The Rodriguez-Iturbe et al. (1999) model was further developed and applied to model the soil moisture dynamics of water-controlled ecosystems with intermittent and unpredictable hydrologic drivers (Bartlett et al. 2015b; Bartlett et al. 2015a; Botter et al. 2007; Dralle and Thompson 2016; Entekhabi and Rodriguez-Iturbe 1994; Ghannam et al. 2016; Guswa et al. 2002; Laio 2006; Rodríguez-Iturbe and Porporato 2005). This study extended the analytical stochastic approach to the

analysis of LID practices.

1.7 Objectives and Organizations

The overall objective of this thesis is to obtain analytical models which can provide estimations of the hydrologic performance of structural LID devices such as infiltration facilities, RWH systems, and PPSs. This thesis also aims at overcoming the aforementioned limitations due to the simplifying assumptions about the antecedent moisture conditions and providing a more general and reliable analytical tool for the planning and design of structural LID practices with wider application ranges.

To achieve the overall objective of this thesis, three individual papers have been completed. These three papers are presented in Chapters 2 through 4. Chapter 2 applied and verified the existing analytical probabilistic approach to infiltration facilities with previously adopted simplifying assumption about the antecedent moisture condition. The focus of Chapter 3 is to remove the aforementioned simplifying assumptions about the antecedent moisture conditions, develop the analytical stochastic model for RWH systems, and derive analytical equations for evaluating their water supply reliability and stormwater capture efficiency. In Chapter 4, with the PDF of the antecedent moisture content derived from the adopted analytical stochastic approach, an analytical probabilistic model is

developed to model the hydrologic processes involved in PPSs, and then analytical equations are derived to evaluate the stormwater capture efficiencies of PPSs. Following these three chapters, Chapter 5 summarizes the major findings of this research and lists some recommendations for future research. A discussion paper illustrating the advantages of our analytical probabilistic approach in evaluating the performance of green infrastructure systems under series of rainfall events is also included in this thesis as supplemental findings.

References

Adams, B., and Bontje, J. (1984). Microcomputer applications of analytical models for urban stormwater management. *Emerging Computer Techniques in Stormwater and Flood Management*, 138-162.

Adams, B. J., Fraser, H. G., Howard, C. D., and Sami Hanafy, M. (1986). Meteorological data analysis for drainage system design. *Journal of Environmental Engineering*, 112(5), 827-848.

Adams, B. J., and Papa, F. (2000). *Urban Stormwater Management Planning with Analytical Probabilistic Models*, John Wiley & Sons, Inc., New York, USA.

Ahiablame, L. M., Engel, B. A., and Chaubey, I. (2012). Effectiveness of low impact development practices: literature review and suggestions for future research. *Water, Air, & Soil Pollution*, 223(7), 4253-4273.

Ahiablame, L. M., Engel, B. A., and Chaubey, I. (2013). Effectiveness of low impact development practices in two urbanized watersheds: Retrofitting with rain barrel/cistern and porous pavement. *Journal of Environmental Management*, 119, 151-161.

Akan, A. O. (2002a). Modified rational method for sizing infiltration structures. *Canadian Journal of Civil Engineering*, 29(4), 539-542.

Akan, A. O. (2002b). Sizing stormwater infiltration structures. *Journal of Hydraulic Engineering*, 128(5), 534-537.

Aron, G., and Kibler, D. F. (1990). Pond sizing for rational formula hydrographs. *Water Resources Bulletin*, 26(2), 255-258.

Bacchi, B., Balistrocchi, M., and Grossi, G. (2008). Proposal of a semi-probabilistic approach for storage facility design. *Urban Water Journal*, 5(3), 195-208.

Balistrocchi, M., Grossi, G., and Bacchi, B. (2009). An analytical probabilistic model of the quality efficiency of a sewer tank. *Water Resources Research*, 45(12).

Ball, J. E., and Rankin, K. (2010). The hydrological performance of a permeable pavement. *Urban Water Journal*, 7(2), 79-90.

Bartlett, M., Daly, E., McDonnell, J., Parolari, A., and Porporato, A. (2015). Stochastic rainfall-runoff model with explicit soil moisture dynamics. *Proceedings of the Royal Society*, 471(2183), 20150389.

Bartlett, M., Daly, E., McDonnell, J., Parolari, A., and Porporato, A. (2015). Stochastic rainfall-runoff model with explicit soil moisture dynamics. *Proc. R. Soc. A*, 471(2183), The Royal Society, 20150389.

Bean, E. Z., Hunt, W. F., and Bidelspach, D. A. (2007). Field survey of permeable

pavement surface infiltration rates. *Journal of Irrigation and Drainage Engineering*, 133(3), 249-255.

Bonta, J. V., and Rao, A. R. (1988). Factors affecting the identification of independent storm events. *Journal of Hydrology*, 98(3), 275-293.

Bontje, J. B., 1. K. Ballantyne, and B. J. Adams (1984). User interfacing techniques for interactive hydrologic models on microcomputers. *Proceedings of conference on Stormwater and Water Quality Management Modeling,* E. M. and W. James (ed.), McMaster University, Ontario, 75-89.

Botter, G., Porporato, A., Rodriguez-Iturbe, I., and Rinaldo, A. (2007). Basin-scale soil moisture dynamics and the probabilistic characterization of carrier hydrologic flows: Slow, leaching-prone components of the hydrologic response. *Water Resources Research*, 43(2).

Coffman, L. (2000). *Low-Impact Development Design Strategies, An Integrated Design Approach*, Prince George's County, Maryland: Department of Environmental Resources, Programs and Planning Division.

Collins, K. A., Hunt, W. F., and Hathaway, J. M. (2008). Hydrologic comparison of four types of permeable pavement and standard asphalt in eastern North Carolina. *Journal of Hydrologic Engineering*, 13(12), 1146-1157.

Cox, D., and Isham, V. (1986). The virtual waiting-time and related processes. *Advances in Applied Probability*, 18(02), 558-573.

De Souza, V. C. B., Goldenfum, J. A., and Barraud, S. (2002). An experimental and numerical study of infiltration trenches in urban runoff control. *Global Solutions for Urban Drainage*, 1-10.

Di Toro, D. M., and Small, M. J. (1979). Stormwater interception and storage. *Journal of the Environmental Engineering*, 105(EE1), 43-54.

Díaz-Granados, M., Valdes, J., and Bras, R. (1984). A physically based flood frequency distribution. *Water Resources Research*, 20(7), 995-1002.

Dietz, M. E. (2007). Low impact development practices: A review of current research and recommendations for future directions. *Water, Air, & Soil Pollution*, 186, 351-363.

Dralle, D. N., and Thompson, S. E. (2016). A minimal probabilistic model for soil moisture in seasonally dry climates. *Water Resources Research*, 52(2), 1507-1517.

Duchene, M., and McBean, E. A. (1992). Discharge characteristics of perforated pipe for use in infiltration trenches. *Journal of the American Water Resources Association*, 28(3), 517-524.

Eagleson, P. S. (1972). Dynamics of flood frequency. *Water Resources Research*, 8(4), 878-898.

Eagleson, P. S. (1978). Climate, soil, and vegetation, 2, the distribution of annual precipitation derived from observed storm sequences. *Water Resources Research*, 14 (15), 713-721.

Elliott, A. H., and Trowsdale, S. A. (2007). A review of models for low impact urban stormwater drainage. *Environmental modelling & software*, 22(3), 394-405.

Entekhabi, D., and Rodriguez-Iturbe, I. (1994). Analytical framework for the characterization of the space-time variability of soil moisture. *Advances in Water Resources*, 17(1-2), 35-45.

Fach, S., and Dierkes, C. (2011). On-site infiltration of road runoff using pervious pavements with subjacent infiltration trenches as source control strategy. *Water Science and Technology*, 64(7), 1388-1397.

Farahbakhsh, K., Despins, C., and Leidl, C. (2009). Developing capacity for large-scale rainwater harvesting in Canada. *Water Quality Research Journal of Canada*, 44(1), 92.

Fassman, E. A., and Blackbourn, S. (2010). Urban runoff mitigation by a permeable

pavement system over impermeable soils. *Journal of Hydrologic Engineering*, 15(6).

Fewkes, A. (2000). Modelling the performance of rainwater collection systems: towards a generalised approach. *Urban water*, 1(4), 323-333.

Fewkes, A., and Butler, D. (2000). Simulating the performance of rainwater collection and reuse systems using behavioural models. *Building Services Engineering Research and Technology*, 21(2), 99-106.

Fewkes, A., and Wam, P. (2000). Method of modelling the performance of rainwater collection systems in the United Kingdom. *Building Services Engineering Research and Technology*, 21(4), 257-265.

Flatt, P. E., and Howard, C. D. D. (1978). Preliminary screening procedure for economic storage-treatment trade-offs in storm water control. *Proceedings of International Symposium on Urban Stormwater Management*, University of Kentucky, Lexington, Kentucky 219-228.

Freni, G., and Oliveri, E. (2005). Mitigation of urban flooding: A simplified approach for distributed stormwater management practices selection and planning. *Urban Water Journal*, 2(4), 215-226.

Ghannam, K., Nakai, T., Paschalis, A., Oishi, C. A., Kotani, A., Igarashi, Y.,

Kumagai, T. o., and Katul, G. G. (2016). Persistence and memory time scales in root-zone soil moisture dynamics. *Water Resources Research*, 52, 1427-1445.

Guo, J. C., and Hughes, W. (2001). Storage volume and overflow risk for infiltration basin design. *Journal of Irrigation and Drainage Engineering*, 127(3), 170-175.

Guo, J. C., Urbonas, B., and MacKenzie, K. (2013). Water quality capture volume for storm water BMP and LID designs. *Journal of Hydrologic Engineering*, 19(4), 682-686.

Guo, Y. (2001). Hydrologic design of urban flood control detention ponds. *Journal of Hydrologic Engineering*, 6(6), 472-479.

Guo, Y., and Adams, B. J. (1998). Hydrologic analysis of urban catchments with event-based probabilistic models: 1. Runoff volume. *Water Resources Research*, 34(12), 3421-3431.

Guo, Y., and Adams, B. J. (1999a). Analysis of detention ponds for storm water quality control. *Water Resources Research*, 35(8), 2447-2456.

Guo, Y., and Adams, B. J. (1999b). An analytical probabilistic approach to sizing flood control detention facilities. *Water Resources Research*, 35(8), 2457-2468.

Guo, Y., and Baetz, B. W. (2007). Sizing of rainwater storage units for green

building applications. *Journal of Hydrologic Engineering*, 12(2), 197-205.

Guo, Y., Zhang, S., and Liu, S. (2014). Runoff reduction capabilities and irrigation requirements of green roofs. *Water Resources Management*, 28(5), 1363-1378.

Guswa, A. J., Celia, M., and Rodriguez-Iturbe, I. (2002). Models of soil moisture dynamics in ecohydrology: A comparative study. *Water Resources Research*, 38(9), 1166.

Hajani, E., and Rahman, A. (2014). Reliability and cost analysis of a rainwater harvesting system in peri-urban regions of Greater Sydney, Australia. *Water*, 6(4), 945-960.

Hammer, T. R. (1972). Stream channel enlargement due to urbanization. *Water Resources Research*, 8(6), 1530-1540.

Hanson, L. S., Vogel, R. M., Kirshen, P., and Shanahan, P. (2009). Generalized storage-reliability-yield equations for rainwater harvesting systems. *In World Environmental and Water Resources Congress 2009: Great Rivers*, 1-10.

Hebson, C., and Wood, E. F. (1982). A derived flood frequency distribution using Horton order ratios. *Water Resources Research*, 18(5), 1509-1518.

Howard, C., and Associates, L. (1977). *Wilson Creek Experimental Watershed Flood Frequency from RainfaIl Data, Report to the Manitoba Department of*

Mines, Resources and Environmental Management, Water Resources Division.

Howard, C., and Associates, L. (1986). *Hydrologic design methodologies for small-scale hydro at ungauged sites, Phase ILA - British Columbia; Theory and modeling procedures, integrated method for power analysis IMP*, Report to Environment Canada and Energy, Mines and Resources Canada.

Howard, C. D. (1976). Theory of storage and treatment-plant overflows. *Journal of the Environmental Engineering Division*, 102(4), 709-722.

Howard, C. D. D., and Smith, D. I. (1977). Floods on ungaged watersheds. *Proceedings of Canadian Hydrology Symposium,* Edmonton, Alberta, Canada, 221-231.

Kim, H., Han, M., and Lee, J. Y. (2012). The application of an analytical probabilistic model for estimating the rainfall–runoff reductions achieved using a rainwater harvesting system. *Science of The Total Environment*, 424, 213-218.

Kim, K., and Yoo, C. (2009). Hydrological modeling and evaluation of rainwater harvesting facilities: case study on several rainwater harvesting facilities in Korea. *Journal of Hydrologic Engineering*, 14(6), 545-561.

Laio, F. (2006). A vertically extended stochastic model of soil moisture in the root zone. *Water Resources Research*, 42(2).

Leopold, L. B. (1968). *Hydrology for Urban Land Planning: A Guidebook on the Hydrologic Effects of Urban Land Use*, U.S. Geologzcal Survey Circular 554. .

Loganathan, G. V., and Delleur, J. W. (1984). Effects of urbanization on frequencies of overflows and pollutant loadings from storm sewer overflows: A derived distribution approach. *Water Resources Research*, 20(7), 857-865.

Lopes, V. A., Marques, G. F., Dornelles, F., and Medellin-Azuara, J. (2017). Performance of rainwater harvesting systems under scenarios of non-potable water demand and roof area typologies using a stochastic approach. *Journal of Cleaner Production*, 148, 304-313.

Matos, C., Santos, C., Pereira, S., Bentes, I., and Imteaz, M. (2013). Rainwater storage tank sizing: Case study of a commercial building. *International Journal of Sustainable Built Environment*, 2(2), 109-118.

Mun, J. S., and Han, M. Y. (2012). Design and operational parameters of a rooftop rainwater harvesting system: definition, sensitivity and verification. *Journal of Environmental Management*, 93(1), 147-153.

OMOE (Ontario Ministry of Environment) (2003). *Stormwater Management Planning and Design Manual*, Ontario Ministry of Environment, Toronto, Ontario, Canada.

Palla, A., Gnecco, I., and Lanza, L. (2011). Non-dimensional design parameters and performance assessment of rainwater harvesting systems. *Journal of Hydrology*, 401(1), 65-76.

Papalexiou, S. M., and Koutsoyiannis, D. (2012). Entropy based derivation of probability distributions: A case study to daily rainfall. *Advances in Water Resources*, 45, 51-57.

Pitt, R., Clark, S., and Field, R. (1999). Groundwater contamination potential from stormwater infiltration practices. *Urban water*, 1(3), 217-236.

Rodríguez-Iturbe, I., and Porporato, A. (2005). *Ecohydrology of Water-Controlled Ecosystems: Soil Moisture and Plant Dynamics*, Cambridge University Press, Cambridge, U.K.

Rodriguez-Iturbe, I., Porporato, A., Ridolfi, L., Isham, V., and Coxi, D. (1999). Probabilistic modelling of water balance at a point: the role of climate, soil and vegetation. *Proceedings of the Royal Society of London A,* 455(1990), 3789-3805.

Rossman, L. A. (2015). *Storm Water Management Model User's Manual, Version 5.1 (EPA- 600/R-14/413b)*, National Risk Management Research Laboratory, Office of Research and Development, US Environmental Protection Agency, Cincinnati, OH, U.S.

Sample, D. J., Liu, J., and Wang, S. (2012). Evaluating the dual benefits of rainwater harvesting systems using reliability analysis. *Journal of Hydrologic Engineering*, 18(10), 1310-1321.

Sanchez, L. (1986). Flood frequency analysis for ungauged watersheds using a derived kinematic wave model. M. Eng. Thesis, Department of Civil Engineering, University of Toronto, Toronto, Ontario.

Sanchez, L., and Adams, B. J. (1990). Flood frequency analysis using a derived kinematic wave model. *Proceedings of the Flood Plain Management Conference*, Toronto, Ontario.

Santos, C., and Taveira-Pinto, F. (2013). Analysis of different criteria to size rainwater storage tanks using detailed methods. *Resources, Conservation and Recycling*, 71, 1-6.

Schwarz, R. B. (1980). Distributed storage for urban stormwater control: an analytical model with economic optimization. M.A.Sc. Thesis, Department of Civil Engineering, University of Toronto, Toronto, Ontario.

Seto, M. Y. K. (1984). Comparison of alternative derived probability distribution models for stormwater management. M.A.Sc. Thesis, Department of Civil Engineering, University of Toronto, Toronto, Ontario.

Silva, A., Nascimento, N., Seidl, M., and Vieira, L. (2009). Infiltration and detention systems for stormwater control in Belo Horizonte: assessment of demo performance and perspectives for use. *4th Switch Scientific Meetings*, 10.

Siriwardene, N. R., Deletic, A., and Fletcher, T. D. (2007). Clogging of stormwater gravel infiltration systems and filters: Insights from a laboratory study. *Water Research*, 41(7), 1433-1440.

Smith, D. I. (1980). Probability of storage overflows for stormwater management. M.A.Sc. Thesis, Department of Civil Engineering, University of Toronto, Toronto, Ontario.

Sturm, M., Zimmermann, M., Schütz, K., Urban, W., and Hartung, H. (2009). Rainwater harvesting as an alternative water resource in rural sites in central northern Namibia. *Physics and Chemistry of the Earth, Parts A/B/C*, 34(13), 776-785.

Sun, Y., Li, Q., Liu, L., Xu, C., and Liu, Z. (2014). Hydrological simulation approaches for BMPs and LID practices in highly urbanized area and development of hydrological performance indicator system. *Water Science and Engineering*, 7(2), 143-154.

Takács, L. (1955). Investigation of waiting time problems by reduction to Markov processes. *Acta Mathematica Hungarica*, 6(1-2), 101-129.

TRCA and CVCA (Toronto and Region Conservation Authority and Credit Valley Conservation Authority) (2010). *Low Impact Development Stormwater Management Planning and Design Guide*, Ontario, Canada.

USEPA (U. S. Environmental Protection Agency) (2003). *Bacterial Water Quality Standards for Recreational Waters (Freshwater and Marine Waters) Status Report. Rep. No. EPA-823-R-03-008*, Washington, D.C., USA.

USEPA (U. S. Environmental Protection Agency) (2010). *Low Impact Development (LID), A literature review, EPA-841-B-00-005*, Office of Water, Washington, D.C, US.

Vaes, G., and Berlamont, J. (2001). The effect of rainwater storage tanks on design storms. *Urban Water*, 3(4), 303-307.

Warnaars, E., Larsen, A. V., Jacobsen, P., and Mikkelsen, P. S. (1999). Hydrologic behaviour of stormwater infiltration trenches in a central urban area during 2¾ years of operation. *Water Science and Technology*, 39(2), 217-224.

WEF and ASCE/EWRI (Water Environment Federation and American Society of Civil Engineers/Environmental & Water Resources Institute) (2012). *Design of Urban Stormwater Controls*, McGraw-Hill Companies, New York. USA.

Woolhiser, D. A., and Pegram, G. (1979). Maximum likelihood estimation of

Fourier coefficients to describe seasonal variations of parameters in stochastic daily precipitation models. *Journal of Applied Meteorology*, 18(1), 34-42.

Zhang, S. (2014). Analytical probabilistic models for evaluating the hydrologic performance of structural low impact development practices. Ph.D Thesis, McMaster University, Hamilton, Canada.

Zhang, S., and Guo, Y. (2012a). Analytical probabilistic model for evaluating the hydrologic performance of green roofs. *Journal of Hydrologic Engineering*, 18(1), 19-28.

Zhang, S., and Guo, Y. (2012b). Explicit equation for estimating storm-water capture efficiency of rain gardens. *Journal of Hydrologic Engineering*, 18(12), 1739-1748.

Zhang, S., and Guo, Y. (2014a). Analytical equation for estimating the stormwater capture efficiency of permeable pavement systems. *Journal of Irrigation and Drainage Engineering*, 141(4), 06014004.

Zhang, S., and Guo, Y. (2014b). Stormwater capture efficiency of bioretention systems. *Water Resources Management*, 28(1), 149-168.

Zhang, Y., Chen, D., Chen, L., and Ashbolt, S. (2009). Potential for rainwater use in high-rise buildings in Australian cities. *Journal of Environmental*

Management, 91(1), 222-226.

Zukovs, G. (1983). Development of a probabilistic runoff storage/treatment model. M.Eng. Thesis, Department of Civil Engineering, University of Toronto, Toronto, Ontario.

Chapter 2

Analytical Equations for Use in the Planning of Infiltration Facilities

Rui Guo and Yiping Guo

Abstract: This paper applies on an analytical probabilistic approach to examine the hydrologic operations of non-vegetated infiltration facilities. Two sets of analytical equations for estimating infiltration facilities' stormwater capture efficiencies and overflow frequencies are derived, one applying the Horton infiltration model and the other considering infiltration rates as constant. The acceptability of all the adopted simplifying assumptions is verified by comparing analytical results with continuous simulation results. Using Concord, New Hampshire as an example location and infiltration trenches as an example type of infiltration facilities, the influences of underlying soil types, area ratios and infiltration trench dimensions on their performance statistics are investigated. Both the Horton infiltration model and constant infiltration rates are shown to be acceptable for the tested location. The closed-form analytical equations can be applied as an alternative to continuous simulations for the planning of infiltration facilities.

Keywords: Non-vegetated infiltration facility; Infiltration trench; Stormwater management; Stormwater capture efficiency; Probabilistic approach

2.1 Introduction

The urbanization process is accelerating worldwide. This leads to increases in impervious surfaces and thus adversely affects the natural hydrologic cycles. To provide both quantity and quality control of urban stormwater, many best management practices (BMPs) and low-impact development practices (LIDs) have been developed. Infiltration facilities such as infiltration trenches, infiltration chambers/vaults, dry wells, and infiltration basins are one type of structural practice. These infiltration facilities are constructed to collect rainwater, temporarily store it in their storage spaces, filter the suspended pollutants, and infiltrate the water into the surrounding soils. These infiltration facilities can reduce surface runoff volume, attenuate flood peak, recharge groundwater, and remove pollutants.

An infiltration trench generally consists of a storage reservoir lined with geotextile filter clothes and filled with clean granular stones or plastic lattice structures. The storage reservoir is generally covered by a vegetated or non-vegetated (e.g. gravel) surface. Vegetated infiltration trenches can remove more nutrients and/or other types of pollutants, whereas non-vegetated trenches can more effective reduce runoff volumes and peak discharges. Surface runoff from the source area and rainfall falling directly onto the surface can flow through the surface layer to enter the storage reservoir. Stormwater flows downward through the storage reservoir, whereas sediments and other suspended pollutants can be filtered out by the void

forming materials. Stormwater inside the storage reservoir can infiltrate into the surrounding native soils. When the storage space is completely filled, overflow occurs and can be conveyed downstream by overflow pipes. Infiltration chambers/vaults are a design variation of trenches where stones or other void forming materials are replaced with a series of chamber/vault-shaped, pre-manufactured modular structures fuctioning as stormwater storage spaces. Dry wells are another design variation of trenches in which excavated pits instead of trenches are lined with geotextile fabrics and filled with gravel aggregates or other void forming materials. Infiltration basins are natural or constructed shallow impoundments lined with relatively permeable soils.

In the initial operation stage of an infiltration facility, the storage space is relatively clean, the vertical hydraulic gradients dominate the infiltration process, and thus infiltration occurs mainly through the bottom of the infiltration facility. As sediments gradually deposit in the bottom of the storage space, clogging of the bottom might occur and lateral infiltration generally dominates. Some jurisdictions specify that only infiltration through the bottom of an infiltration facility should be considered for design (e.g., TRCA and CVCA 2010, MDE 2000) and some other jurisdictions (e.g., PDEP 2006) consider both lateral and bottom infiltrations.

During the planning stage, the performance of an infiltration facility with different sizes need to be explored. Among all the benefits that infiltration facilities

can provide, water quality control is the primary benefit. The criterion for water quality control is selected so that a required fraction of runoff volume from the drainage area can be captured and infiltrated by an infiltration facility on a long-term basis. This fraction is referred to as the stormwater capture efficiency (WEF and ASCE/EWRI 2012), and is one of the performance indicators of an infiltration facility. Continuous simulation models are widely used to estimate this hydrologic performance indicator (Freni and Oliveri 2005). However, continuous simulations are too time consuming, especially for planning purposes in which various design scenarios need to be considered.

This study focuses on non-vegetated infiltration facilities and aims at obtaining an alternative approach to continuous simulation that can be more easily used to estimate these facilities' performance statistics. Previously, Guo and Gao (2016) used the exponential distributions of rainfall characteristics to establish event-based probabilistic stormwater models and derive analytical equations for estimating the runoff reduction rates of infiltration trenches. However, they only considered infiltration through the bottom of an infiltration trench; assumed that the infiltration rates remain constant, equal to the saturated hydraulic conductivity of the soils, and only take into account infiltration trenches receiving runoff from 100% impervious catchments. To obtain more widely applicable analytical equations, the present study makes many improvements.

The constant infiltration rate assumption may underestimate the stormwater volume treated by infiltration trenches for some locations. To examine whether a more sophisticated infiltration model is necessary, this study used the Horton infiltration model with a more detailed description of the infiltration process as a comparison. The stormwater capture efficiencies based on both infiltration models were calculated and compared with continuous simulation results using the US EPA Storm Water Management Model (SWMM). Furthermore, this study derived analytical equations that can be used for not only infiltration trenches but also other infiltration facilities with drainage areas having different levels of imperviousness. To gain more insight into the hydrologic operation of infiltration facilities, this research also provides analytical equations for estimating the long-term average overflow frequencies.

2.2 Probabilistic Models of Rainfall Event Characteristics

To probabilistically represent local rainfall characteristics, a continuous historical rainfall data series should first be separated into discrete and statistically independent rainfall events based on a selected minimum inter-event time (MIET). Rainfall episodes separated by a dry period longer than the selected MIET are considered as separate rainfall events. Each rainfall event is characterized by its rainfall event volume (v), rainfall event duration (t), and the inter-event time (b) preceding it. The frequency distributions of v, t, and b can be modeled using

theoretical distribution models, such as the exponential (Guo and Adams 1998), the log-normal (Guo and Hughes 2001), the one-parameter Poisson (Wanielista and Yousef 1993), and the two-parameter Gamma distribution (Woolhiser and Pegram 1979) models. This study adopts the exponential distribution model. Table 2.1 gives the probability density functions (PDFs) of v, t, and b, where ζ, λ, and ψ are distribution parameters, and $\bar{v}$, $\bar{t}$, and $\bar{b}$ are the mean rainfall event volume (mm), mean rainfall event duration (h), and mean inter-event time (h), respectively.

Table 2.1 Probability Density Functions (PDFs) of Rainfall Event Characteristics

Rainfall Event Characteristic	Exponential PDF	Distribution Parameter
Rainfall Event Volume v, mm	$f(v) = \zeta e^{-\zeta v}, \quad v \geq 0$	$\zeta = 1/\bar{v}$
Rainfall Event Duration t, h	$f(t) = \lambda e^{-\lambda t}, \quad t \geq 0$	$\lambda = 1/\bar{t}$
Rainfall Inter-event Time b, h	$f(b) = \psi e^{-\psi b}, \quad b \geq 0$	$\psi = 1/\bar{b}$

This study seleted Concord, New Hampshire, USA as one test location and its historical rainfall record was obtained from the National Climate Data Center (NCDC). The rainfall data were from the ASOS station of Concord (43°11'43" N, 71°30'04" W, with an elevation of 346 m above the mean sea level) and covered the years from 1945 to 2005. For each year, the non-winter period rainfall data from April 1 to November 30 were analyzed. To ensure stochastic independence between consecutive storms, the MIET of 6-12 hours were tested for Concord. Many previous studies found this range of the MIET values to be appropriate for

small urban catchments (e.g., Restrepo-Posada and Eagleson 1982; Guo and Baetz 2007). Autocorrelation analysis on the observed successive hourly rainfall data of Concord was performed with lag times ranging from 6 to 12 hours. The autocorrelation coefficients between successive hourly rainfall volumes are all less than 0.08 for lag times ranging from 6 to 12 hours, which suggests that separating rainfall episodes by an interval of 6 to 12 hours can result in statistically independent rainfall episodes. Because the 6-hour MIET gave the best fit between the fitted exponential distributions and the observed frequencies of occurrence, this study selected the 6-hour MIET. A rainfall volume threshold of 1 mm was also used to censor out extremely small rainfall events (event volumes less than 1 mm). The continuous rainfall record was thus separated into 3,410 individual rainfall events. Adams and Papa (2000) gave details of the rainfall event-based analysis. The mean values of the rainfall event volume, duration and inter-event time were found to be 11.9 mm, 9.2 h, and 93.7 h, respectively.

The random variables v, t, and b are usually assumed to be statistically independent. To verify that this independence assumption was acceptable for the Concord station, the correlation coefficients between v and b (r_{vb}), t and b (r_{tb}), and v and t (r_{vt}) were calculated and found to be 0.04, 0.01, and 0.66, respectively. The results for r_{vb} and r_{tb} are nearly 0, indicating that $v \sim b$ and $t \sim b$ were not linearly correlated. To further illustrate the $v \sim b$, $t \sim b$, and $v \sim t$ relationships,

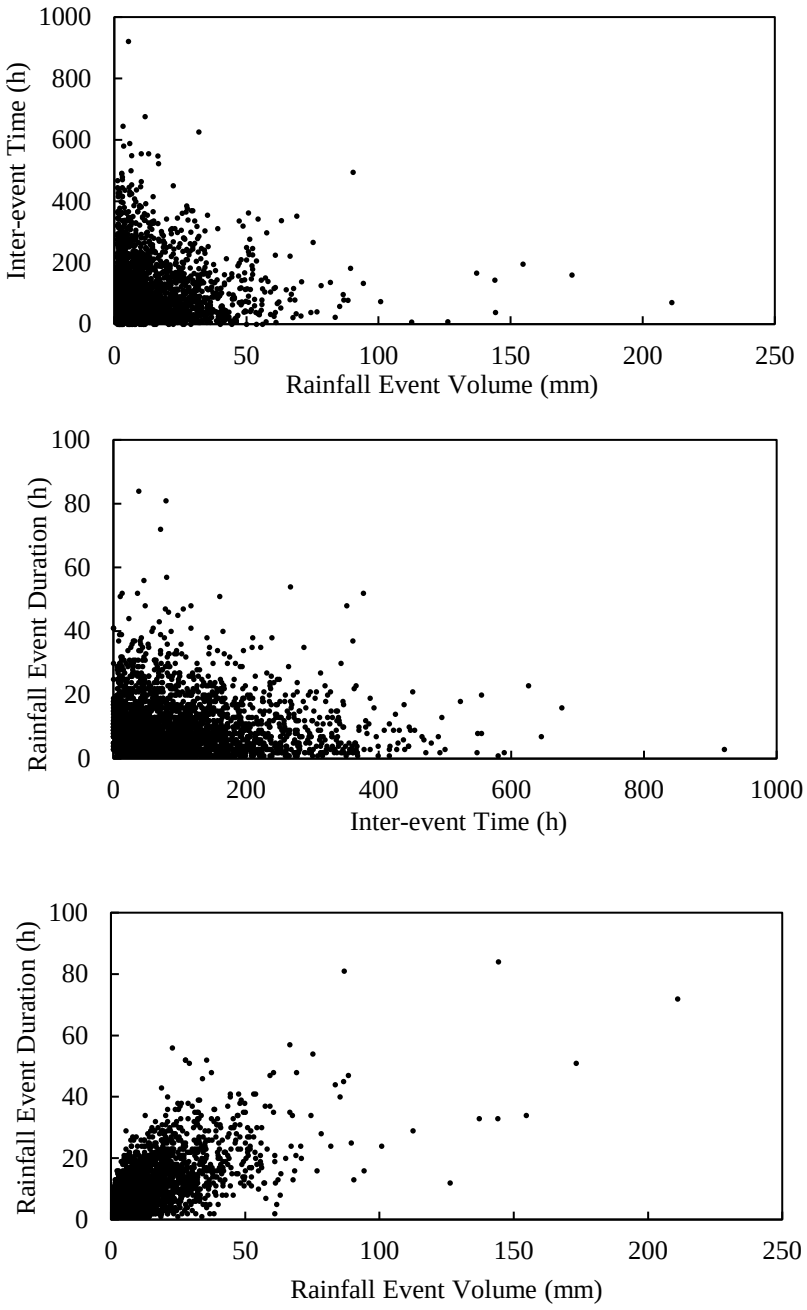

Fig. 2.1 Scattergrams of (a) rainfall event volume versus inter-event time, (b) inter-event time versus rainfall event duration, and (c) rainfall event volume versus duration at Concord

Fig. 2.1 shows scattergarms between them; v and b as well as t and b were not likely correlated, and therefore v and b as well as t and b can be considered as mutually independent for practical purposes. The result for r_{vt} was relatively high and demonstrates a possible linear correlation. However, the $v \sim t$ scattergram (Fig. 2.1) shows that the linear correlation between v and t was very weak, and treating v and t as statistically independent may not cause a significant loss of accuracy. Comparison results presented subsequently confirmed the acceptability of this independence assumption between v and t for Concord.

2.3 Analytical Derivations

The derivations in this study focused on the response of an infiltration facility during a random rainfall event. An infiltration facility is usually modeled as a storage space underlined with relatively permeable soils. The inflow starts to fill a facility when rainfall occurs, and overflow from the facility may occur when the facility's available storage capacity is fully used and the facility cannot receive any more inflow. Denoting the random rainfall event to be fully analyzed as the current rainfall event (CRE), the volume of overflow from the infiltration facility during the CRE can be calculated based on the event-based water balance equation as

$$v_o = \begin{cases} v_i - F_{CRE} - R_c, & v_i > F_{CRE} + R_c \\ 0, & v_i \le F_{CRE} + R_c \end{cases} \tag{2.1}$$

where v_o = volume of overflow from the infiltration facility occurring during the CRE; v_i = volume of inflow into the infiltration facility during the CRE; F_{CRE} = volume of infiltration occurring during the CRE; and R_c = available storage space at the beginning of the CRE. All the terms in Eq. (2.1) are expressed in mm of water over the facility's surface area. Eq. (2.1) does not consider the evaporation occurring during the CRE because evaporation rates are usually very small compared with infiltration rates. This study takes non-vegetated infiltration trenches as an example type of non-vegetated infiltration facilities and applies the event-based probabilistic approach for analysis. With proper modifications of the definitions of variables, the obtained results can also be applied for the study of infiltration basins, chambers/vaults, and dry wells.

2.3.1 Inflow from a Rainfall Event

The volume of inflow entering an infiltration trench as a result of a random rainfall event includes two parts: (1) surface runoff generated from the catchment areas serviced by the infiltration trench; and (2) rainwater directly falling onto the trench surface. For infiltration trenches constructed to service roofs and/or paved areas, such as walkways and roadways, the contributing areas are usually 100% impervious (PDEP 2016). The equations for this case were derived first, and cases with catchments that are not 100% impervious (e.g., residential lots) are discussed

subsequently. For catchments that are 100% impervious, surface depressions must be filled before any runoff occurs for each rainfall event. To simplify derivations, it was assumed that the depression storage capacity (S_{dc}) of the contributing area is always available when a rainfall event starts. This is justified because the value of S_{dc} is usually quite small [e.g., less than 3 mm, (WEF and ASCE/EWRI 2012)] and water held in these small depressions can quickly evaporate. The volume of surface runoff (v_r) generated from the contributing catchment under a random rainfall event can therefore be estimated as

$$v_r = \begin{cases} 0, & v \le S_{dc} \\ v - S_{dc}, & v > S_{dc} \end{cases} \tag{2.2}$$

where v_r is expressed in mm of water over the catchment area.

To simplify derivations, runoff from the catchment was assumed to fill the trench as soon as the rain began and to end when the rain stopped, i.e., the time of concentration of the catchment area was negligible. This is justified because catchments serviced by infiltration trenches are usually very small, and their times of concentration are usually very short (e.g., less than 15 minutes) compared with t and b. For an infiltration trench with a vegetated surface, part of the inflow may become plant uptake. For a non-vegetated infiltration trench, the amount of water absorbed by the gravel surfaces is very small and can be neglected; therefore all the surface runoff and rainfall falling on the surface of the trench becomes inflow into

the storage reservoir of the trench. Denoting the ratio between the contributing area and the footprint area of the infiltration trench as the area ratio r (dimensionless), the total volume of inflow v_i into the infiltration trench under a random rainfall event with rainfall event volume v can be expressed as

$$v_i = v + rv_r = \begin{cases} v, & v \le S_{dc} \\ v + r(v - S_{dc}), & v > S_{dc} \end{cases} \tag{2.3}$$

where v_i is expressed in mm of water over the trench's surface area. Based on the probability distribution of v and the functional relationship between v_i and v, the expected value of v_i can be derived as

$$E(v_i) = \int_0^{S_{dc}} v\zeta e^{-\zeta v} dv + \int_{S_{dc}}^{+\infty} [v + r(v - S_{dc})]\zeta e^{-\zeta v} dv = (1/\zeta)(1 + r\,\mathrm{e}^{-\zeta S_{dc}}) \tag{2.4}$$

2.3.2 Available Storage Capacity at the Beginning of a Rainfall Event

During a rainfall event, if the rainfall volume is small and the infiltration rate is large enough, all the inflow into the infiltration trench can be infiltrated and the trench will be empty at the end of the rainfall event. Otherwise, stormwater will remain in the trench when the rainfall event ends. In this case, if the following dry period is long and the rates of evaporation and infiltration are large enough, the stormwater held in the storage space can be depleted at the start of the next rainfall event. Otherwise, water will remain in the storage space when the next rainfall event starts. As such, the infiltration trench may be completely empty or partly

empty at the start of a random rainfall event. Therefore, the value of R_c in Eq. (2.1) is a random variable that varies depending on the response of the infiltration trench to previous rainfall events and dry periods.

It is difficult to quantify the effects of all the rainfall events and dry periods preceding the CRE; however, it is known for certain that the earlier the event, the less effect it has on the CRE. Therefore, in order to simply the derivation and obtain a closed-form analytical solution, this study analyzed only the rainfall event and the dry period that immediately precede the CRE. The rainfall event that immediately precedes the CRE is referred to as the previous rainfall event (PRE), and the dry period that immediately precedes the CRE is referred to as the previous dry period (PDP).

For simplification, this study assumed that the storage space of the infiltration trench was completely empty at the start of the PRE. This simplification is justifiable because (1) the inter-event times are usually very long (e.g., the average value is 93.7 h), infiltration trenches are usually constructed in permeable soils, and infiltration trenches are usually completely drained during the vast majority of inter-event times; (2) for the CRE which starts at the end of the PDP, R_c will still be assessed more realistically and accurately; and (3) the trench's main performance statistics are obtained by analyzing the CRE. The acceptability of this simplification is also demonstrated subsequently by comparing the analytical and

continuous simulation results. Based on this simplification, the volume of water (S_r) remaining in the trench when the PRE ends can be expressed as

$$S_r = \begin{cases} 0, & v_i \le F_{PRE} \\ v_i - F_{PRE}, & F_{PRE} < v_i \le F_{PRE} + R_{cmax} \\ R_{cmax}, & v_i > F_{PRE} + R_{cmax} \end{cases} \quad (2.5)$$

where F_{PRE} = volume of stormwater infiltrated from the infiltration trench to the surrounding soils during the PRE (mm); and R_{cmax} = maximum storage capacity of the infiltration trench (mm). For any type of infiltration facilities, its storage capacity R_{cmax} can be simply calculated as the maximum storage space it can provide divided by the facility's bottom area through which infiltration of collected stormwater takes place. For example, an infiltration trench located in permeable soils is usually constructed without underdrains, and the total pore volume of the gravel aggregates filling the storage space functions as its full storage capacity. An infiltration trench located in less permeable soils is usually installed with underdrains, and runoff from adjacent areas and rainfall falling directly on the trench surface reach the bottom of the trench almost instantaneously because of the extremely high permeability of the trench's fill materials. When rainwater stored in the storage reservoir reaches an elevation that is above the underdrains, it is quickly drained by the underdrains; therefore, the actual useful storage capacity of an infiltration trench with underdrains is the void space of the storage reservoir underneath the underdrains.

During dry periods, stormwater held in the storage reservoir can be depleted through evaporation and infiltration. The time needed to drain all the stormwater (S_r) stored in the trench when the PDP starts is denoted as t_d. By comparing t_d with b, R_c can be calculated as

$$R_c = \begin{cases} E_a b + R_{cmax} - S_r + F_{PDP}, & b \le t_d \\ R_{cmax}, & b > t_d \end{cases} \quad (2.6)$$

where E_a = average evaporation rate from the infiltration trench (mm/h); and F_{PDP} = volume of stormwater infiltrated from the infiltration trench to the surrounding soils during the PDP (mm). The values of t_d and F_{PDP} are estimated subsequently.

2.3.3 Infiltration during a Rainfall Event

Some jurisdictions recommend that only bottom infiltration need to be considered for the design of infiltration facilities. This study focuses on the planning of infiltration facilities in those regions where only bottom infiltration needs to be considered in design calculations, and not on the detailed operations of individual facilities; therefore, only infiltration through the bottom of a facility is taken into account. Some simplified approaches for the modeling of the hydrologic operation of infiltration facilities were proposed based on the assumption that the infiltration rate into the soils remains constant and is equal to the saturated hydraulic conductivity (or the final infiltration capacity if the Horton infiltration model is

used) of the soils. This constant infiltration rate assumption may underestimate the infiltration volume for some locations. Using the results derived in this paper, the infiltration volume can be calculated by assuming constant infiltration rate or with the Horton infiltration model, which is well documented and has been verified in various studies.

This study analyzed the response of the system under the CRE fully and more accurately, whereas it analyzed the response of the system under the PRE and PDP less accurately. This is justifiable because analysis of the response of the system under the PRE and PDP was mainly used for establishing the initial conditions when the CRE starts. Therefore, only the infiltration volume during the CRE was calculated using the two different models, and the infiltration rate of the soils underneath the trench was assumed to remain at its ultimate constant value f_c during the entire PRE and PDP for simplicity. Thus F_{PRE} and F_{PDP} can be calculated as $F_{PRE} = f_c t$ and $F_{PDP} = f_c b$, respectively, where t and b represents the random duration of the PRE and PDP.

When the infiltration rate during the entire infiltration process is considered as a constant, F_{CRE} can be calculated as $f_c t$, where t represents the random duration of the CRE. The same variable t is used to represent the durations of both the PRE and CRE, this is viable because they are treated as statistically independent and

identically distributed random variables. When the Horton infiltration model is applied to represent the infiltration process, the infiltration capacity of the soils can be expressed as $f_p = f_c + (f_0 - f_c)\mathrm{e}^{-kT}$, where f_p is the infiltration capacity of the soils at time T (mm/h), T is the length of time elapsed from the start of a storm (h), f_c is the ultimate constant value of f_p (mm/h), f_0 is the initial infiltration capacity of the soils when the storm event starts (mm/h), and k is the infiltration capacity decay coefficient (h^{-1}). When stormwater flowing into the trench is of sufficient quantity, the actual infiltration rate is always equal to the infiltration capacity of the soils, and the total volume infiltrated during the rainfall event can be calculated as

$$F = \int_0^t (f_0 - f_c)\mathrm{e}^{-kT} dT + f_c t \tag{2.7}$$

Based on Eq. (2.7), the total volume of infiltration can be viewed as comprised of two parts: (1) the volume of water needed to wet the soils underneath the bottom of the trench; and (2) the volume of water infiltrated at a constant rate f_c during the rainfall event. The first term in Eq. (2.7) is referred to as the initial soil wetting infiltration volume, denoted as F_{iw} and given by

$$F_{iw} = \int_0^t (f_0 - f_c)\mathrm{e}^{-kT} dT = [(f_0 - f_c)/k](1 - \mathrm{e}^{-kt}) \tag{2.8}$$

Because F_{iw} is usually satisfied during a very short initial period of a rainfall event (Guo and Adams 1998), it is assumed that F_{iw} is satisfied before any overflow

occurs from an infiltration trench.

The value of f_0 in Eq. (2.7) varies from one rainfall event to another and depends on the infiltration capacity regeneration of the soils during the PDP. It can be determined using the procedure developed by Huber and Dickinson (1988) for the *SWMM* model, $f_{T_S} = f_m - (f_m - f_c)\mathrm{e}^{-Rk(T_s - T_w)}$, where T_s is the length of dry period that the soils have experienced already, f_{T_S} is the infiltration capacity at time T_s, f_m is the soil's maximum infiltration capacity, and T_w is a hypothetical start time at which the infiltration capacity equals f_c on the infiltration capacity recovery curve. In the preceeding relationship, R is a constant ratio calculated as $R = -\ln(0.02)/24Dk$, where D is the time in days for a fully saturated soil to dry completely. Considering T_w as the time when the infiltration trench is completely drained during the PDP (i.e., t_d) and T_s as the time when the CRE starts (i.e., when the PDP ends), f_{T_S} can be used as the f_0 when the CRE starts

$$f_0 = \begin{cases} f_c, & b \le t_d \\ f_m - (f_m - f_c)\mathrm{e}^{-Rk(b-t_d)}, & b > t_d \end{cases} \tag{2.9}$$

Substituting Eq. (2.9) into Eq. (2.8) obtains

$$F_{iw} = \begin{cases} 0, & b \le t_d \\ [(f_m - f_c)/k](1-\mathrm{e}^{-kt})(1-\mathrm{e}^{-Rk(b-t_d)}), & b > t_d \end{cases} \tag{2.10}$$

The expected value of F_{iw} can thus be determined as

$$E(F_{iw}) = \int_{t=0}^{+\infty}\int_{b=t_d}^{+\infty} \frac{(f_m - f_c)}{k}(1-\mathrm{e}^{-kt})(1-\mathrm{e}^{-Rk(b-t_d)})\psi e^{-\psi b}\lambda e^{-\lambda t} dbdt$$
$$= \frac{Rk(f_m - f_c)}{(\lambda + k)(\psi + Rk)} e^{-\psi t_d} \quad (2.11)$$

To simplify the following derivations, the value of F_{iw} for each rainfall event is assumed to be the same and equals $E(F_{iw})$. This is justifiable because, as is shown subsequently, F_{iw} is relatively small compared to $f_c t$, the second component in Eq. (2.7). The total infiltration volume during the CRE can thus be obtained as

$$F_{CRE} = \begin{cases} f_c t, & b \le t_d \\ E(F_{iw}) + f_c t, & b > t_d \end{cases} \quad (2.12)$$

All the preceding calculations are for the total potential infiltration volumes. For cases where the infiltration capacity of the trench exceeds the inflow rates, the actual infiltrated volume equals the total inflow volume.

Because of the deposition of sediments, clogging might occur and the infiltration rates into surrounding soils can be reduced during the lifespan of infiltration trenches. In the planning and design of a facility, a safety factor for clogging and compaction can be applied to the infiltration rate of the soils in order to obtain a design infiltration rate.

2.3.4 Overflow during a Rainfall Event

Replacing F_{PRE} with $f_c t$ in Eq. (2.5) and then substituting Eq. (2.3) for v_i into Eq.

(2.5), S_r can be expressed as

$$S_r = \begin{cases} 0, & v \le \dfrac{rS_{dc} + f_c t}{r+1} \\ (r+1)v - rS_{dc} - f_c t, & \dfrac{rS_{dc} + f_c t}{r+1} < v \le \dfrac{rS_{dc} + f_c t + R_{cmax}}{r+1} \\ R_{cmax}, & v > \dfrac{rS_{dc} + f_c t + R_{cmax}}{r+1} \end{cases} \tag{2.13}$$

Based on the PDF of v and t and the functional relationship in Eq. (2.13), the expected value of S_r can be derived as

$$\begin{aligned} E(S_r) &= \int_{t=0}^{+\infty} \int_{v=(rS_{dc}+f_c t)/(r+1)}^{v=(rS_{dc}+f_c t+R_{cmax})/(r+1)} [(r+1)v - rS_{dc} - f_c t]\zeta \, \mathrm{e}^{-\zeta v} \, \lambda e^{-\lambda t} dv dt \\ &\quad + \int_{t=0}^{+\infty} \int_{v=(rS_{dc}+f_c t+R_{cmax})/(r+1)}^{+\infty} R_{cmax} \zeta \, \mathrm{e}^{-\zeta v} \, \lambda e^{-\lambda t} dv dt \\ &= [(r+1)/\zeta] C_1 C_3 (1 - C_2) \end{aligned} \tag{2.14}$$

where C_1 through C_3 are constants introduced in order to simplify the final expressions. These constants are defined as follows:

$$C_1 = \frac{\lambda(r+1)}{\lambda(r+1) + \zeta f_c}, \; C_2 = \exp(-\frac{\zeta R_{cmax}}{r+1}), \; C_3 = \exp(-\frac{\zeta r S_{dc}}{r+1}).$$

For a specific infiltration trench, knowing the characteristics of local rainfall events and the infiltration system, the values of C_1 through C_3 can be easily determined. The value of $E(S_r)$ estimated using Eq. (2.14) can be viewed as the long-term average volume of water remaining in the trench at the end of rainfall events. For simplicity, it can be assumed that the volume of stormwater stored in the trench at the end of the PRE is equal to $E(S_r)$. Thus the average time needed (t_d) to drain

the storage reservoir during the PDP can be calculated as

$$t_d = \frac{E(S_r)}{E_a + f_c} = \frac{r+1}{\zeta(E_a + f_c)} C_1 C_3 (1 - C_2) \tag{2.15}$$

In Eq. (2.6), when $b \le t_d$, $F_{PDP} = f_c b$. Substituting $F_{PDP} = f_c b$ into Eq. (2.6) and replacing S_r with $E(S_r)$, R_c can be expressed as

$$R_c = \begin{cases} E_a b + R_{cmax} - E(S_r) + f_c b, & b \le t_d \\ R_{cmax}, & b > t_d \end{cases} \tag{2.16}$$

Compared with Eq. (2.6), the randomness of R_c is reduced and it is now only related to the randomness of b, because t_d can now be treated as a constant and calculated using Eq. (2.15). Nevertheless, the infiltration capacity recovery process is considered in the estimation of $E(S_r)$ and therefore affects the values of t_d and R_c. By estimating the available storage space R_c at the beginning of a random rainfall event (the CRE as analyzed here) using Eq. (2.16), the maximum available storage space of the trench, the possible occupation of the storage space by runoff from previous rainfall events, and depletion of the stored water during rainfall events and inter-event dry periods are all taken into consideration. The random variable R_c itself is incorporated into the estimation of the volume of overflow from the trench. Even though this consideration of the effects of previous rainfall events and dry periods is still approximate in nature, it is much better than not considering them at all.

Knowing the expressions of v_i, F_{CRE}, and R_c, the volume of overflow from the infiltration trench during the CRE can be calculated based on Eq. (2.1). It can be safely assumed that no overflow would be generated from the infiltration trench when no surface runoff is generated from its contributing areas. In other words, receiving inflow only from rainfall falling directly onto the infiltration trench's surface alone will not cause the trench to overflow. Thus, only for overflow estimation purposes, Eq. (2.3) representing the total volume of runoff entering into the infiltration trench during the CRE is simplified as

$$v_i = v + r(v - S_{dc}) = (r+1)v - rS_{dc} \tag{2.17}$$

When the Horton infiltration model is adopted to calculate the total infiltration volume during the CRE, by substituting v_i calculated using Eq. (2.17), F_{CRE} calculated using Eq. (2.12), and R_c calculated using Eq. (2.16) into Eq. (2.1), the volume of overflow (v_{oH}) can be expressed as

$$v_{oH} = \begin{cases} (r+1)v - rS_{dc} & b \le t_d \\ -R_{c1} - f_c t, & \text{and } v > \dfrac{f_c t + rS_{dc} + R_{c1}}{r+1} \\ (r+1)v - rS_{dc} & b > t_d \\ -R_{cmax} - f_c t - E(F_{iw}), & \text{and } v > \dfrac{f_c t + E(F_{iw}) + rS_{dc} + R_{cmax}}{r+1} \\ 0, & \text{otherwise} \end{cases} \tag{2.18}$$

where $R_{c1} = E_a b + R_{cmax} - E(S_r) + f_c b$. Eq. (2.18) shows that the v, t, and b

combinations that result in zero v_{oH} includes cases where the infiltration capacity of the trench always exceeds the inflow volume.

Similarly, with v_i also calculated using Eq. (2.17), R_c also calculated using Eq. (2.16), but F_{CRE} calculated as $f_c t$ when the infiltration rate is assumed to be always constant, the volume of overflow (v_{oC}) can be expressed as

$$v_{oC} = \begin{cases} (r+1)v - rS_{dc} - R_{c1} - f_c t, & b \le t_d \text{ and } v > \dfrac{f_c t + rS_{dc} + R_{c1}}{r+1} \\ (r+1)v - rS_{dc} - R_{cmax} - f_c t, & b > t_d \text{ and } v > \dfrac{f_c t + rS_{dc} + R_{cmax}}{r+1} \\ 0, & \text{otherwise} \end{cases} \quad (2.19)$$

2.3.5 Overflow Frequency and Stormwater Capture Efficiency

Overflow frequency is defined as the probability that a random rainfall event generates overflow. Based on the probability distributions of v, t, and b and on Eqs. (2.18) and (2.19), the overflow frequencies with the infiltration process described by the Horton [denoted as $P(v_{oH} > 0)$] and constant infiltration models [denoted as $P(v_{oC} > 0)$] can be derived respectively as

$$\begin{aligned} P(v_{oH} > 0) &= \int_{t=0}^{+\infty} \int_{b=0}^{b=t_d} \int_{v=\frac{f_c t + rS_{dc} + R_{c1}}{r+1}}^{+\infty} \zeta \, \mathrm{e}^{-\zeta v} \psi e^{-\psi b} \lambda e^{-\lambda t} dv db dt \\ &\quad + \int_{t=0}^{+\infty} \int_{b=t_d}^{+\infty} \int_{v=\frac{f_c t + E(F_{iw}) + rS_{dc} + R_{cmax}}{r+1}}^{+\infty} \zeta \, \mathrm{e}^{-\zeta v} \psi e^{-\psi b} \lambda e^{-\lambda t} dv db dt \quad (2.20) \\ &= C_1 C_2 C_3 [C_4 (C_5 - C_6) + C_6 C_7] \end{aligned}$$

and

$$P(v_{oC}>0)=\int_{t=0}^{+\infty}\int_{b=0}^{b=t_d}\int_{v=\frac{f_c t+rS_{dc}+R_{c1}}{r+1}}^{+\infty}\zeta\,\mathrm{e}^{-\zeta v}\,\psi e^{-\psi b}\lambda e^{-\lambda t}dvdbdt$$
$$+\int_{t=0}^{+\infty}\int_{b=t_d}^{+\infty}\int_{v=\frac{f_c t+rS_{dc}+R_{cmax}}{r+1}}^{+\infty}\zeta\,\mathrm{e}^{-\zeta v}\,\psi e^{-\psi b}\lambda e^{-\lambda t}dvdbdt \qquad (2.21)$$
$$=C_1C_2C_3[C_4(C_5-C_6)+C_6]$$

where C_4 through C_7 are constants introduced in order to simplify the final expressions. These constants are defined as follows:

$$C_4=\frac{\psi(r+1)}{\psi(r+1)+\zeta(E_a+f_c)}\quad,\quad C_5=exp[\frac{\zeta E(S_r)}{r+1}]\quad,\quad C_6=exp^{-\psi t_d}\quad,$$

$$C_7=exp[-\frac{\zeta E(F_{iw})}{r+1}].$$

Similarly, the expected overflow volume with the infiltration processes described by the Horton [$E(v_{oH})$] and constant infiltration models [$E(v_{oC})$] can be derived respectively as

$$E(v_{oH})=\int_{t=0}^{+\infty}\int_{b=0}^{b=t_d}\int_{v=\frac{f_c t+rS_{dc}+R_{c1}}{r+1}}^{+\infty}[(r+1)v-rS_{dc}-R_{c1}-f_c t]$$
$$\zeta\,\mathrm{e}^{-\zeta v}\,\psi e^{-\psi b}\lambda e^{-\lambda t}dvdbdt$$
$$+\int_{t=0}^{+\infty}\int_{b=t_d}^{+\infty}\int_{v=\frac{f_c t+E(F_{iw})+rS_{dc}+R_{cmax}}{r+1}}^{+\infty}[(r+1)v-rS_{dc}-R_{cmax}-f_c t-E(F_{iw})] \qquad (2.22)$$
$$\zeta\,\mathrm{e}^{-\zeta v}\,\psi e^{-\psi b}\lambda e^{-\lambda t}dvdbdt$$
$$=[(r+1)/\zeta]C_1C_2C_3[C_4(C_5-C_6)+C_6C_7]$$

and

$$E(v_{oC}) = \int_{t=0}^{+\infty}\int_{b=0}^{b=t_d}\int_{v=\frac{f_c t+rS_{dc}+R_{c1}}{r+1}}^{+\infty}[(r+1)v - rS_{dc} - f_c t - R_{c1}]$$
$$\zeta\, \mathrm{e}^{-\zeta v}\psi e^{-\psi b}\lambda e^{-\lambda t}dvdbdt$$
$$+\int_{t=0}^{+\infty}\int_{b=t_d}^{+\infty}\int_{v=\frac{f_c t+rS_{dc}+R_{cmax}}{r+1}}^{+\infty}[(r+1)v - rS_{dc} - f_c t - R_{cmax}] \qquad (2.23)$$
$$\zeta\, \mathrm{e}^{-\zeta v}\psi e^{-\psi b}\lambda e^{-\lambda t}dvdbdt$$
$$= [(r+1)/\zeta]C_1C_2C_3[C_4(C_5 - C_6) + C_6]$$

Eqs. (2.22) and (2.23) show that $E(v_{oH}) = [(r+1)/\zeta]P(v_{oH} > 0)$ and $E(v_{oC}) = [(r+1)/\zeta]P(v_{oC} > 0)$, i.e., the expected overflow volume is simply the product of the overflow frequency and $(r+1)/\zeta$. The long-term average stormwater capture efficiency or ratio (denoted as C_e, also referred to as the runoff reduction rate or ratio) of the trench can be expressed in terms of the expected values of the inflow [$E(v_i)$] and overflow [$E(v_o)$] of an infiltration trench during a random rainfall event as

$$C_e = \frac{E(v_i) - E(v_o)}{E(v_i)} \qquad (2.24)$$

Substituting Eq. (2.4) for $E(v_i)$ and Eq. (2.22) for $E(v_o)$ into Eq. (2.24), the long-term average stormwater capture efficiency C_{eH} with the infiltration process described by the Horton infiltration model is obtained as

$$C_{eH} = 1 - \frac{(r+1)C_1C_2C_3[C_4(C_5 - C_6) + C_6C_7]}{[1 + r\,\mathrm{e}^{-\zeta S_{dc}}]} \qquad (2.25)$$

Substituting Eq. (2.4) for $E(v_i)$ and Eq. (2.23) for $E(v_o)$ into Eq. (2.24), the long–

term average stormwater capture efficiency C_{eC} with the infiltration rate treated as a constant is obtained as

$$C_{eC} = 1 - \frac{(r+1)C_1C_2C_3[C_4(C_5 - C_6) + C_6]}{[1 + r\,\mathrm{e}^{-\zeta\,\mathrm{e}^{-\zeta S_{dc}}}]} \tag{2.26}$$

Eq. (2.26) is applicable for cases in which the infiltration process is such that the infiltration rates into the soils remain constant and equal to the final infiltration capacity or saturated hydraulic conductivity of the soils. This would likely occur for infiltration chambers/vaults where stormwater is stored inside a deep underground chamber and evaporation of moisture contained in the soils under the bottoms of the chambers/vaults does not occur easily.

The contributing catchments for facilities such as infiltration basins and chambers are usually not 100% impervious, so the inflow into these types of facilities therefore needs to be determined differently. Runoff from the impervious areas can still be calculated using Eq. (2.2). The pervious areas can be viewed as an infiltration trench with the surface depression storage of the pervious areas (S_{dp}) equated to the stormwater storage capacity of the infiltration trench (R_{cmax}). Thus runoff from the pervious areas can be estimated as the overflow from an equivalent infiltration trench with the trench receiving only rainfall falling on its surface. With $r = 0$, replacing R_{cmax} with S_{dp}, the C_{eH} or C_{eC} calculated using Eq. (2.25) or Eq. (2.26) represents the runoff reduction rate of such a trench with different infiltration

models. Denoting the value of the calculated C_{eH} or C_{eC} for the equivalent pervious areas as α, $1-\alpha$ represents the ratio of the runoff generated from the previous area to the rainfall falling on the pervious areas. Treating this $1-\alpha$ as the runoff coefficient of the contributing pervious areas and adding the $1-\alpha$ fraction of the pervious areas to the contributing impervious areas, the area of the equivalent 100% impervious contributing catchment can be calculated. By replacing the actual area ratio with the calculated equivalent area ratio, all the equations derived in this paper can still be used.

The derived analytical equations for stormwater capture efficiency of trenches are dependent on the storage capacity R_{cmax} and area ratio r in addition to the characteristics of local rainfall, contributing catchment, and site location affecting evaporation rates. These equations can also be applied for other infiltration facilities by calculating properly the facility's storage capacity and area ratio. All other parameters required for input into Eq. (2.25) or Eq. (2.26) are the same as for infiltration trenches.

2.4 Comparison with Continuous Simulation Results

The derived analytical equations [Eqs. (2.25) and (2.26)] together with the expressions for C_1 through C_6 constitute a computationally efficient analytical model for estimating the stormwater capture efficiencies of infiltration facilities.

The derivation process used several assumptions. In presenting a suitable probabilistic model of rainfall characteristics, it was assumed that the rainfall event volume, duration, and inter-event time are statistically independent and exponentially distributed random variables. To calculate the runoff generated from an impervious contributing area, it was assumed that the depression storage of the contributing area is fully available at the start of a random rainfall event. The mathematical model describing the hydrologic processes of the infiltration facility under a random rainfall event was based on the assumptions that (1) the storage space is completely empty at the beginning of the PRE and analysis of the PRE and its subsequent PDP is conducted to establish more accurate initial conditions of the CRE; and (2) infiltration takes place at a rate equaling the hydraulic conductivity of the underlying soils during the PRE and PDP. In addition, when the Horton infiltration model is applied to describe the infiltration processes, the following assumptions were adopted: (1) initial soil wetting infiltration is always satisfied before any overflow occurs from an infiltration facility for each rainfall event; and (2) the initial soil wetting infiltration for each rainfall event is a constant equaling its expected value.

To test the validity of the simplifying assumptions made in deriving the analytical expressions, a set of continuous simulations were conducted. The *SWMM* software uses continuous rainfall data, does not require similar simplifying

assumptions and is usually used to perform time step-by-time step simulations of the operation of infiltration facilities (Baek et al. 2015; Ghodsi et al. 2016; Sun et al. 2014). Therefore this study used *SWMM*.

Verifications of results for infiltration trenches are taken as an example. To ensure that the infiltration calculation in *SWMM* is consistent with what is considered in the analytical derivations, two subcatchments were established in a *SWMM* model. Subcatchment A represented the contributing area and Subcatchment B represented the infiltration trench area. To verify the accuracy of Eq. (2.26) which is derived based on the constant infiltration rates assumption, Subcatchment B was modeled using the *SWMM*'s LID module, in which the infiltration rate through the bottom of an infiltration trench was assumed to be constant. To verify the accuracy of Eq. (2.25) derived by adopting the Horton infiltration model, Subcatchment B was modeled in *SWMM* as a regular subcatchment with its surface depression storage equaling R_{cmax}, and the Horton Model was selected to simulate the infiltration of rainwater over the subcatchment area, which in reality is the infiltration through the bottom of the trench. Runoff from Subcatchment A was routed through Subcatchment B.

The *SWMM* simulations used the previously analyzed non-winter (April through November) hourly rainfall record of Concord, New Hampshire as the rainfall input, evaporation was set to occur only during dry times and the average

evaporation rate was 0.11 mm/h. Table 2.2 lists the main parameters for soils. Based on the approximating non-linear reservoir model of subcatchments, the continuous *SWMM* simulations output the total volume of runoff generated from Subcatchment A ($V_{runoffA}$, i.e., inflow from the contributing area), rainfall falling on Subcatchment B (V_{rainB}), and runoff (i.e., overflow) from Subcatchment B ($V_{runoffB}$). Thus the stormwater capture efficiency can be calculated as $[(V_{runoffA}+V_{rainB}-V_{runoffB})/(V_{runoffA}+V_{rainB})]$.

Table 2.2 Main Parameters for the Surrounding Soils of Infiltration Trenches

Soil Type	f_m (mm/hr)	f_c (mm/hr)	k (1/hr)	D (days)	R (fraction)
Sand	127	36	3	4	0.01
Sandy loam	101.9	10.9	4	7.8	0.005
Loam	76.2	3.6	4.5	8	0.004

Stormwater capture efficiencies of trenches built in different soils with varying storage capacities and varying area ratios calculated by the analytical equations were compared with those determined from *SWMM* simulations. For a fixed 2-hectare and 100% impervious catchment with surface depression storages of 2 mm, Table 2.3 compares the results for infiltration trenches with varying storage capacities (5 ~ 900 mm). For a fixed 2-hectare and 70% impervious catchment (with surface depression storages for impervious areas of 2 mm and for pervious areas of 5 mm respectively), Table 2.4 compares the results for trenches with

varying area ratios (5-50). The absolute differences between the analytical and *SWMM* results were all within 0.09, with an average of 0.04; the relative differences were all within 11%, with an average of 5%. The analytically estimated stormwater capture efficiencies were always slightly lower (i.e., more conservative) than those determined from *SWMM* simulation results. This close agreement illustrates that the analytical equations may be used as an alternative to continuous simulations to estimate the stormwater capture efficiencies of infiltration trenches. Tables 2.3 and 2.4 also show that the stormwater capture efficiencies calculated applying the Horton infiltration model were slightly larger than those obtained based on constant infiltration rates, but the differences were very small. This seems to suggest that, at least for New Hampshire and for infiltration trenches, use of both the Horton infiltration model and constant infiltration rates are acceptable.

Table 2.3 Comparison of Analytical and *SWMM* Results for Stormwater Capture Efficiencies of Infiltration Trenches (Area Ratio: 15; Soil Type: Sand)

Stormwater Capture Efficiency	R_{cmax} (mm)												
	15	30	60	100	150	200	300	400	500	600	700	800	900
C_{eC}	0.66	0.69	0.73	0.78	0.83	0.87	0.92	0.96	0.97	0.98	0.99	1	1
C_{eCSWMM}	0.73	0.76	0.82	0.86	0.90	0.93	0.96	0.97	0.98	0.99	0.99	1	1
C_{eH}	0.66	0.69	0.73	0.78	0.83	0.88	0.93	0.96	0.98	0.99	0.99	1	1
C_{eHSWMM}	0.73	0.76	0.82	0.86	0.90	0.96	0.96	0.97	0.98	0.99	0.99	1	1

Table 2.4 Comparison of Analytical and *SWMM* Results for Stormwater Capture Efficiencies of Infiltration Trenches (Infiltration Trench Storage Capacity: 200 mm; Soil Type: Sandy loam)

Stormwater Capture Efficiency	Area Ratio						
	5	10	15	20	30	40	50
C_{eC}	0.99	0.94	0.86	0.78	0.65	0.55	0.47
C_{eCSWMM}	0.99	0.95	0.88	0.81	0.68	0.57	0.49
C_{eH}	0.99	0.94	0.87	0.79	0.66	0.56	0.49
C_{eHSWMM}	1.00	0.97	0.92	0.85	0.72	0.62	0.53

Overflow frequency is sometimes considered as another important performance indicator for some types of infiltration facilities. Over a long period of operation, overflow frequency is calculated as the average percentage of rainfall events which resulted in overflow from an infiltration facility. The number of rainfall events that generated overflow is simply the product of overflow frequency and the total number of rainfall events. Continuous *SWMM* simulations do not output directly the information needed for calculating a facility's overflow frequency, so a direct comparison between analytically calculated and *SWMM*-simulated overflow frequency is not easy to perform. Nevertheless, Eqs. (2.20) through (2.23) showed that stormwater capture efficiency is simply the product of overflow frequency and $(r+1)/\zeta$, which is a constant for a given facility. Because the analytical results for stormwater capture efficiencies were fairly close to those

based on *SWMM* simulation results, the analytically calculated overflow frequency must be close to those determined from continuous simulations as well. Tables 2.5 and 2.6 show the analytically calculated overflow frequency with varying storage capacities (200~1000 mm) and varying area ratios (5~20), respectively. For example, when a trench with a storage capacity of 200 mm and area ratio of 15 is constructed in sandy loam soils, 20% of the rainfall events generate overflow and 80% of the rainfall events are totally captured by the infiltration trench (Table 2.5). Based on the 3,410 total rainfall events in 61 years (56 events per year), every year approximately 11 rainfall events will generate overflow and approximately 45 rainfall events will be completely captured by the trench. Tables 2.5 and 2.6 also illustrates that (1) overflow frequency decreases with increases in storage capacity and decreases in area ratio; and (2) applying the Horton infiltration model does not change the results very much compared with results obtained by applying the constant infiltration rate assumption.

Table 2.5 Analytical Results for Overflow Frequency of Infiltration Trenches (Area Ratio: 15; Soil Type: Sandy Loam)

Overflow Frequency	R_{cmax} (mm)								
	200	300	400	500	600	700	800	900	1000
$P(v_{oC} > 0)$	0.20	0.12	0.07	0.04	0.03	0.01	0.01	0.01	0
$P(v_{oH} > 0)$	0.19	0.11	0.07	0.04	0.02	0.01	0.01	0	0

Table 2.6 Analytical Results for Overflow Frequency of Infiltration Trenches (Infiltration Trench Storage Capacity: 500 mm; Soil Type: Sandy Loam)

Overflow Frequency	Area ratio			
	5	10	15	20
$P(v_{oC} > 0)$	0	0.01	0.04	0.09
$P(v_{oH} > 0)$	0	0.01	0.04	0.08

2.5 Summary and Conclusions

This study used the exponential distributions of rainfall characteristics, developed event-based probabilistic models, and derived analytical equations to estimate the stormwater capture efficiencies and overflow frequencies of non-vegetated infiltration trenches. Those derived analytical equations can also be applied for other types of non-vegetated infiltration facilities, such as infiltration basins, infiltration chambers/vaults, and dry wells, although care must be taken to estimate a facility's storage capacity and area ratio in a way consistent with how the two parameters are defined and estimated for infiltration trenches. The stormwater capture efficiencies of non-vegetated infiltration trenches with different area ratios, trench sizes, and soil types in Concord, New Hampshire calculated using the analytical equations were compared with those determined from continuous *SWMM* simulation results. Close agreement demonstrates that the analytical equations can be used as an alternative to continuous simulations to estimate the hydrologic performances of non-vegetated infiltration facilities.

The analytical equations can be implemented in a spreadsheet and are computationally much more efficient than continuous simulations. Compared with continuous simulations, the analytical equations provide an easier and direct way of conducting sensitivity analysis for routine planning projects. This study considered only infiltration through the bottom of an infiltration facility, therefore the analytical equations are valid for regions specifying that only bottom infiltration should be considered for the design of infiltration facilities. The analytical results were only verified by comparing with *SWMM* simulation results; therefore the analytical equations reflect the limitations of the *SWMM* model and the calculation methods chosen.

This study analyzed the bottom infiltration process in two ways; one applied the Horton infiltration model and the other assumed a constant infiltrate rate. The small differences in stormwater capture efficiencies and overflow frequencies calculated using the two infiltration calculation methods suggest that either method is acceptable for infiltration trenches constructed in the test location. For infiltration basins in which the bottom is directly exposed to the atmosphere and may be dried much faster, use of the Horton model may be more appropriate in order to properly account for the faster recovery of infiltration capacities. For locations with drier climate conditions, the use of the Horton model may also be necessary.

Acknowledgements

This work has been supported by the Natural Sciences and Engineering Research Council of Canada and the China Scholarship Council.

Notation

The following symbols are used in this paper:

b = rainfall inter-event time (h);

$\bar{b}$ = average rainfall inter-event time (h);

C_{eC} = stormwater capture efficiency of an infiltration facility with the infiltration rate treated as a constant (dimensionless);

C_{eH} = stormwater capture efficiency of an infiltration facility with the infiltration process described by the Horton infiltration model (dimensionless);

D = time for a fully saturated soil to dry completely (days);

$E[\cdot]$ = expected value of a random variable;

E_a = average evaporation rate (mm);

F_{CRE} = stormwater infiltrated from an infiltration facility during the current rainfall event (mm);

F_{PDP} = stormwater infiltrated from an infiltration facility during the previous dry period (mm);

F_{PRE} = stormwater infiltrated from an infiltration facility during the previous rainfall event (mm);

F_{iw} = initial soil wetting infiltration loss (mm);

f_c = ultimate infiltration capacity of soil (mm/h);

f_m = soil's maximum infiltration capacity (mm/h);

f_p = soil's infiltration capacity at a specific time T (mm/h);

f_{T_s} = infiltration capacity reached after a soil has been dried for T_s hours (mm/h);

f_0 = soil's initial infiltration capacity (mm/h);

k = infiltration capacity decay coefficient (h^{-1});

R_c = available storage capacity of an infiltration facility at the start of a random rainfall event (mm);

R_{cmax} = maximum storage capacity of an infiltration facility (mm);

r = area ratio between the contributing area and the infiltration facility surface are (dimensionless);

S_{dc} = depression storage of an impervious contributing area (mm);

S_r = stormwater remaining in an infiltration facility at the end of a rainfall event (mm);

T = time elapsed since the start of a storm (h);

T_w = a hypothetical start time at which the infiltration capacity equals to f_c on the

infiltration capacity recovery curve (h);

t = rainfall event duration (h);

$\bar{t}$ = average rainfall event duration (h);

t_d = time needed to drain all the stormwater stored in a facility during a dry period (h);

v = rainfall event volume (mm);

$\bar{v}$ = average rainfall event volume (mm);

v_i = inflow into an infiltration facility (mm);

v_{oC} = overflow from an infiltration facility assuming infiltration rates as constants (mm);

v_{oH} = overflow from an infiltration facility adopting the Horton infiltration model (mm);

v_r = surface runoff from the contributing area of an infiltration facility (mm);

V_{rain} = rainfall within a SWMM simulation period (mm);

V_{runoff} = runoff from a catchment within a SWMM simulation period (mm);

ζ = distribution parameter of rainfall event volume (mm^{-1});

λ = distribution parameter of rainfall event duration (h^{-1});

and

ψ = distribution parameter of inter-event time (h^{-1}).

References

Adams, B. J., and Papa, F. (2000). *Urban stormwater management planning with analytical probabilistic models*, Wiley, New York.

Baek, S. S., et al. (2015). "Optimizing low impact development (LID) for stormwater runoff treatment in urban area, Korea: Experimental and modeling approach." *Water research*, 86, 122-131.

Freni, G., and Oliveri, E. (2005). "Mitigation of urban flooding: A simplified approach for distributed stormwater management practices selection and planning." *Urban Water Journal,* 2(4), 215-226.

Ghodsi, S. H., Kerachian, R., Estalaki, S. M., Nikoo, M. R., and Zahmatkesh, Z. (2016). "Developing a stochastic conflict resolution model for urban runoff quality management: application of Info-gap and Bargaining theories." *J. Hydrol.*, 533, 200-212.

Guo, Y., and Adams, B. J. (1998). "Hydrologic analysis of urban catchments with event-based probabilistic models: 1. Runoff volume." *Water Resour Res*, 34(12), 3421-3431.

Guo, Y., and B. W. Baetz (2007), "Sizing of rainwater storage units for green building applications." *J. Hydrol. Eng.*, 10.1061/(ASCE)1084-

0699(2007)12:2(197), 197–205.

Guo, Y., and Gao, T. (2016). "Analytical Equations for Estimating the Total Runoff Reduction Efficiency of Infiltration Trenches." *Journal of Sustainable Water in the Built Environment*, ASCE, 2(3), 06016001.

Huber, W. C., and Dickinson, R. E. (1988). *Storm water management model, version 4: user's manual*. U.S. Environmental Protection Agency, Athens, GA, USA.

MDE (Maryland Department of the Environment) (2000). *Maryland Stormwater Design Manual, Vols. I and II*. Center for Watershed Protection and the Maryland Department of the Environment, Water Management Administration, Baltimore, MD.

PDEP (Pennsylvania Department of Environmental Protection) (2006). *Pennsylvania Stormwater Best Management Practices Manual. PA DEP Document.* No. 363-0300-002, Bureau of Watershed management, Harrisburg, PA.

Restrepo-Posada, P. J., and P. S. Eagleson (1982), "Identification of independent rainstorms." *J. Hydrol*., 55(1-4), 303– 319.

Sun, Y., Li, Q., Liu, L., Xu, C., and Liu, Z. (2014). "Hydrological simulation

approaches for BMPs and LID practices in highly urbanized area and development of hydrological performance indicator system." *Water Science and Engineering*, 7(2), 143-154.

Toronto and Region Conservation Authority (TRCA) and Credit Valley Conservation Authority (CVCA) (2010). *Low impact development stormwater management planning and design guide*, Ontario, Canada.

Wanielista, M. P., and Yousef, Y. A. (1993). *Stormwater Management*, Wiley, New York, USA

WEF (Water Environment Federation) and ASCE/EWR (American Society of Civil Engineers/Environmental & Water Resources Institute) (2012). *Design of Urban Stormwater Controls*, McGraw-Hill Companies, New York, USA.

Woolhiser, D. A., and Pegram, G. (1979). "Maximum likelihood estimation of Fourier coefficients to describe seasonal variations of parameters in stochastic daily precipitation models." *Journal of Applied Meteorology*, 18(1), 34-42.

Chapter 3

Stochastic Modelling of the Hydrologic Operation of Rainwater Harvesting Systems

Rui Guo and Yiping Guo

Abstract: Rainwater harvesting (RWH) systems are an effective low impact development practice that provides both water supply and runoff reduction benefits. A stochastic modelling approach is proposed in this paper to quantify the water supply reliability and rainwater capture efficiency of RWH systems. The input rainfall series is represented as a marked Poisson process and two typical water use patterns are analytically described. The stochastic mass balance equation is solved analytically, and based on this, explicit expressions relating system performance to system characteristics are derived. The performances of a wide variety of RWH systems located in five representative climatic regions of the United States are examined using the newly derived analytical equations. Close agreements between analytical and continuous simulation results are shown for all the compared cases. In addition, an analytical equation is obtained expressing the required storage size as a function of the desired water supply reliability, average water use rate, as well as rainfall and catchment characteristics. The equations developed herein constitute a convenient and effective tool for sizing RWH systems and evaluating their

performances.

Key words: rainwater harvesting, stochastic model, water supply reliability, rainwater capture efficiency

3.1. Introduction

A rainwater harvesting (RWH) system is generally designed to capture, convey and store (in storage units, e.g. rain barrels or cisterns) the rainwater falling upon a catchment surface (e.g. rooftops or other impervious areas) for domestic or municipal uses (PDEP, 2006). It provides a promising alternative to reduce potable water demand or minimize water scarcity by harvesting the nonuniformly distributed rainfall both in urban and rural areas (Fewkes and Wam, 2000; Sturm et al., 2009; Matos et al., 2013). Meanwhile, the collection and use of rainwater can effectively reduce the volume of runoff, especially in rapidly expanding urban areas (Guo and Baetz, 2007; Kim et al., 2012; Sample et al., 2012). Hence, this low-impact development (LID) practice has been increasingly studied and implemented worldwide during the last two decades (Fewkes and Wam, 2000; Kim and Yoo, 2009; Sturm et al., 2009; Zhang et al., 2009; Jones and Hunt, 2010; Campisano and Modica, 2012; Palla et al., 2012; Zhang et al., 2012).

In analyzing the performance of a RWH system, its water supply reliability (or water-saving efficiency) and stormwater capture efficiency (or runoff reduction rate) are the two most commonly used indices for evaluation (Santos and Taveira-Pinto, 2013). Various methods have been developed to evaluate them for the purpose of optimizing the system design and/or operation (Kim et al., 2012). Among these methods, continuous simulation based on mass equilibrium models

has been used most frequently (Fewkes, 2000; Mun and Han, 2012; Hajani and Rahman, 2014; Lopes et al., 2017). Empirical and semi-empirical equations expressing directly the relationship between the storage volume, water supply reliability, water demand, and climate conditions have also been developed based on regression analysis of simulation results (Fewkes, 2000; Lee et al., 2000; Su et al., 2009; Campisano and Modica, 2012; Youn et al., 2012; Hajani and Rahman, 2014). To ensure the accuracy of the fitted empirical relationships, a large number of simulations covering a sufficiently large design-parameter space are inevitably required.

Alternatively, incorporating probabilistic rainfall models, an appealing analytical probabilistic approach has been developed to investigate the long-term average hydrologic performance of RWH systems (Guo and Baetz, 2007; Kim et al., 2012). By analyzing an event-based water balance using the derived probability distribution theory, analytical solutions for quantifying key indicators were derived for regions where the rainfall event characteristics follow exponential probability distributions. However, in deriving those analytical solutions, an initial condition about the water level in the storage unit at the beginning of a dry period preceding a rainfall event has to be assumed. Although appropriate simplifications would adequately represent a vast majority of design cases, the accuracy that can be provided by this method for some unusual or special cases is limited. Therefore,

further improvement of the analytical probabilistic approach is required.

As an extension and improvement of the analytical probabilistic approach, an analytical stochastic approach is developed in this paper for evaluating the performance of RWH systems. First of all, a differential mass balance equation is used to describe the instantaneous water balance which governs the operation of a RWH system. Secondly, the input rainfall series is represented as a marked Poisson process, and the inflow into the RWH system is expressed analytically considering the contributing catchment characteristics. Thirdly, two common water use patterns are considered and approximate methods are proposed for modelling these two patterns. Finally, an equilibrium solution in probabilistic terms is derived by solving the stochastic mass balance equation. Based on that solution, explicit expressions for rainwater capture efficiency, water supply reliability, and the required storage size are all derived analytically. The accuracy of the analytical solutions are examined by comparing with results from continuous simulations. Using the analytical solutions, the influences of rainfall characteristics, storage volume, anticipated water demand, and the contributing catchment characteristics on the hydrologic performance of RWH systems are all demonstrated.

3.2. The Dynamic Water Balance of a Rainwater Storage Unit

3.2.1. Instantaneous Water Balance Equation

In a RWH system, rainwater captured by the catchment area is conveyed to a storage device after receiving some forms of pretreatment (e.g. filtration or first-flush diversion) (Mun and Han, 2012) and then drained to the discharge system when the storage capacity of the system is fully utilized. The stored water is often utilized for domestic and/or municipal purposes. As depicted in Fig. 3.1, the involved hydrological processes have often been described as those associated with a simple storage reservoir (Fewkes and Butler, 2000; Vaes and Berlamont, 2001; Guo and Baetz, 2007; Hanson et al., 2009; Kim and Yoo, 2009). For describing the dynamic water balance of a water storage unit, the mass balance equation can be expressed in differential form as

$$w_0 \frac{ds(t)}{dt} = I[s(t),t] - L[s(t)] \tag{3.1}$$

where w_0 is the maximum storage capacity of a RWH system expressed as depth of water over the storage unit's bottom area, mm; $s(t)$ represents the fraction of the maximum storage capacity that is occupied by water at time t [$0 \le s(t) \le 1$]; $I[s(t),t]$ represents the net rate of water filling into the storage unit at time t when $s(t)$ fraction of the storage unit is filled with water, $I[s(t),t]$ equals zero except when rainfall occurs, at the instant when rainfall occurs, $I[s(t),t]$ would be such

that available water will all be stored as long as the storage unit is not full; $L[s(t)]$ is the water depletion rate from the storage unit other than overflow which may occur under some rainfall events, this depletion rate depends on s which is a function of t, that is why it is denoted as $L[s(t)]$.

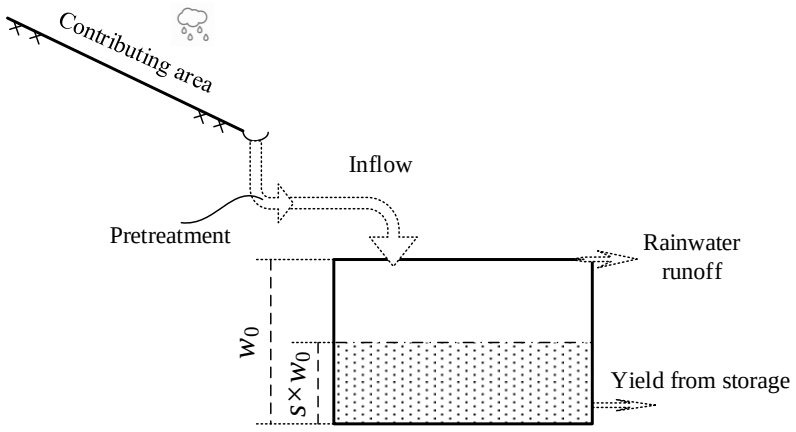

Fig. 3.1 Schematic of inflow into and outflow from a rainwater storage unit

Eq. (3.1) provides the basis for quantifying the dynamics of a RWH system. It demonstrates that the water availability in the storage unit at a specific time *t* [i.e. $s(t)$] depends on the balance of water inflow (the amount of water which can be captured and stored) and demand (the volume of water that will be used/depleted). Coupled with the input of a time series of local rainfall data, water demand, conditions of contributing area, and the size of a RWH system, Eq. (3.1) can be used to model the system's hydrologic operations through either numerical calculations or analytical derivations. In this paper, an analytical approach is introduced, with mathematical representations of the required input terms

introduced first.

3.2.2. Net Inflow Represented as a Marked Poisson Process

A long-term continuous rainfall record can be viewed as being comprised of a series of rainfall pulses occurring at various times. To facilitate its application in theoretical analyses, a rainfall data series is usually discretized into statistically independent individual rainfall events by selecting a minimum inter-event time (MIET). The MIET is defined as the minimum number of dry hours between two rainfall events. Two consecutive rainfall episodes are considered as belonging to the same rainfall event if the dry time between them is less than the adopted MIET, otherwise they are considered as belonging to two different events. Each rainfall event can be characterized by its volume, duration and inter-event time. The exponential probability density functions (PDFs) were found to fit the histograms of rainfall event volume (v), duration (u), and inter-event time (b) satisfactorily, especially in many regions of North America (Restrepo-Posada and Eagleson, 1982; Wanielista and Yousef, 1993; Adams and Papa, 2000; Guo and Baetz, 2007). The PDFs of rainfall event characteristics are

$$f(v) = \zeta \exp(-\zeta v), \quad v > 0 \tag{3.2}$$

$$f(u) = \lambda \exp(-\lambda u), \quad u > 0 \tag{3.3}$$

$$f(b) = \psi \exp(-\psi b), \quad b > 0 \tag{3.4}$$

where ζ, λ and ψ are distribution parameters. A rigorous data processing

technique for obtaining these parameters is provided by Hassini and Guo (2016). Hourly rainfall data from five stations (varying from humid to arid climates) are used in this study and their rainfall statistics obtained from previous studies are tabulated in Table 3.1, where $\langle v \rangle$, $\langle u \rangle$, and $\langle b \rangle$ are the mean rainfall event volume (mm), mean rainfall event duration (h), and mean inter-event time (h), respectively.

Table 3.1 Rainfall Statistics and Climate Classifications

Station	Data series		MIET	$\langle v \rangle = \zeta^{-1}$	$\langle u \rangle = \lambda^{-1}$	$\langle b \rangle = \psi^{-1}$	Annual precipitation (NOAA, 2011)	Climate classification[a]
			h	mm	h	h	mm	
Atlanta, GA.	1945-2005	Jan.-Dec.	8	15.68	9.18	101.84	1236	Humid
Concord, NH.	1945-2005	Apr.-Nov.	6	11.9	9.2	93.7	1031	Humid
Detroit, MI.	1960-2006	Apr.-Oct.	8	14.35	8.2	97.95	850	Humid
Flagstaff, AZ.	1947-2005	Jan.-Dec.	12	11.63	13.54	170.75	555	Semi-arid
Billings, MT.	1945-2005	Apr.-Oct.	8	9.8	10.7	192.5	347	Arid

Note: Rainfall statistics for Atlanta and Flagstaff were presented in Zhang and Guo (2013); data for Concord were presented in Guo and Guo (2017); data for Detroit were presented in Zhang and Guo (2013); data for Billings were presented in Guo et al. (2014). [a] The climate is roughly classified based on the annual precipitation (AP) as follows: AP < 400 mm - Arid climate; AP = 400~750 mm - Semi-arid climate; AP > 750 mm - Humid climate (Raghunath, 2006).

The rainfall event durations are usually much shorter than the inter-event times. As such, an individual rainfall event may be considered as fallen at an instant of time and a point rainfall series can be idealized as a point process comprised of instantaneous rainfall jumps separated by random arrival times. The random

rainfall depths of individual events are statistically independent, and the time series of rainfall events is therefore a marked Poisson process with a mean rainfall event arrival rate μ' approximately equalling to $[\langle u \rangle + \langle b \rangle]^{-1}$ (Eagleson, 1978; Guo, 2016). The mark (or ancillary variable) of this marked Poisson process is the rainfall event volume v.

The volume of runoff generated from a catchment that can be collected by the storage unit as the result of a rainfall event with volume (v) can be expressed as

$$v_{in} = \begin{cases} 0, & v \le v_{ff} \\ \varphi_{st}(v - v_{ff}), & v > v_{ff} \end{cases} \tag{3.5}$$

where v_{in} is the generated runoff or the available volume of inflow into the storage unit, expressed as depth (mm) of water over the storage unit's bottom area; φ_{st} is the contributing ratio and can be calculated as $\varphi_{st} = R_a \phi$, where R_a is the ratio between the contributing catchment area and the bottom area of the storage unit, R_a is referred to as the area ratio hereafter, and ϕ is the runoff coefficient of the catchment, mainly reflecting the effect of evaporation during the rainfall events and surface depressions in converting rainfall to runoff, ϕ has values from 0 to unity [e.g., the suggested roof runoff coefficients vary in a range of 0.75-0.95 (Jennings et al., 2015)]; v_{ff} is the first-flush diversion height typically ranges from 0.5 mm to 1.5 mm (TRCA and CVCA, 2010) . Eq. (3.5) reflects the effect that the first v_{ff}

mm of rainfall of every rainfall event will not be collected by the storage unit.

As shown in Eq. (3.5), since the first-flush diversion is considered, the runoff process is censored from the rainfall process with events having $v \le v_{ff}$ removed, this runoff process forms a new marked Poisson process. The new marked Poisson process has a less frequent arrival rate of $\mu = \mu' \int_{v_{ff}}^{+\infty} f(v)dv = \mu' \exp(-\zeta v_{ff})$ (Laio et al., 2001). The volume of rainfall events remaining in the new marked Poisson process has the same distribution as $(v - v_{ff})$ conditioned on $v > v_{ff}$, which is the same as described by Eq. (3.2). The mark of the new marked Poisson process is the generated runoff volume v_{in} with events having $v_{in} = 0$ removed (i.e., rainfall events with $v \le v_{ff}$ removed). The cumulative distribution function of v_{in} is denoted as $F(v_{in})$ and can be derived considering that v_{in} is simply the product of φ_{st} and $(v - v_{ff})$ conditioned on $v > v_{ff}$, i.e.,

$$F(v_{in}) = P[\,\varphi_{st}(v - v_{ff}) \le v_{in} \mid v > v_{ff}\,] = \frac{\int_0^{v_{in}/\varphi_{st}+v_{ff}} \zeta \exp(-\zeta v)dv}{\int_{v_{ff}}^{+\infty} \zeta \exp(-\zeta v)dv}$$

$$= \frac{1}{\exp(-\zeta v_{ff})} - \exp(-\frac{\zeta}{\varphi_{st}} v_{in})$$

Therefore, the PDF of the generated runoff or available inflow v_{in} [denoted as $f(v_{in})$] can be derived as

$$f(v_{in}) = \frac{dF(v_{in})}{dv_{in}} = \frac{\zeta}{\varphi_{st}} \exp(-\frac{\zeta}{\varphi_{st}} v_{in}) = \zeta' \exp(-\zeta' v_{in}) \qquad (3.6)$$

where $\zeta' = \zeta / \varphi_{st}$ is the exponential distribution parameter of the available inflow. Normalizing v_{in} by dividing it by w_0, the PDF of the normalized available inflow (denoted as r and $r = v_{in} / w_0$) can be expressed as

$$f(r) = \gamma \exp(-\gamma r), \quad r > 0 \qquad (3.7)$$

where r is dimensionless and $\gamma = \zeta' w_0$ is the normalized dimensionless distribution parameter. The rainwater amount that is lost prior to entering the storage unit due to first flush diversion, depression storage and other losses have been excluded from the r values considered in Eq. (3.7).

The actual/net normalized inflow into the storage unit as a result of a runoff event generating a normalized available inflow r is denoted as y. The value of y depends on not only r, but also s, the fraction of the maximum storage capacity that is already filled with water when the runoff event occurs. The conditional PDF of y given an antecedent saturation level s is therefore required for further analysis. This conditional PDF is denoted as $f(y|s)$, considering the PDF of r as given in Eq. (3.7) and the possible relations between y, r, and s, it can be shown that

$$f(y \mid s) = \begin{cases} \gamma \exp(-\gamma y), & 0 < y < 1-s \\ \exp[-\gamma(1-s)]\delta(y-1+s), & y = 1-s \end{cases} \quad (3.8)$$

where $\delta(\cdot)$ is the Dirac delta function. Eq. (3.8) shows that y can only take on values from 0 to $(1-s)$. Eq. (3.8) also states that additional water can not be stored by the system as soon as its maximum storage capacity is reached; therefore, there is an atom of probability at $y = 1-s$. Under a rainfall event with normalized available inflow $r \le (1-s)$, $y = r$; this explains why for this region of y values (i.e., $0 < y < 1-s$), the PDF of y is the same as the PDF of r. The probability mass at $y = (1-s)$ represents the probability that a storm will fill up the storage unit to its maximum capacity given that the storage unit has s fraction of it already occupied by water at the beginning of the storm. The time series of net inflows into the storage unit can therefore be represented as a new marked Poisson process with arrival rate μ and individual marks y obeying the PDF of $f(y \mid s)$.

3.2.3. Water Use Rate

RWH systems usually supply water to meet the demand for toilet flushing, landscape irrigation, pavement washing or even as complementary water sources for drinking purpose inside or outside buildings (Sturm et al., 2009; Palla et al., 2011; Jennings et al., 2012; Matos et al., 2013). Such water use may have significant daily and seasonal variations, and may also change depending on whether it is during a rainfall event or dry period. For the sake of simplicity, the

rate of anticipated water demand is treated as a constant equalling its long-term average value in the sizing of RWH systems (Fewkes and Wam, 2000; Su et al., 2009; Campisano et al., 2013; Hajani and Rahman, 2014). The water use is therefore assumed to proceed at the average water demand rate except when the system is completely dry. Hence, the normalized water use rate can be expressed as

$$L[s(t)] = \begin{cases} 0, & s = 0 \\ \eta, & 0 < s \leq 1 \end{cases} \tag{3.9}$$

where $\eta = \varpi / w_0$ is the long-term average normalized water demand rate, with ϖ being the average water demand rate expressed as depth of water in the storage unit per unit time.

3.2.4. Steady State Solution of the Stochastic Water Balance Equation

With the net inflow $I[s(t),t]$ in Eq. (3.1) described as a marked Poisson process with arrival rate μ and individual marks having a PDF as shown in Eq. (3.8), Eq. (3.1) can therefore be considered as a stochastic differential equation, with its solution $s(t)$ also being a stochastic process, which is meaningful only in probabilistic terms. Since $s(t)$ is driven by a marked Poisson process, it would be a Markov process with jumps and drifts (Gardiner, 2004). The state PDF of s at time t is denoted as $p(s,t)$ which can be obtained by solving the Chapman-Kolmogorov forward equation for the Markov process governed by Eq. (3.1)

(Gardiner, 2004). The Chapman-Kolmogorov forward equation of a Markov process relates the state probability distribution [$p(s,t)$ in this case] at different times. Based on Eq. (3.1) and adapting from the solutions provided by (Cox and Isham, 1986), (Rodriguez-Iturbe et al., 1999), and (Rodríguez-Iturbe and Porporato, 2005), the Chapman-Kolmogorov forward equations describing the temporal evolution of $p(s,t)$ were found to be

$$\frac{\partial}{\partial t}p(s,t)=\eta\frac{\partial}{\partial s}p(s,t)-\mu p(s,t)+\mu\int_0^s p(z,t)f[(s-z)|z]dz+\mu p_0(t)f(s|0) \quad (3.10)$$

$$\frac{d}{dt}p_0(t)=-\mu p_0(t)+\eta p(0,t) \quad (3.11)$$

where $f[(s-z)|z]$ is the conditional probability distribution expressed in Eq. (3.8), z is the dummy variable of integration; $p(0,t)$ is the value of the PDF $p(s,t)$ when s approaches zero at time t [i.e., $p(0,t)=\lim_{s\to 0}p(s,t)$], and $p_0(t)$ is the probability that s is zero (or the storage unit is empty) at time t. Eq. (3.11) appears as a part of the Chapman-Kolmogorov forward equations because of the probability mass $p_0(t)$ at $s=0$.

By taking the limit as $t\to\infty$, an equilibrium or steady-state solution of the above Chapman-Kolmogorov forward equations exists. Under this steady state, although s still changes randomly with time, the PDF of s does not change with time any more, and the time series of s afterwards can be described as a strictly

stationary process. Mathematically, steady state can only be reached with $t \to \infty$, but practically, since the storage volume of a RWH system is relatively small compared to monthly or seasonal total rainfall, a nearly steady-state condition would be reached after a few months of operation. For planning and design purposes, only the system's steady-state condition is of interests.

The steady-state solution for $p(s,t)$ is denoted as $p(s)$ and the steady-state solution for $p_0(t)$ is denoted as p_0. These steady-state solutions can be obtained by setting the left-hand-sides of Eqs. (3.10) and (3.11) to zero and replacing $p(s,t)$ with $p(s)$ and $p_0(t)$ with p_0, i.e.:

$$\eta \frac{\partial}{\partial s} p(s) - \mu p(s) + \mu \int_0^s p(z) f[(s-z) \mid z] dz + \mu p_0 f(s \mid 0) = 0 \quad (3.12)$$

$$-\mu p_0 + \eta p(0) = 0 \quad (3.13)$$

Substituting $f(y \mid s)$ with what is given in Eq. (3.8), Eq. (3.12) turns to be

$$\eta \frac{\partial}{\partial s} p(s) - \mu p(s) + \mu \int_0^s p(z) \gamma \exp[-\gamma(s-z)] dz + \mu p_0 \gamma \exp(-\gamma s) = 0 \quad (3.14)$$

Multiplying by $\exp(\gamma s)$ to eliminate the term containing p_0, differentiating with respect to s and then dividing by $\exp(\gamma s)/(\gamma\eta)$, Eq. (3.14) becomes

$$\frac{1}{\gamma} \frac{d^2}{ds^2} p(s) + (1-\alpha) \frac{d}{ds} p(s) = 0$$

In the above expression, for simplicity in notation, we let $\alpha = \mu/\gamma\eta$. The general

solution of the above equation is

$$p(s) = \begin{cases} C_1 \exp[\gamma(\alpha - 1)s] + C_2, & \alpha \neq 1 \\ C_3 s + C_4, & \alpha = 1 \end{cases}$$

where C_1, C_2, C_3 and C_4 are integration constants. It can be seen already that the special case with $\alpha = 1$ needs to be dealt with separately.

The value of $p(0)$ can be obtained from the above general solution as follows:

$$p(0) = \lim_{s \to 0} p(s) = \begin{cases} C_1 + C_2, & \alpha \neq 1 \\ C_4 & \alpha = 1 \end{cases}$$

Substitute the value of $p(0)$ into Eq. (3.13), p_0 can be obtained as follows:

$$p_0 = \frac{\eta}{\mu} p(0) = \begin{cases} \frac{\eta}{\mu}(C_1 + C_2), & \alpha \neq 1 \\ \frac{\eta}{\mu} C_4 & \alpha = 1 \end{cases}$$

To determine the values of C_1, C_2, C_3 and C_4, the general solution of $p(s)$ and p_0 are substituted back into Eq. (3.14) to ensure that they together still satisfy Eq. (3.14). It can be shown that satisfaction of Eq. (3.14) requires that

$$C_2 = 0, \text{ if } \alpha \neq 1; \text{ and } C_3 = 0, \text{ if } \alpha = 1$$

The value of p_0 and the general solution of $p(s)$ for cases where $\alpha \neq 1$ becomes

$$p_0 = \eta / \mu C_1, \text{ and } p(s) = C_1 \exp[\gamma(\alpha - 1)s] \text{ with } 0 < s \leq 1$$

The value of p_0 and the general solution of $p(s)$ for the special case where $\alpha = 1$

becomes

$$p_0 = C_4\,\eta/\mu\text{, and } p(s) = C_4 \text{ for } 0 < s \le 1$$

Since s is physically bounded in [0, 1], $p_0 + \int_0^1 p(s)ds$ must equal to unity. To ensure that this requirement is satisfied, C_1 and C_4 were determined to be

$$C_1 = \frac{\gamma\alpha(\alpha-1)}{\alpha\exp[\gamma(\alpha-1)]-1}, \text{ if } \alpha \ne 1\text{; and } C_4 = \frac{\gamma}{1+\gamma}, \text{ if } \alpha = 1$$

The steady-state solution for cases where $\alpha \ne 1$ is therefore

$$p_0 = \frac{\alpha-1}{\alpha\exp[\gamma(\alpha-1)]-1}; \tag{3.15a}$$

$$p(s) = \frac{\mu}{\eta}\,p_0\exp[(\frac{\mu}{\eta}-\gamma)s] = \frac{\gamma\alpha(\alpha-1)}{\alpha\exp[\gamma(\alpha-1)]-1}\exp[(\frac{\mu}{\eta}-\gamma)s], \text{ for } 0 < s \le 1 \tag{3.15b}$$

Similarly, the solution for the special case where $\alpha = 1$ is

$$p_0 = \frac{1}{1+\gamma}; \tag{3.16a}$$

$$p(s) = \frac{\gamma}{1+\gamma}\text{, for } 0 < s \le 1 \tag{3.16b}$$

In the above expressions, η is the normalized water demand rate, μ/γ represents the normalized mean inflow rate (i.e., the inflow rate averaged through both dry and wet periods), therefore $\alpha = \mu/\gamma\eta$ [i.e., $(\mu/\gamma)/\eta$] is the ratio between the normalized mean inflow rate and water demand rate. This ratio α can also be

viewed as the ratio between annual runoff collected by a RWH system and the annual total water demand, it is considered as an important parameter in previous studies (Fewkes, 2000). The solutions above show that when the average inflow rate is equal to the average water demand rate (i.e. when $\alpha = 1$), the steady-state fluctuation of s is only related to γ; otherwise it depends on not only γ, but also on η and μ.

3.2.5. Water Use Patterns and Effective Storage Capacity

When rainwater collected by a RWH system is designed only for outdoor uses (e.g. garden irrigation, pavement washing), water use may primarily take place during dry periods. For large buildings or communities, use of water supplied by RWH systems may take place no matter if it rains or not. Therefore, depending on the purposes and period of water demand, RWH systems can be analyzed for two typical water use patterns: Pattern 1, water is only used during dry periods; and Pattern 2, water is used during both rainfall events and dry periods (Guo and Baetz, 2007; Ward et al., 2010; Palla et al., 2011; Matos et al., 2013). Because of these different water-use patterns, there may be some inaccuracies resulting from the use of Eq. (3.9) to represent the water demand rate.

For RWH systems with Pattern 1 water use, physically, water use occurs only during dry periods and starts when the dry period starts; however, in the established

stochastic model, the random inflow are treated as instantaneous pulses with an arrival rate of $[\langle u \rangle + \langle b \rangle]^{-1}$. The starting point of water use is thus moved forward to the start point of the rainfall event and an additional period (i.e., the duration of the rainfall event) is added prior to the actual water use occurrence time. Rainfall event duration is statistically much shorter than inter-event dry period (e.g. the average values of rainfall event durations are only 1/10-1/20 of those of the dry periods as shown in Table 3.1); therefore, it is reasonable to assume that only a slight overestimation of the overall water use would result from the use of Eq. (3.9) for Pattern 1 cases. If necessary, this overestimation may be eliminated by proportionally adjusting the value of η used in the stochastic model.

For cases with Pattern 2 water use, stored water is used the same way during both dry and wet times, and storage capacity in addition to what is physically provided by the tank is created as a result of water use simultaneously occurring during a rainfall event. However, in the stochastic model, rainfall events are assumed to occur instantaneously, so the additional storage capacity generated while water is used is not considered. To take into account this additional storage capacity due to the water use occurring during rainfall events, it is assumed that the maximum effective storage capacity of a RWH system prior to a rainfall event is approximately equal to the maximum physical storage volume of the system V_{st} plus the average volume of water used during a rainfall event. For Pattern 1 water

use, no adjustment on the storage capacity is needed. The maximum effective storage capacity can therefore be expressed as

$$w_0 = \begin{cases} V_{st} / A_{st}, & \text{Pattern 1 water use} \\ V_{st} / A_{st} + \varpi \langle u \rangle, & \text{Pattern 2 water use} \end{cases} \quad (3.17)$$

where V_{st} is the storage volume measured in the unit of lites (L) or m^3 and A_{st} is the bottom area of the storage unit measured in the unit consistent with V_{st}; $\varpi \langle u \rangle$ is the average volume of water used during a rainfall event. The acceptability of this simplification will be confirmed later.

3.2.6. Long-term Water Balance and Performance Statistics

Performance indicators of a RWH system can be analytically expressed based on the preceding stochastic solutions. First of all, the performance of a RWH system in reducing potable water consumption is often examined by quantifying its volumetric reliability defined as the ratio between the total volume of rainwater supplied by the system and the total demand. Another time-based reliability is defined as the fraction of time when the water demand is met by the RWH system (Guo and Baetz, 2007; Palla et al., 2011; Mun and Han, 2012; Santos and Taveira-Pinto, 2013). Since water use rate is considered to be constant whenever there is water in the storage tank, the long-term average volumetric reliability and the time-based reliability are the same (denoted as R_e and also referred to as water saving

efficiency). Using the stochastic model results presented earlier, R_e can be calculated as:

$$R_e = \frac{\langle L \rangle}{\langle D \rangle} = \frac{\int_0^1 \eta\, p(s) ds}{\eta} = 1 - p_0 \tag{3.18}$$

where $\langle L \rangle = \int_0^1 \eta\, p(s) ds$ is the normalized mean water use rate (i.e., the actual average rate of water supplied by the system for use averaged through both wet and dry periods); $\langle D \rangle = \eta$ is the normalized water demand rate. Furthermore, the water use rate described in Eq. (3.9) depends only on the availability of water in the storage tank, which means that the RWH system can supply water for use as long as there is water in the system. Therefore, $(1 - p_0)$, which is the average fraction of time when there is water in storage, can indeed represent this water supply reliability. Moreover, p_0, which is the average fraction of time when there is no water in storage, has also been defined as the water deficit rate in the performance analysis of RWH systems (Su et al., 2009; Youn et al., 2012).

Additionally, an unnecessarily large storage tank would be a misuse of investment and space, yet it may still not meet the reliability requirement when the catchment size is too small. Amongst the performance indicators, water supply reliability is found to be the most appropriate criterion to size a RWH system, ensuring that the system may achieve a high water-saving performance at a

relatively low cost (Zhang et al., 2009; Santos and Taveira-Pinto, 2013; Hajani and Rahman, 2014). Substituting $\gamma = \zeta w_0 / \varphi_{st}$, $\eta = \varpi / w_0$ into Eq. (3.15a) or Eq. (3.16a) for calculating p_0 and then substituting that p_0 expression into Eq. (3.18), solving for w_0 from the resulting expression of R_e, the following was obtained:

$$w_0 = \begin{cases} \dfrac{\varpi}{\mu} \dfrac{\ln\left[(1-\frac{\zeta}{\varphi_{st}}\frac{\varpi}{\mu}R_e)/(1-R_e)\right]}{1-\frac{\zeta}{\varphi_{st}}\frac{\varpi}{\mu}}, & \alpha \neq 1 \\ \dfrac{\varphi_{st}}{\zeta}\dfrac{R_e}{1-R_e}, & \alpha = 1 \end{cases} \tag{3.19}$$

Eq. (3.19) may provide an easy-to-use tool for sizing storage tanks with specified reliability requirements. Given an optimized R_e [e.g., the storage tank sized with a reliability of 80% was found to achieve the highest ratio between water savings and installation cost (Santos and Taveira-Pinto (2013)] and based on Eq. (3.19), the required storage volume for cases under Pattern 1 water use can be calculated as $V_{st} = w_0 A_{st}$, and the required storage volume for cases under Pattern 2 water use can be calculated as $V_{st} = [w_0 - \varpi \langle u \rangle] A_{st}$.

Also, the runoff reduction benefit can be quantified by the long-term average stormwater capture efficiency (or runoff reduction rate, denoted as C_e) which can be derived as follows:

$$C_e = \frac{\langle L \rangle}{\langle R \rangle} = \frac{\int_0^1 \eta\, p(s) ds}{\mu / \gamma} = \frac{\gamma \eta}{\mu}(1 - p_0) = \frac{R_e}{\alpha} \tag{3.20}$$

where $\langle R \rangle = \mu / \gamma$ is the normalized mean inflow rate. Eq. (3.20) shows that C_e and R_e are linearly related, which is consistent with their respective definitions.

In addition, considering the discontinuous nature of the loss function $L[s(t)]$ at $s = 0$, the cumulative distribution function (CDF) of s [denoted as $C_u(s)$] for cases where $\alpha \neq 1$ can be determined as follows:

$$C_u(s) = p_0 + \int_{s=0}^{s} p(s) ds = \frac{\alpha \exp[\gamma(\alpha - 1)s] - 1}{\alpha \exp[\gamma(\alpha - 1)] - 1} \tag{3.21}$$

$C_u(s)$ for cases where $\alpha = 1$ can be derived as follows:

$$C_u(s) = p_0 + \int_{s=0}^{s=1} p(s) ds = \frac{1 + \gamma s}{1 + \gamma} \tag{3.22}$$

The expected long-term average value of s (i.e., $\langle s \rangle$) for cases where $\alpha \neq 1$ can be derived as follows:

$$\langle s \rangle = \int_{s=0}^{s=1} s p(s) ds = \frac{\gamma\alpha \exp[\gamma(\alpha - 1)] + 1}{\gamma\alpha \exp[\gamma(\alpha - 1)] - \gamma} - \frac{1}{\gamma(\alpha - 1)} \tag{3.23}$$

The value of $\langle s \rangle$ for cases where $\alpha = 1$ can be derived as follows:

$$\langle s \rangle = \int_{s=0}^{s=1} s p(s) ds = \frac{\gamma}{1 + \gamma} \tag{3.24}$$

Eq. (3.23) or Eq. (3.24) provide a convenient estimate of the long-term average

water level in the storage tank.

3.3. Validation of the Stochastic Solutions by Comparing with SWMM Continuous Simulation Results

In establishing the stochastic model, several assumptions were made: rainfall events are assumed to occur instantaneously, the arrival of the rainfall events are treated as a Poisson process, the volume for any rainfall event is randomly drawn from an exponential distribution, and the maximum effective storage capacity of RWH systems is assumed to be equal to what is described by Eq. (3.17). To verify the accuracy of the derived stochastic results and test the validity of the simplifying assumptions, continuous simulations using the U.S. Environmental Protection Agency's Storm Water Management Model (SWMM) version 5.1 (Rossman, 2015) were conducted with results compared to those from stochastic analysis. The SWMM model does not employ similar assumptions and continuous simulation results should therefore be much more accurate.

In a SWMM model, two subcatchments are established; Subcatchment A represents the contributing area with depression storage equaling the value of first flush, while Subcatchment B represents the RWH system. To model RWH systems under Pattern 2 water use, Subcatchment B is modelled using SWMM's LID module, in which water in the RWH system can be used during both dry and rainfall

periods. Since SWMM's LID module does not provide a water use option for systems where water use only occurs during dry periods, to model cases under Pattern 1 water use, Subcatchment B is modeled in SWMM as a regular 100% impervious subcatchment with its surface depression storage equaling V_{st} / A_{st} and evaporation set to occur only in dry periods with a constant rate equaling to ϖ. Using continuous rainfall data, the SWMM model performs time-step-by-time-step simulations of the operation of the RWH system, and can output the inflow into Subcatchment B (denoted as V_{inB}) and runoff (i.e., discharge) from Subcatchment B (denoted as V_{outB}). Thus, the stormwater capture efficiency can be calculated as $(1-V_{outB}/V_{inB})$.

Local rainfall statistics, conditions of contributing area, storage tank size, and water demand rate are the main factors influencing the performance of RWH systems (Fewkes and Wam, 2000; Guo and Baetz, 2007; Kim and Yoo, 2009; Imteaz et al., 2011; Mun and Han, 2012; Campisano et al., 2013). RWH systems in locations with different climates (i.e., Atlanta, Concord, Detroit, Flagstaff and Billings as shown in Table 3.1) with varying contributing area conditions (φ_{st} changing from 5 to 500), storage tank sizes (V_{st} changing from 200 L to 500 L) and water demand rates (hereafter l_{st} is used to denote the volumetric water demand rate, i.e., $l_{st} = \varpi A_{st}$, l_{st} varies from 100 L/day to 1000 L/day) are modeled.

Stormwater capture efficiencies of various RWH systems under Pattern 1 and Pattern 2 water uses calculated using the analytical stochastic solutions [Eq. (3.20) with w_0 expressed in Eq. (3.17)] are compared with SWMM simulation results. The comparisons for 206 different cases under Pattern 1 water use and 158 different cases under Pattern 2 water use are shown in Figs. 3.2 and 3.3, respectively. Treating SWMM results as observed data, the Nash-Sutcliffe model efficiency coefficient (NSME), the root mean square error (RMSE), and the correlation coefficient between stochastic results and observed values were also calculated and the results are also presented in Figs. 3.2 and 3.3. It can be seen from the two figures that the analytical and simulation results are well within agreement. Taking the continuous simulation results as a benchmark, the summary statistics indicate that the derived analytical solutions can provide an accurate and reliable method for estimating stormwater capture efficiencies.

To save space, only some cases in Atlanta are illustrated in Figs. 3.4 and 3.5. The two figures show that the stormwater capture efficiency of a RWH system would generally rise with the increase of the storage tank size and the water use rate, and rapidly drop with the increase of the contributing ratio. Additionally in Fig. 3.4, the derived stochastic solution is also compared with the analytical probabilistic solution that adopted the same water use pattern (Pattern 1) and derived by Guo and Baetz (2007). As previously discussed, a simplifying

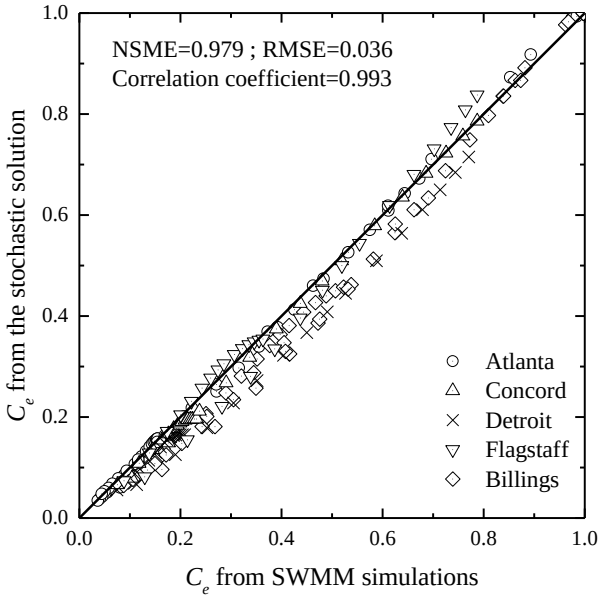

Fig. 3.2 Comparisons of stormwater capture efficiencies (C_e) for 206 cases with Pattern 1 water use

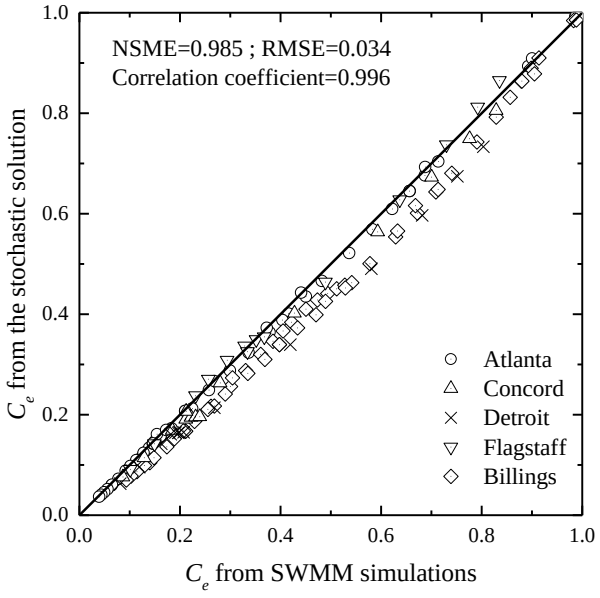

Fig. 3.3 Comparisons of stormwater capture efficiencies (C_e) for 158 cases with Pattern 2 water use

assumption about the initial water content of the storage tank had to be made in that event-based probabilistic approach. In the Guo and Baetz's (2007) solution, it was assumed that the storage unit would be full at the beginning of a dry period preceding a rainfall event which is the end of the last rainfall event. Only small storage units (e.g. rain barrels) were considered and probabilistic results were obtained by analyzing the operation of the system during the dry and subsequent rainfall period preceded by the last rainfall event. In comparison with the continuous simulation results, results based on the Guo and Baetz's (2007) solution performed well when the storage volume is relatively small, but would underestimate the stormwater capture efficiency when the storage tank size gets larger and the water use rate also reaches a certain high value, or when the contributing ratio is relatively small. This is because the contributing ratio determines the amount of inflow into the storage tank, and when the contributing ratio is small, the inflow volume is small and there is less a possibility for a RWH system with a larger storage capacity to be filled when a rainfall event ends. With a large water use rate, the runoff into the storage tank can be used quickly during a rainfall event. That is why for these cases, the assumption that the storage space is filled when the last storm ends becomes more unrealistic, the average storage capacity available at the beginning of a random rainfall event would be larger than what is calculated in the analytical probabilistic approach. Therefore, the stormwater capture efficiency for these cases will be slightly underestimated by the

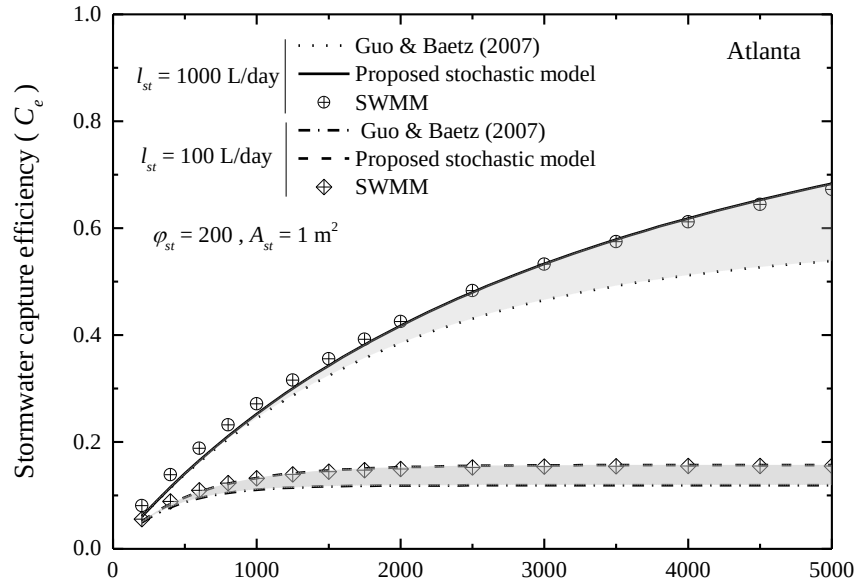

(a) Storage volume [V_{st} , liters (L)]

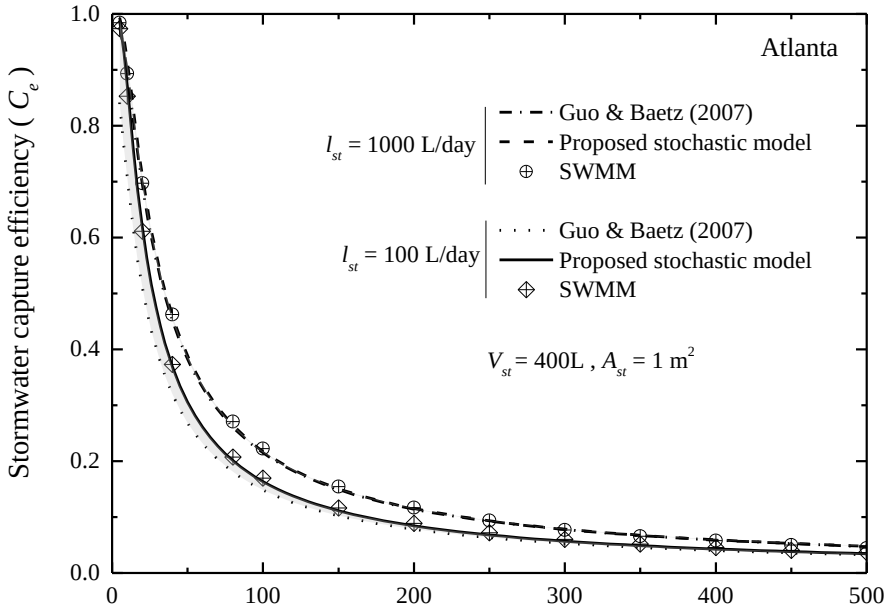

(b) Contributing ratio ($\varphi_{st} = \phi R_a$)

Fig. 3.4 Stormwater capture efficiency C_e of RWH systems with varying storage volumes, contributing ratios, and water use rates in Atlanta (Pattern 1 water use)

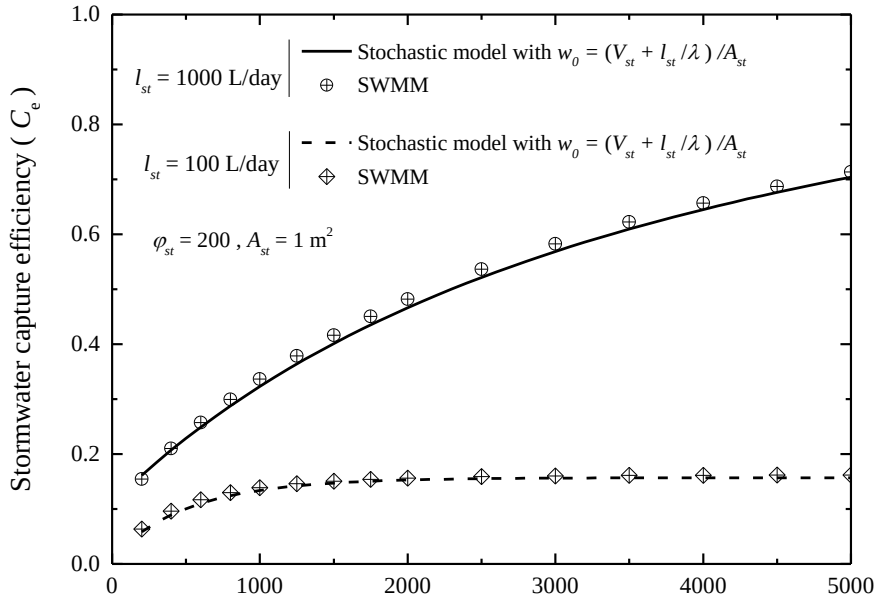

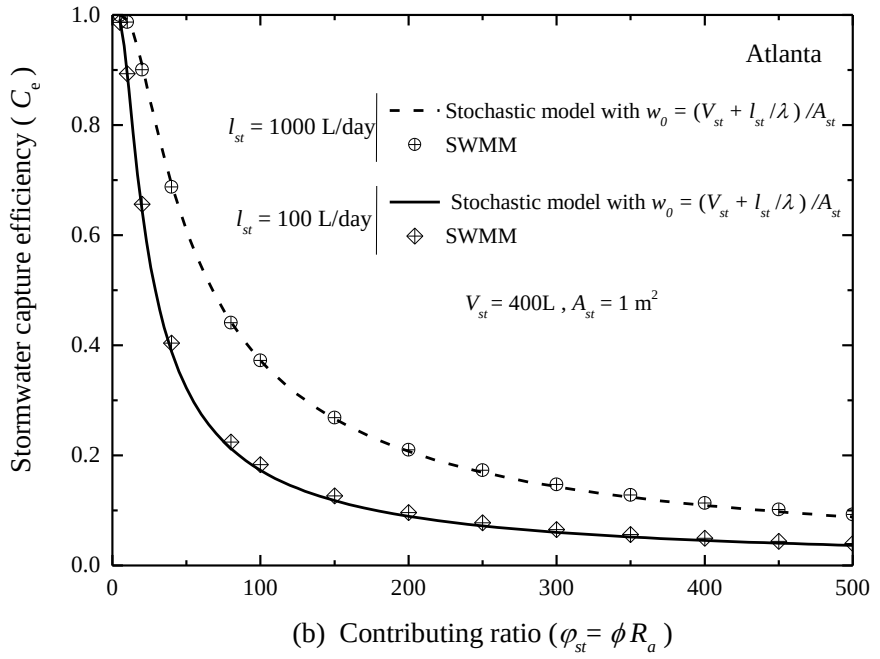

Fig. 3.5 Stormwater capture efficiencies (C_e) of RWH systems with varying storage volumes, contributing ratios, and water use rates in Atlanta (Pattern 2 water use)

previous analytical probabilistic solutions. The proposed stochastic method effectively gets rid of this restriction and may provide a more general and reliable analytical tool for evaluating the long-term hydrologic performance of RWH systems.

3.4. Example Analysis Results

In addition to stormwater capture efficiency, many other valuable indicators can also be conveniently obtained using the derived formulas. These results are also of great interest in the performance evaluation and design of RWH systems, but continuous simulation models do not directly output these results. The commonly used Pattern 2 water use was applied as an example in the following analysis.

The cumulative frequency distribution of normalized water level in the storage tank and its long-term average value can be calculated using Eq. (3.21) or Eq. (3.22) and Eq. (3.23) or Eq. (3.24), respectively. Taking Atlanta as an example, Fig. 3.6 shows that the fluctuation of the water level in the storage tank is greater with larger contributing ratio, larger storage tank size and smaller water demand rate. $\langle s \rangle$ rises with the increase in contributing ratio and storage tank size and with the decrease in water demand rate. Note that the rate of change of $\langle s \rangle$ with these factors are significantly different; this should be taken into account in the optimum design of

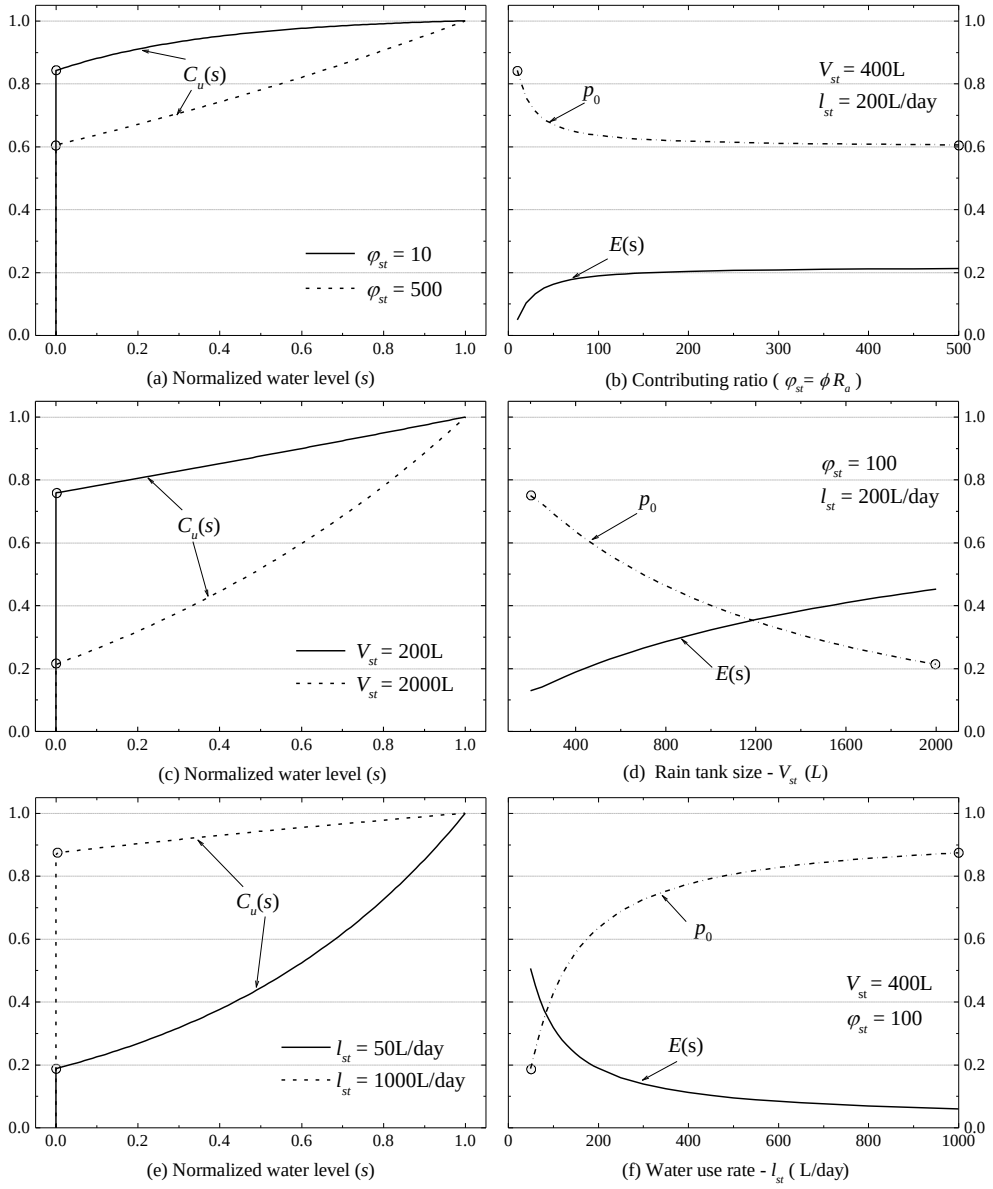

Fig. 3.6 The water balance of a rainwater tank (Atlanta) [(a) CDF of normalized water levels for two different contributing ratios (φ_{st}); (b) $\langle s \rangle$ and p_0 varying with φ_{st}; (c) CDF of normalized water levels with two different tank sizes (V_{st}); (d) $\langle s \rangle$ and p_0 varying with V_{st}; (e) CDF of normalized water levels with two different water use rates; (f) $\langle s \rangle$ and p_0 varying with the water use rate]

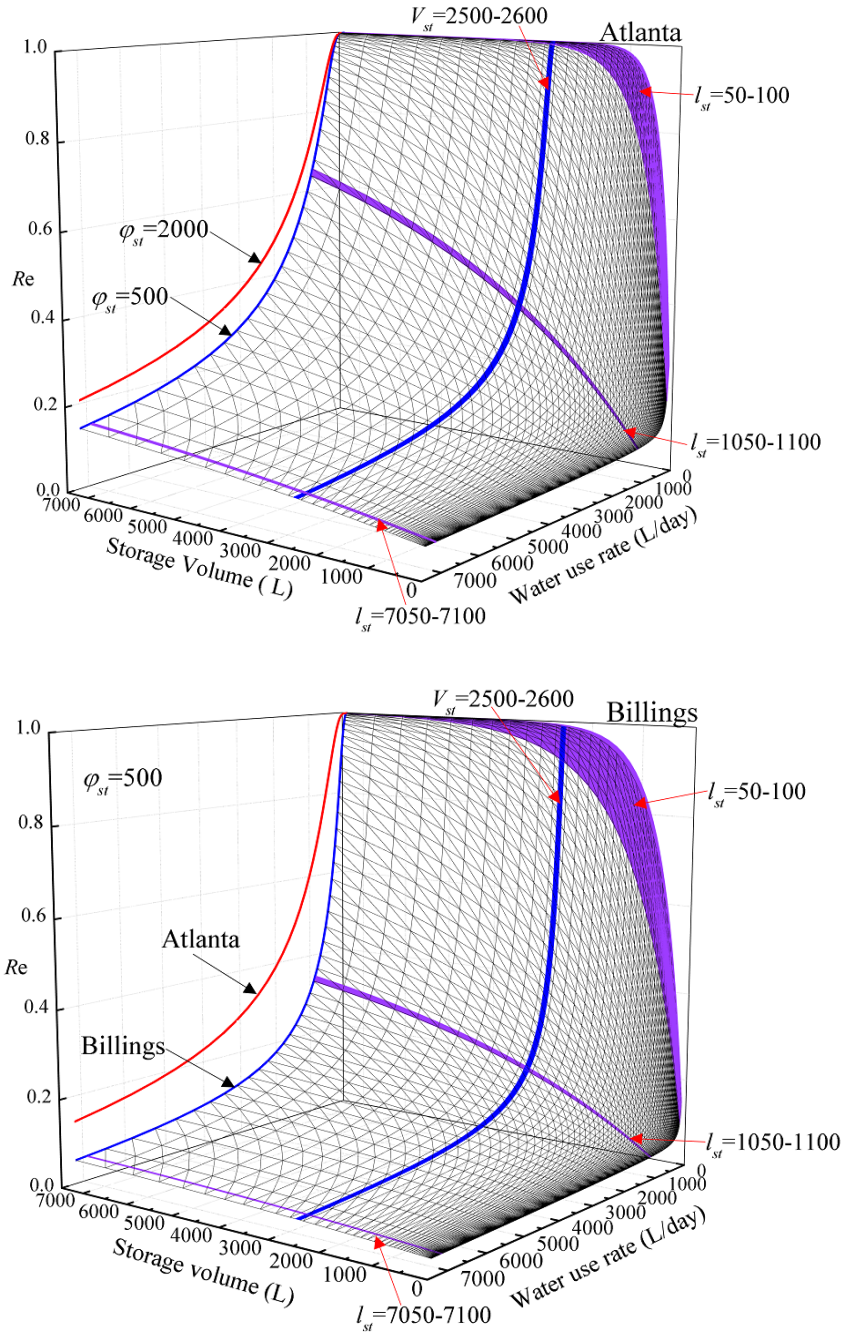

Fig. 3.7 Water supply reliability R_e varying with climate conditions, contributing ratios, storage volumes and water use rates

storage tanks. Meanwhile, the water deficit rate p_0 also changes significantly as the design factors change.

The water supply reliability of RWH systems in Atlanta and Billings are presented in Fig. 3.7. It can be seen that the water supply reliabilities of RWH systems in a humid region (Atlanta) are generally higher than those that can be obtained in an arid region (Billings) with the same system configurations. Fig. 3.7 further highlights that gradual increases of storage tank size and contributing ratio, and decreases of water use rate would both lead to nonlinear increases of R_e. These nonlinearities should be adequately considered in the sizing of RWH systems.

3.5. Concluding Remarks

Runoff reduction and water supply are the two most important benefits of rainwater harvesting (RWH) systems. Based on a stochastic water balance equation, analytical solutions were derived, which can be used for the detailed analysis of the hydrological performance of RWH systems. Two typical water use patterns were considered, and the analytical solutions for both of them were compared with the corresponding continuous simulation results. The analytical solutions are fairly accurate for a wide range of cases with different contributing ratios, storage sizes, and water use rates located in five representative climate regions. Overall, it was demonstrated that this stochastic approach is feasible and reliable in modeling the

long-term water balance of RWH systems. It is worth emphasizing that the presented solutions are valid for RWH systems located in regions where the rainfall series may be approximated as marked Poisson processes.

The analytical solutions relate the stormwater capture efficiency and water supply reliability of RWH systems directly and explicitly to the rainfall conditions, sizes of contributing areas, water collection/conveyance efficiencies, storage tank sizes, and average water use rates. Significant nonlinear dependencies of the system performance on these factors have been observed, and design optimization is therefore necessary to balance the cost and performance. The proposed analytical solutions are accurate, concise, and can be conveniently implemented in computer spreadsheets. They may provide a robust and easy-to-use tool for the performance evaluation and optimum design of RWH systems.

Acknowledgement

This work has been supported by the Natural Sciences and Engineering Research Council of Canada [RGPIN-5112-2016] and the China Scholarship Council [201306220046].

References

Adams, B. J., Papa, F. 2000. Urban Stormwater Management Planning with Analytical Probabilistic Models. John Wiley & Sons, Inc., New York, USA.

Campisano, A., Modica, C. 2012. Optimal sizing of storage tanks for domestic rainwater harvesting in Sicily. Resources, Conservation and Recycling, **63**: 9-16.

Campisano, A., Nie, L. M., Li, P. Y. 2013. Retention performance of domestic rain water harvesting tank under climate change conditions. Applied Mechanics and Materials, **438**: 451-458.

Cox, D., Isham, V. 1986. The virtual waiting-time and related processes. Advances in Applied Probability, **18**: 558-573.

Eagleson, P. S. 1978. Climate, soil, and vegetation: 2. The distribution of annual precipitation derived from observed storm sequences. Water Resources Research, **14**: 713-721.

Fewkes, A. 2000. Modelling the performance of rainwater collection systems: towards a generalised approach. Urban Water, **1**: 323-333.

Fewkes, A., Butler, D. 2000. Simulating the performance of rainwater collection and reuse systems using behavioural models. Building Services Engineering

Research and Technology, **21**: 99-106.

Fewkes, A., Wam, P. 2000. Method of modelling the performance of rainwater collection systems in the United Kingdom. Building Services Engineering Research and Technology, **21**: 257-265.

Gardiner, C. W. 2004. Handbook of Stochastic Methods for Physics, Chemistry and the Natural Sciences (3rd Ed.). Springer, Berlin.

Guo, R., Guo, Y. 2017. Analytical equations for use in the planning of infiltration facilities. Journal of Sustainable Water in the Built Environment: Accepted for publication, August 2017.

Guo, Y. 2016. Stochastic analysis of hydrologic operation of green roofs. Journal of Hydrologic Engineering: 04016016.

Guo, Y., Baetz, B. W. 2007. Sizing of rainwater storage units for green building applications. Journal of Hydrologic Engineering, **12**: 197-205.

Guo, Y., Zhang, S., Liu, S. 2014. Runoff reduction capabilities and irrigation requirements of green roofs. Water Resources Management, **28**: 1363-1378.

Hajani, E., Rahman, A. 2014. Reliability and cost analysis of a rainwater harvesting system in peri-urban regions of Greater Sydney, Australia. Water, **6**: 945-960.

Hanson, L. S., Vogel, R. M., Kirshen, P., Shanahan, P. 2009. Generalized storage-reliability-yield equations for rainwater harvesting systems. World Environmental and Water Resources Congress 2009: Great Rivers: 1-10.

Hassini, S., Guo, Y. 2016. Exponentiality test procedures for large samples of rainfall event characteristics. Journal of Hydrologic Engineering, **21**: 04016003.

Imteaz, M. A., Shanableh, A., Rahman, A., Ahsan, A. 2011. Optimisation of rainwater tank design from large roofs: A case study in Melbourne, Australia. Resources, Conservation and Recycling, **55**: 1022-1029.

Jennings, A. A., Adeel, A. A., Hopkins, A., Litofsky, A. L., Wellstead, S. W. 2012. Rain barrel–urban garden stormwater management performance. Journal of Environmental Engineering, **139**: 757-765.

Jennings, A. A., Berger, M. A., Hale, J. D. 2015. Hydraulic and hydrologic performance of residential rain gardens. Journal of Environmental Engineering, **141**: 04015033.

Jones, M. P., Hunt, W. F. 2010. Performance of rainwater harvesting systems in the southeastern United States. Resources, Conservation and Recycling, **54**: 623-629.

Kim, H., Han, M., Lee, J. Y. 2012. The application of an analytical probabilistic

model for estimating the rainfall–runoff reductions achieved using a rainwater harvesting system. Science of the Total Environment, **424**: 213-218.

Kim, K., Yoo, C. 2009. Hydrological modeling and evaluation of rainwater harvesting facilities: case study on several rainwater harvesting facilities in Korea. Journal of Hydrologic Engineering, **14**: 545-561.

Laio, F., Porporato, A., Ridolfi, L., Rodriguez-Iturbe, I. 2001. Plants in water-controlled ecosystems: active role in hydrologic processes and response to water stress: II. Probabilistic soil moisture dynamics. Advances in Water Resources, **24**: 707-723.

Lee, K. T., Lee, C.-D., Yang, M.-S., Yu, C.-C. 2000. Probabilistic design of storage capacity for rainwater cistern systems. Journal of Agricultural Engineering Research, **77**: 343-348.

Lopes, V. A., Marques, G. F., Dornelles, F., Medellin-Azuara, J. 2017. Performance of rainwater harvesting systems under scenarios of non-potable water demand and roof area typologies using a stochastic approach. Journal of Cleaner Production, **148**: 304-313.

Matos, C., Santos, C., Pereira, S., Bentes, I., Imteaz, M. 2013. Rainwater storage tank sizing: Case study of a commercial building. International Journal of Sustainable Built Environment, **2**: 109-118.

Mun, J. S., Han, M. Y. 2012. Design and operational parameters of a rooftop rainwater harvesting system: definition, sensitivity and verification. Journal of Environmental Management, **93**: 147-153.

NOAA. 2011. 1981-2010 United States Climate Normals. (National Climatic Data Center).

Palla, A., Gnecco, I., Lanza, L. 2011. Non-dimensional design parameters and performance assessment of rainwater harvesting systems. Journal of Hydrology, **401**: 65-76.

Palla, A., Gnecco, I., Lanza, L., La Barbera, P. 2012. Performance analysis of domestic rainwater harvesting systems under various European climate zones. Resources, Conservation and Recycling, **62**: 71-80.

PDEP (Pennsylvania Department of Environmental Protection). 2006. Pennsylvania Stormwater Best Management Practices Manual. Bureau of Watershed management, Harrisburg, PA, USA.

Raghunath, H. M. 2006. Hydrology: Principles, Analysis and Design (2ed Ed.). New Age International (P) Ltd., New Delhi.

Restrepo-Posada, P. J., Eagleson, P. S. 1982. Identification of independent rainstorms. Journal of Hydrology, **55**: 303-319.

Rodríguez-Iturbe, I., Porporato, A. 2005. Ecohydrology of Water-Controlled Ecosystems: Soil Moisture and Plant Dynamics. Cambridge University Press, Cambridge, U.K.

Rodriguez-Iturbe, I., Porporato, A., Ridolfi, L., Isham, V., Coxi, D. 1999. Probabilistic modelling of water balance at a point: the role of climate, soil and vegetation. In: Proceedings of the Royal Society of London A, pp: 3789-3805.

Rossman, L. A. 2015. Storm Water Management Model User's Manual, Version 5.1 (EPA- 600/R-14/413b). National Risk Management Research Laboratory, Office of Research and Development, US Environmental Protection Agency, Cincinnati, OH, U.S.

Sample, D. J., Liu, J., Wang, S. 2012. Evaluating the dual benefits of rainwater harvesting systems using reliability analysis. Journal of Hydrologic Engineering, **18**: 1310-1321.

Santos, C., Taveira-Pinto, F. 2013. Analysis of different criteria to size rainwater storage tanks using detailed methods. Resources, Conservation and Recycling, **71**: 1-6.

Sturm, M., Zimmermann, M., Schütz, K., Urban, W., Hartung, H. 2009. Rainwater harvesting as an alternative water resource in rural sites in central northern Namibia. Physics and Chemistry of the Earth, Parts A/B/C, **34**: 776-785.

Su, M.-D., Lin, C.-H., Chang, L.-F., Kang, J.-L., Lin, M.-C. 2009. A probabilistic approach to rainwater harvesting systems design and evaluation. Resources, Conservation and Recycling, **53**: 393-399.

TRCA and CVCA (Toronto and Region Conservation Authority and Credit Valley Conservation Authority). 2010. Low Impact Development Stormwater Management Planning and Design Guide. Ontario, Canada.

Vaes, G., Berlamont, J. 2001. The effect of rainwater storage tanks on design storms. Urban Water, **3**: 303-307.

Wanielista, M. P., Yousef, Y. A. 1993. Stormwater Management. John Wiley & Sons, New York, USA

Ward, S., Memon, F., Butler, D. 2010. Rainwater harvesting: model-based design evaluation. Water Science and Technology, **61**: 85-96.

Youn, S.-g., Chung, E.-S., Kang, W. G., Sung, J. H. 2012. Probabilistic estimation of the storage capacity of a rainwater harvesting system considering climate change. Resources, Conservation and Recycling, **65**: 136-144.

Zhang, S., Guo, Y. 2013. Analytical probabilistic model for evaluating the hydrologic performance of green roofs. Journal of Hydrologic Engineering, **18**: 19-28.

Zhang, S., Guo, Y. 2013. Explicit equation for estimating storm-water capture efficiency of rain gardens. Journal of Hydrologic Engineering, **18**: 1739-1748.

Zhang, X., Hu, M., Chen, G., Xu, Y. 2012. Urban rainwater utilization and its role in mitigating urban waterlogging problems - a case study in Nanjing, China. Water Resources Management, **26**: 3757-3766.

Zhang, Y., Chen, D., Chen, L., Ashbolt, S. 2009. Potential for rainwater use in high-rise buildings in Australian cities. Journal of Environmental Management, **91**: 222-226.

Chapter 4

Stormwater Capture and Antecedent Moisture Characteristics of Permeable Pavements

Rui Guo, Yiping Guo, and Jun Wang

Abstract: An approach based on individual rainfall events is introduced to mathematically describe the hydrologic response and estimate the stormwater capture efficiency of permeable pavement systems (PPSs). A stochastic model describing the instantaneous dynamic water balance of a PPS is then established; from which, the probability distribution of the antecedent moisture content of the PPS at the beginning of a rainfall event is analytically derived. Based on this probability distribution and the event-based approach, an analytical equation that can be used for estimating the stormwater capture efficiencies of PPSs is also derived. The derived analytical equation is verified by comparing its results with those from continuous simulations for a wide range of PPSs with different sizes and underlying soils, and operating under various climate conditions. Example analyses also illustrate that the antecedent moisture contents of PPSs are usually fairly close to zero, suggesting that PPSs are always almost empty at the start of a rainfall event. The derived analytical equation accounts for many key processes influencing the behaviour and operation of PPSs; it may serve as an easy-to-use

tool that is essential for the preliminary planning and design of PPSs.

Key Words: Permeable pavement systems; Stormwater management; Stormwater capture efficiency; Analytical probabilistic approach; Stochastic approach

4.1 Introduction

Urbanization typically increases impervious surfaces, resulting in greater flood peaks and volumes. Conventional structural stormwater control devices capture storm runoff, and subsequently distribute it to sewer systems or nearby watercourses, which increases the risk of severe downstream flooding and stream channel erosion (Dietz, 2007; Holman-Dodds *et al.*, 2003). Permeable pavement systems (PPSs) emphasizing on-site small-scale runoff control have been constructed as an alternative to traditional impervious pavements for places such as low traffic parking lots, driveways, pedestrian plazas, and walkways. A PPS is usually constructed in permeable soils and consists of two layers: the pavement layer and the storage layer. The surface pavement layer is usually comprised of porous structural pavers and placed on top of the storage layer. The storage layer is filled with uniformly graded coarse aggregate/stones supporting the loading on the pavement layer. Underdrains are usually installed in the storage layer if the local soils are not very permeable. Rainfall falling onto the surface of a PPS and runoff from adjacent impervious areas can pass directly through the surface of the PPS and into the storage layer, which provides temporary storage as water slowly infiltrates into the underlying soils. The sediments and other suspended pollutants in the runoff can be filtered out by the aggregate in the storage layer. PPSs can provide efficient water quality and quantity controls, as they reduce surface runoff

volumes and peak discharges, increase groundwater recharge, and capture pollutants (Ball and Rankin, 2010; Bean *et al.*, 2007b; Collins *et al.*, 2008; Fassman and Blackbourn, 2010).

For urban runoff quality control analysis, the fraction of runoff volume from the drainage area that can be captured by a PPS on a long-term basis, referred to as the stormwater capture efficiency, is required for selecting the most appropriate sizes of PPSs (WEF and ASCE/EWRI 2012) and for evaluating the runoff quality control performance of PPSs with known sizes. The stormwater capture efficiency is also a useful piece of infiltration for urban runoff quantity control analysis. For example, when using the Rational method for estimating peak discharge in storm sewer designs, runoff coefficients are used to represent the runoff generation characteristics of urban areas. The equivalent runoff coefficient values for PPS areas may be determined based on their average runoff generation ratios (i.e., ratios between runoff generated and rainfall received). The runoff generation ratio of a PPS area is simply one minus its stormwater capture efficiency. Additionally, in calculating the stormwater capture efficiencies for individual storms, the volume of water retained in the PPS when a rainfall event starts, i.e., the antecedent moisture content of the PPS, needs to be known. The information about the antecedent moisture contents of a PPS may also be used for urban runoff quantity control analysis in determing the appropriate equivalent curve numbers for the PPS and its

service areas. These equivalent curve numbers can be used in the NRCS curve-number method for the estimation of design runoff volumes or peak discharges needed in flood control studies (Bean *et al.*, 2007a; Leming *et al.*, 2007).

Many hydrological models using a specified design storm or continuous rainfall sequences as input have been developed to examine the performance of PPSs. Hydrological models using a specified rainfall event as input provide only the performance information in response to the individual rainfall event, and cannot provide the required long-term average stormwater capture efficiency of PPSs. Besides, in such models, the antecedent moisture condition of the PPS prior to the occurrence of the input rainfall event is usually not properly considered. Consequently, continuous simulation modeling (Ahiablame *et al.*, 2012; James and von Langsdorf, 2003) using a continuous rainfall sequence as input is more desirable. The long-term average stormwater capture efficiency and the possible antecedent moisture conditions prior to individual rainfall events can both be obtained from continuous simulation results. However, continuous simulations and statistical analysis of simulation results may be too time-consuming for use in individual small-scale stormwater management design cases. Therefore, a reliable and easy-to-use method for evaluating the long-term average stormwater capture efficiency and the statistics of the antecedent moisture conditions of PPSs needs to be developed.

An analytical probabilistic approach, which was developed as a computationally efficient alternative to continuous simulation for urban stormwater management purposes, has been applied to evaluate the long-term average performance of stormwater control facilities (Adams and Bontje, 1984; Bacchi *et al.*, 2008; Balistrocchi *et al.*, 2009; Howard, 1976; Loganathan and Delleur, 1984) and low impact developments practices (LIDs) (Guo and Baetz, 2007; Guo *et al.*, 2014; Zhang and Guo, 2012a; Zhang and Guo, 2012b; Zhang and Guo, 2014a; Zhang and Guo, 2014b). In these previous studies, simplifying assumptions about the moisture condition preceding a random rainfall event or preceding the dry period before the occurrence of a random rainfall event were usually made. Based on these assumptions, analytical equations for estimating the hydrologic performances of urban stormwater management facilities are then derived. Some of the previous simplifying assumptions are not entirely realistic under special circlmustances (Adams and Papa, 2000), therefore, the previously derived analytical equations may not be accurate enough for some extreme cases.

This study also applies the analytical probabilistic approach to model the hydrologic processes involved in the operation of PPSs; but instead of making simplifying assumptions, a stochastic method is used to analytically derive the probability density function (PDF) and the expected value of the antecedent moisture content of a PPS. Use of the expected value of the antecedent moisture

content increases the accuracy of the estimated stormwater capture efficiency.

4.2 Event-Based Analytical Probabilistic Approach for Estimating Stormwater Capture Efficiency

4.2.1 Probabilistic Models of Rainfall Event Characteristics

The foundation of the analytical probabilistic approach is its concise and mathematical representation of the probabilistic nature of local rainfall characteristics. The local rainfall characteristics are usually represented well by the continuous precipitation data collected at the location of interest, if the data series is long enough. This continuous precipitation data series can be separated into discrete rainfall events by selecting a minimum inter-event time (MIET) first. MIET is defined as the minimum number of dry hours between two rainfall events. Two consecutive rainfall episodes are considered as belonging to the same rainfall event if the dry time between them is less than the adopted MIET; otherwise, they are considered as belonging to two separate events. With an appropriately selected MIET, the discrete rainfall events can be considered as statistically independent (Adams and Papa, 2000). Each rainfall event can be characterized by its rainfall volume (v), rainfall duration (u), and inter-event time (b) preceding the occurrence of the next rainfall event. The random variables v, u, and b are usually assumed to be statistically independent. These three rainfall event characteristics

are attested to follow exponential distributions at many different locations (Adams *et al.*, 1986; Guo, 2001; Guo and Adams, 1998; Howard, 1976). Their PDFs are given in Table 4.1, where $\bar{v}$, $\bar{u}$, and $\bar{b}$ are the mean rainfall event volume (mm), mean rainfall event duration (h), and mean inter-event time (h), respectively.

Table 4.1 Probability Density Functions of Rainfall Characteristics

Rainfall Characteristic	Exponential PDF	Distribution parameter
Rainfall Event Volume v, mm	$f(v) = \zeta e^{-\zeta v}, \quad v > 0$	$\zeta = 1/\bar{v}$
Rainfall Event Duration u, h	$f(t) = \lambda e^{-\lambda u}, \quad u > 0$	$\lambda = 1/\bar{u}$
Rainfall Inter-event Time b, h	$f(b) = \psi e^{-\psi b}, \quad b > 0$	$\psi = 1/\bar{b}$

As an example, the 56-year (1945–2000) non-winter (April through November) historical rainfall record of the New Durham station in New Durham, New Hampshire, USA [Data were obtained from the National Climate Data Center (NCDC)] was tested in this study. Guo and Baetz (2007) and Hassini and Guo (2016) described a series of statistical tests that can be used to determine the most appropriate MIET. After applying some of these tests, it was found that an MIET of 6 h is appropriate for this location. Use of slightly longer or shorter MIET is also acceptable and will result in similar results. Strict statistical tests were therefore not conducted and an MIET of 6 h is recommended and used for this location. With an MIET of 6 h, the continuous rainfall record from New Durham was isolated into separate individual rainfall events, and the histograms of the

rainfall events' v, u, and b are shown in Fig. 4.1. The exponential PDFs of rainfall event characteristics were fitted to their respective empirical distributions and are shown in Table 4.2.

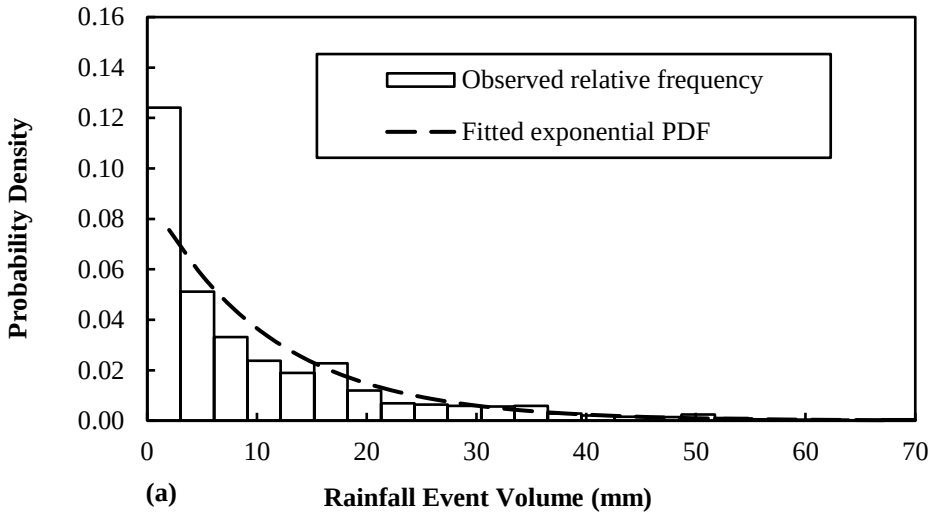

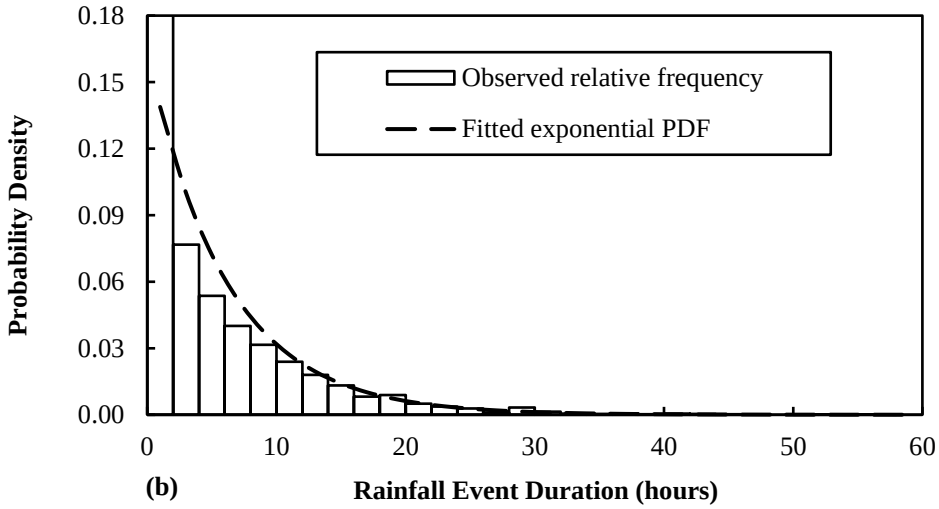

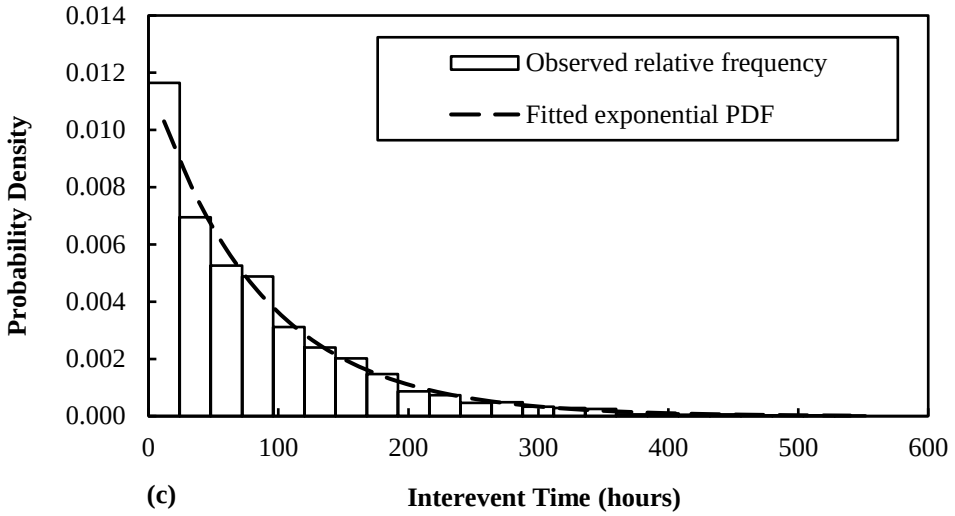

Fig. 4.1. Frequency distributions of the rainfall event (a) volume; (b) duration; and (c) inter-event time at New Durham, New Hampshire, USA (MIET = 6 h)

Table 4.2. Rainfall and other Basic Climatic Statistics of Four Test Locations

Station	Data series		MIET	$\bar{v} = \zeta^{-1}$	$\bar{t} = \lambda^{-1}$	$\bar{b} = \psi^{-1}$	*ET*	Annual precipitation (NOAA, 2011)
			h	mm	h	h	mm/ h	mm
Atlanta, GA	1945-2005	Jan.-Dec.	8	15.68	9.18	101.84	0.116	1236
Charlotte, NC	1945-2005	Mar.-Nov.	12	17.7	11.6	134.7	0.1	1057
New Durham, NH	1945-2000	Apr.-Oct.	6	11.03	6.1	85.5	0.11	879
Flagstaff, AZ	1947-2005	Jan.-Dec.	12	11.63	13.54	170.75	0.18	555

Note: Rainfall and evapotranspiration statistics for Atlanta, Charlotte, and Flagstaff were presented in Guo *et al.* (2014), Zhang and Guo (2012), and Zhang and Guo (2012) respectively; *ET* stands for average potential evapotranspiration rate.

4.2.2 Event-Based Water Balance Equation and Stormwater Capture Efficiency

The pavement layer and the fill materials of the storage layer usually have high permeabilities (Bean, 2005). Therefore, it can be assumed that stormwater can infiltrate into a PPS and reach the bottom almost instantaneously when the PPS is not filled. Thus a PPS is usually modeled as a storage space underlined with permeable soils (Martin and Kaye, 2014; Schwartz, 2010; Zhang and Guo, 2014a). For a PPS without underdrains, the storage spaces consist of the void portions of the pavement and storage layers; and the total storage capacity (S_m) can be calculated as $S_m = S_d + \frac{n_p}{1+n_p} h_p + \frac{n_s}{1+n_s} h_s$, where S_d is the surface depression storage of the pavement layer, expressed in mm of water over the surface area of the pavement; n_p and n_s (dimensionless) are the void ratios of the pavement and storage layer, respectively; h_p is the depth (in mm) of the pavement layer; and h_s is referred to as the effective depth (in mm) of the storage layer and is equal to the maximum physical storage depth for this type of PPSs. For a PPS with underdrains, the drainage capacity of the underdrain pipes is extremely large compared with the underlying soil's infiltration capacity; therefore, water can be assumed to be drained right away whenever it reaches a level that is slightly above the bottom of the underdrain pipe, thus the effective storage space is the void space of the storage

layer below the bottom of the underdrains. The storage capacity for cases with underdrains can therefore be calculated as $S_m = S_d + \frac{n_s}{1+n_s} h_s$, where h_s equals the depth of the storage layer that is below the bottom of the underdrains.

The hydrologic operation associated with a PPS includes storage of the incoming rainfall while water slowly infiltrates into the native soils, and overflow may occur if the PPS is filled. The event-based water balance equation for a PPS resulting from the input of a random rainfall event can be expressed as

$$v_o = \begin{cases} v_i - F + S_i - S_m, & v_i > F - S_i + S_m \\ 0, & v_i \le F - S_i + S_m \end{cases} \tag{4.1}$$

where v_i is the volume of inflow into the PPS resulting from this random rainfall event; v_o is the volume of overflow from the PPS during this random event; F is the volume of water that is infiltrated into the underlying soils of the PPS during the entire duration of this event; S_i is the volume of water retained in the PPS at the beginning of this random event, S_i can be regarded as the antecedent moisture content of the PPS. Evaporation during a rainfall event is not considered because evaporation rate is very small compared with the rate of infiltration into the native soils (Nemirovsky *et al.*, 2012). Analyzing event-by-event over a long-term or probabilistically for a random rainfall event, the long-term average, i.e., the expected values of v_i and v_o can be obtained. Then the long-term average

stormwater capture efficiency of the PPS (denoted as C_e) can be calculated as

$$C_e = \frac{E(v_i) - E(v_o)}{E(v_i)} \tag{4.2}$$

where $E(v_i)$ and $E(v_o)$ are respectively the expected values of v_i and v_o per rainfall event.

4.2.3 Event-Based Inflow Volume and Infiltration Volume

The volume of inflow v_i entering a PPS usually includes two parts: (1) surface runoff generated from adjacent areas, and (2) rain water directly falling onto the PPS surface. The contributing catchments for a PPS are usually 100% impervious (PDEP, 2006; TRCA and CVCA, 2010) with small depressions (e.g., from 0 to 3 mm) (WEF and ASCE/EWRI, 2012) . Surface runoff generates after the depressions are filled. To simplify derivations, the water held in these depressions are assumed to be completely evaporated during dry periods and the depression storage capacity (S_{dc}) is always 100% available when a rainfall event starts. Also for simplicity, the surface runoff is assumed to flow into the PPS as soon as it starts to rain and end when it stops raining, i.e., the time of concentration of the adjacent impervious area is negligible. This is justified because the contributing areas are usually very small and their times of concentration are usually very short when compared with u and b . With the ratio between the

contributing area and the surface area of a PPS defined as the area ratio (denoted as R_a), the inflow (v_i) that enters the PPS per rainfall event can be calculated as

$$v_i = \begin{cases} v, & v \le S_{dc} \\ v + R_a(v - S_{dc}), & v > S_{dc} \end{cases} \tag{4.3}$$

Based on the PDF of v and the functional relationship between v_i and v as described by Eq. (4.3), the expected value of the inflow volume can be derived as

$$E(v_i) = \int_0^{S_{dc}} v\zeta e^{-\zeta v} dv + \int_{S_{dc}}^{+\infty} [v + R_a(v - S_{dc})]\zeta e^{-\zeta v} dv = \frac{1}{\zeta}(1 + R_a e^{-\zeta S_{dc}}) \tag{4.4}$$

Particularly, for a PPS not receiving runoff from any adjacent areas, the area ratio is zero ($R_a = 0$), and the inflow from a rainfall event would be simply v and its expected value would be $1/\zeta$. For contributing areas without surface depressions (i.e., $S_{dc} = 0$), the inflow from a rainfall event can be calculated as $(1 + R_a)v$ and its expected value would be $(1 + R_a)/\zeta$.

Only infiltration through the bottom of a PPS needs to be considered, because percolation through the sides of a PPS is really small when compared with that through the bottom of the PPS. The rate of infiltration into the native soils through the bottom during a rainfall event is usually assumed to be constant, equaling the saturated hydraulic conductivity of the native soils (denoted as f_c, in mm/h) (Martin and Kaye, 2014; Schwartz, 2010). It is conservative and justified because

the native soils are underneath the storage layer, thus, after a rainfall event, its infiltration capacity needs a much longer time to recover than soils exposed to the air (Martin and Kaye, 2014). Besides, results obtained from this study are intended for use in planning-level analysis or preliminary design, where infiltration is usually assumed to be occurring at constant rates. The total volume infiltrated during a rainfall event can therefore be calculated as

$$F = f_c u \tag{4.5}$$

where u is the duration of the event.

4.3 Stochastic Analysis for Estimating Antecedent Moisture Conditions

The water retained in the PPS at the end of a rainfall event will be evaporated and infiltrated during the following dry period. The response of the PPS to a wet-dry cycle varies depending on the preceding conditions. The preceding conditions are random and determines the value of S_i in Eq. (4.1), therefore, S_i in Eq. (4.1) should be treated as a random variable. As shown in Eqs. (4.3) and (4.5), v_i and F in Eq. (4.1) are functions of v and u of the random rainfall event and therefore are random variables as well. If the expected value of S_i can be analytically expressed, then the derived probability distribution theory (Benjamin and Cornell, 1970) can be used to obtain the PDF of v_o and the expected values of v_o based on Eq. (4.1). The PDF of S_i and its expected value are therefore derived first.

4.3.1 Dynamic Water Balance Equation of a PPS

To derive the PDF of S_i, the dynamic water balance equation, which describes how the water level in the storage space of a PPS changes with time, needs to be formulated and solved. Treating a PPS as a storage unit with inflow from infiltration through the surface of the porous pavement layer and outflow in the form of evaporation from the stored water and deep infiltration through the bottom of the storage layer, the dynamic water balance equation can be expressed as

$$S_m \frac{ds}{dt} = I(s,t) - O(s) \tag{4.6}$$

where s is the fraction of the PPS's storage capacity S_m that is occupied by water at an instant of time t (s is therefore a dimensionless variable changing from 0 to 1 and S_m is a constant); $I(s,t)$ represents the rate of net inflow through the surface pavement layer of the PPS into its storage layer at time t when s fraction of the PPS's storage space is filled with water; and $O(s)$ is the rate of outflow from the PPS (including evaporation and deep infiltration) at time t. Since daily and seasonal variations of evaporation and infiltration are not considered, the rate of outflow is a function of s only. The event-based water balance equation [i.e., Eq. (4.1)] is written for a lumped individual random rainfall event, while Eq. (4.6) is written for a random instant of time. At an instant of time, the inflow to a PPS is random, i.e., $I(s,t)$ is a random function of time t. Therefore a time series of $I(s,t)$ can be

viewed as a realization of a stochastic process. Eq. (4.6) is thus a stochastic differential equation.

4.3.2 Rainfall Modelling

Average inter-event time is usually much longer than average rainfall event duration, therefore previous research has shown that rainfall events can be considered as occurring at instant times, and the arrival of rainfall events can be treated as a Poisson process (Botter *et al.*, 2007; Laio *et al.*, 2001; Porporato *et al.*, 2004; Rodriguez-Iturbe *et al.*, 1999). According to the definitions introduced in the event-based approach for analyzing rainfall characteristics, the inter-arrival time of rainfall events can be calculated as $(u+b)$. As Eagleson (1978) pointed out that, when u and b are independent and are exponentially distributed with their distribution parameters meeting the requirement that $\psi/\lambda \ll 1$, the frequency distribution of $(u+b)$ (i.e., the inter-arrival time) approaches exponential as well, which is required for a Poisson process. For all the tested locations, as shown in Table 4.2, the distributions of u and b fit exponential with $\psi/\lambda \ll 1$, thus the inter-arrival time $(u+b)$ can be approximated as exponentially distributed. The exponential distribution parameter value for $(u+b)$ is $(1/\psi+1/\lambda)$ and the storm arrival rate (denoted as μ') is $[1/(1/\psi+1/\lambda)]$. The same exponential distribution of rainfall event volume is adopted in both the event-based analytical probabilistic

approach and the rainfall modelling for the solution of Eq. (4.6). This way the input rainfall series can be represented as a marked Possion process with the storm arrival rate of μ' and an ancillary random variable v (storm volume) following an exponential distribution.

4.3.3 Net Inflow Process

Lumping the contributing area and the surface area of a PPS together, the total inflow into the PPS as a result of a rainfall event with volume v can be calculated as

$$v_i = (1+R_a)(v - S_{di}') \tag{4.7}$$

where S_{di}' is the area-averaged depression storage and it equals $R_a S_{dc}/(R_a+1)$. This is approximately the same as what is calculated in Eq. (4.3), but simplified so that it can be viewed as a fraction of rainfall falling on the lumped area which is $(1+R_a)$ times the pavement area and the lumped area has an area-averaged depression storage of S_{di}'. This also implies that only rainfall events with volumes larger than S_{di}' would generate inflow. Therefore, the process of inflow into a PPS is comprised of rainfall events of the input rainfall Poisson process but with rainfall events having volumes less than or equal to S_{di}' removed. According to the statistical properties of the Poisson process, the PPSs' inflow process turns into a

new marked Poisson process (Rodriguez-Iturbe 1999; Laio 2001) with an arrival rate of $\mu = \mu' \int_{S_{di}'}^{+\infty} f(v)dv = \mu' e^{-\zeta S_{di}'}$. Also based on Eq. (4.7), the PDF of the inflow volume per inflow event is $f(v_i) = \zeta' e^{-\zeta' v_i}$, where $v_i > 0$ and $\zeta' = \zeta/(R_a + 1)$. Particularly, when $R_a = 0$, S_{di}' would be zero as well, the rate of the inflow Poisson process would be μ' and the PDF of inflow would be $\zeta e^{-\zeta v_i}$ with $v_i > 0$, which is the same as the original input rainfall Poisson process. This is true because when $R_a = 0$, the inflow to the PPS is exactly the same as the original rainfall input. When $S_{dc} = 0$, S_{di}' would be zero too, the rate of the inflow Poisson process would be μ which is equal to μ' and the PDF of inflow volume per inflow event would be $f(v_i) = \zeta' e^{-\zeta' v_i}$. This is true because when $S_{dc} = 0$, the inflow arrival rate is the same as the original rainfall input but the volume of each inflow event is $(1 + R_a)$ times the corresponding input rainfall event volume. These verifications for special cases confirm that the approximate way of calculating v_i using Eq. (4.7) is acceptable.

To simplify equations and their solutions, normalized and dimensionless quantities are used. The inflow volume is normalized as $r = v_i / S_m$ and the PDF of r is

$$f(r) = \gamma e^{-\gamma r}, \quad r > 0 \tag{4.8}$$

where $\gamma = \zeta' S_m$. The marked Poisson process representing the total inflow $In(t)$ can be expressed as a temporal sequence as

$$In(t) = \sum_i r_i \delta(t - t_i) \tag{4.9}$$

where $\delta(\cdot)$ is the Dirac delta function, $\{r_i, i = 1, 2, 3, ...\}$ is the sequence of random inflow, each individual r_i follows the same PDF as described by Eq. (4.8) and is statistically independent of each other; t is the current time; and $\{t_i, i = 1, 2, 3, ...\}$ is the sequence of times when individual inflow occurs.

When it rains, if there is enough storage in the PPS to accommodate the inflow, the whole inflow can be infiltrated into the PPS. When the inflow exceeds the available storage, the volume of infiltration from the inflow equals the available storage and the excess water becomes overflow. The PDF of the net inflow volume *y* per inflow event can therefore be expressed as

$$f(y|s) = \begin{cases} \gamma e^{-\gamma y}, & 0 < y < (1-s) \\ e^{-\gamma(1-s)} \delta(y - 1 + s), & y = (1-s) \end{cases} \tag{4.10}$$

In Eq. (4.10), the probability mass at $y = (1-s)$ represents the probability that the system is filled when water stored in the system at the start of a rainfall event is equal to s. Similar to Eq. (4.9), the normalized net inflow, $i(s,t)$, which is equal

to $I(s,t)/S_m$, can be expressed as

$$i(s,t) = I(s,t)/S_m = \sum_i y_i \delta(t - t_i) \tag{4.11}$$

where $\{y_i, i = 1,2,3,...\}$ is the sequence of random net inflow and is statistically independent of each other. Since the net inflow at an instant of time t is also dependent on s, i.e., the fraction of storage space occupied by water at that time, it is denoted as $i(s,t)$.

4.3.4 Outflow Rate

Since water captured in the PPS can percolate into native soils (deep infiltration) and evaporate during inter-arrival periods, deep infiltration and evaporation can be considered as two components of outflow from the PPS. Using the same constant infiltration and evaporation models as described earlier and denoting the normalized rate of the infiltration and evaporation $(E + f_c)/S_m$ as η, the normalized outflow from the PPS can be expressed as

$$\rho(s) = O(s)/S_m = \begin{cases} 0, & s = 0 \\ \eta, & s > 0 \end{cases} \tag{4.12}$$

4.3.5 Analytical Solution of the Dynamic Water Balance Equation

Since $i(s,t)$ is a stochastic input coming from the marked Poisson process representing the random occurrence of net inflows with random magnitudes, Eq.

(4.6) is therefore a stochastic differential equation. The solution S from Eq. (4.6) as a function of time [i.e., $s(t)$ with t taking on values from zero onward and $s(0)$ representing the initial condition of the PPS] is therefore also a stochastic process. As $s(t)$ is driven by a marked Poisson process, $s(t)$ solved from Eq. (4.6) is a Markov process with jumps and drifts (Gardiner, 2004).

Rodriguez-Iturbe *et al.* (1999) and Rodríguez-Iturbe and Porporato (2005) established a dynamic water balance equation similar to Eq. (4.6) when studying the ecohydrology of water-controlled ecosystems and derived the Chapman-Kolmogorov forward equations of the Markov process governed by an equation essentially the same as Eq. (4.6). The Chapman-Kolmogorov forward equations of a Markov process relate the state (in this case, the state is represented by S) probability distributions at different times (Gardiner, 2004). For Eq. (4.6) and its related $I(s,t)$ and $O(s)$ functions, the corresponding Chapman-Kolmogorov forward equations are

$$\frac{\partial}{\partial t}p(s,t)=\eta\frac{\partial}{\partial s}p(s,t)-\mu p(s,t)+\mu\int_0^s p(z,t)f[(s-z)|z]dz+\mu p_0(t)f(s|0) \quad (4.13)$$

$$\frac{\partial}{\partial t}p_0(t)=-\mu p_0(t)+\eta p(0,t) \quad (4.14)$$

where $f(s|0)$ and $f[(s-z)|z]$ are both the conditional probability distribution as expressed in Eq. (4.10), z is the dummy variable of integration; $p(s,t)$ is the PDF

of s at time t; $p_0(t)$ is the probability of having $s=0$ at time t; and $p(0,t)=\lim_{s\to 0} p(s,t)$. Here it can be seen that the probability distribution of s at a specific time t is comprised of two parts: a discrete point at $s=0$ with a probability mass $p_0(t)$ and a continuous range of $s>0$ with a PDF $p(s,t)$. $p_0(t)$ and $p(0,t)$ are therefore different. Two equations [i.e., Eqs. (4.13) and (4.14)] are required to solve for the two parts.

Given stationary climate conditions, a steady state operation condition of a PPS will soon be reached after initiation. Steady state means that, although s still changes randomly with time, the PDF of s does not change with time anymore, and the time series of s can be described as a strictly stationary stochastic process. For the planning and design of a PPS, only its steady-state operation condition is of interest; therefore, only the steady state solutions of Eqs. (4.13) and (4.14) are sought here. The steady state solutions can be obtained by setting the left-hand-sides of Eqs. (4.13) and (4.14) to zero, while replacing $p(s,t)$ with $p(s)$, and replacing $p_0(t)$ with p_0:

$$\eta \frac{\partial}{\partial s} p(s) - \mu p(s) + \mu \int_0^s p(z) f[(s-z)\,|\,z]dz + \mu p_0 f(s\,|\,0) = 0 \tag{4.15}$$

$$-\mu p_0 + \eta p(0) = 0 \tag{4.16}$$

Eqs. (4.15) and (4.16) constitute a set of integro-differential equations. In

these two equations, p_0 is a probability mass whereas $p(0)$ is the value of the PDF $p(s)$ when s approaches zero. Substituting Eq. (4.10) for $f(y|s)$, multiplying both sides by $e^{\gamma s}$, differentiating with respect to s, and then dividing every term by $e^{\gamma s}/\gamma$, Eq. (4.15) is transformed to a simple differential equation:

$$\frac{1}{\gamma}\frac{d^2}{ds^2}p(s)+(1-\alpha)\frac{d}{ds}p(s)=0$$

where $\alpha=\mu/\gamma\eta$. Depending on whether α is equal to one or not, the general solution to the above equation is different. For both cases, the general solution of $p(s)$ based on the above equation can be obtained and the value of $p(0)$ can also be obtained since $p(0)=\lim_{s\to 0}p(s)$. Substituting the expression of $p(0)$ into Eq. (4.16), p_0 can be obtained as well. Substituting the general solutions of $p(s)$ and p_0 back into Eq. (4.15) for further verification and determination of some of the integration constants, the resulting general solutions of Eqs. (4.15) and (4.16) were found to be

$$p(s)=\begin{cases} C_1e^{\gamma(\alpha-1)s}+\dfrac{\eta}{\mu}C_1\delta(s), & 0\le s\le 1 \text{ and } \alpha\neq 1 \\ C_2+\dfrac{\eta}{\mu}C_2\delta(s), & 0\le s\le 1 \text{ and } \alpha=1 \end{cases}$$

where C_1 and C_2 are the remaining integration constants. It is noted here that the general solutions of Eqs. (4.15) and (4.16) are different for cases with $\alpha=1$. In the above solutions, use of the Dirac delta function eliminates the need to write the

probability mass at $s=0$ (i.e., p_0) separately. The values of C_1 and C_2 can be determined by satisfying the requirement that $p_0+\int_0^1 p(s)ds=1$, i.e., the total probability combining the discrete portion ($s=0$) and continuous portion ($0<s\le 1$) has to be one. C_1 and C_2 can thus be determined and the solution of Eqs. (4.15) and (4.16) can then be expressed as

$$p(s)=\begin{cases}\dfrac{\alpha-1}{\alpha e^{\gamma(\alpha-1)}-1}e^{\gamma(\alpha-1)s}+\dfrac{\alpha-1}{\alpha e^{\gamma(\alpha-1)}-1}\delta(s), & 0\le s\le 1 \text{ and } \alpha\ne 1\\ \dfrac{\gamma}{1+\gamma}+\dfrac{1}{1+\gamma}\delta(s), & 0\le s\le 1 \text{ and } \alpha=1\end{cases} \tag{4.17}$$

Eq. (4.17) also shows that depending on whether α equals one or not, the probability distribution of s is different. As a special case, when $\alpha=1$, the probability distribution of s comprises a continuous part with a uniform density of $\gamma/(1+\gamma)$. With $\gamma=\zeta' S_m$ and $\eta=(E+f_c)/S_m$, α can also be expressed as $\mu/[\zeta'(E+f_c)]$, in which $1/\zeta'$ is the average inflow volume into the PPS per rainfall event, $(E+f_c)/\mu$ represents the average outflow volume per wet-dry cycle, thus α (i.e., $[1/\zeta']/[(E+f_c)/\mu]$) is the ratio between the average inflow to and outflow from a PPS per wet-dry cycle. Whether α equals one or not depends on the local climate conditions (rainfall volume, rainfall duration, dry periods, and evaporation rates) and PPS characteristics (area ratio and deep infiltration rates). Although in actual applications, the chances of having α exactly equal to one are

almost negligible, to be mathematically rigorous, the solution for cases with $\alpha = 1$ is included here as well.

In the above-described stochastic model, s represents the storage level of the PPS at a random point in time, which can be the time when a rainfall event starts. The random variable S_i (i.e., the antecedent moisture content of the PPS) as required in Eq. (4.1) can therefore be simply calculated as ($s \cdot S_m$) with s following the PDF described in Eq. (4.17). The expected value of s (denoted as $\langle s \rangle$) can be calculated as $\langle s \rangle = \int_0^1 sp(s)ds$, carrying out the integration the following is obtained:

$$\langle s \rangle = \begin{cases} \dfrac{\alpha\gamma e^{\gamma(\alpha-1)s}+1}{\alpha\gamma e^{\gamma(\alpha-1)}-\gamma} - \dfrac{1}{\gamma(\alpha-1)}, & \alpha \neq 1 \\ \dfrac{\gamma}{1+\gamma}, & \alpha = 1 \end{cases} \tag{4.18}$$

$\langle s \rangle$ can be treated as the long-term average normalized antecedent moisture content. The long-term average value of S_i can be simply calculated as $\langle s \rangle S_m$, and in the event-based water balance equation [i.e., Eq. (4.1)], S_i may be replaced by $\langle s \rangle S_m$, the resulting equation will provide a more accurate approximation of the long-term average water balance.

4.3.6 Long-Term Average Stormwater Capture Efficiency

As shown in Eq. (4.3), for small rainfall events with $v \leq S_{dc}$, the inflow is v

and it can be safely assumed that no overflow would be generated from the PPS for such small rainfall events. Thus, only the part with $v > S_{dc}$ in Eq. (4.3) is substituted into Eq. (4.1), the event-based water balance equation. This way the v_i that will be used in Eq. (4.1) is expressed as

$$v_i = v + R_a(v - S_{dc}) = (R_a + 1)v - R_a S_{dc} \tag{4.19}$$

Substituting Eq. (4.19) for v_i, Eq. (4.5) for F, and $\langle s \rangle S_m$ for S_i into Eq. (4.1), the event-based water balance equation becomes

$$v_o = \begin{cases} (R_a + 1)v - R_a S_{dc} - f_c t - (1 - \langle s_i \rangle)S_m, & v > \dfrac{R_a S_{dc} + f_c t + (1 - \langle s \rangle)S_m}{R_a + 1} \\ 0, & \text{otherwise} \end{cases} \tag{4.20}$$

The expected value of overflow v_o can therefore be derived as

$$E(v_o) = \int_{t=0}^{+\infty}\int_{v=0}^{+\infty} v_o \zeta e^{-\zeta v} \lambda e^{-\lambda t} dv dt = \frac{1}{\zeta}\frac{(R_a + 1)\lambda}{\lambda + \frac{\zeta}{R_a + 1} f_c} e^{-\frac{\zeta}{R_a + 1}\alpha S_{dc} - \frac{\zeta}{R_a + 1}(1 - \langle s \rangle)S_m} \tag{4.21}$$

By substituting $E(v_i)$ as expressed in Eq. (4.4) and $E(v_o)$ as expressed in Eq. (4.21) into Eq. (4.2), the long-term average stormwater capture efficiency of a PPS can be determined as

$$C_e = 1 - \frac{(R_a + 1)\lambda}{(1 + R_a e^{-\zeta S_{dc}})(\lambda + \frac{\zeta}{R_a + 1} f_c)} e^{-\frac{\zeta}{R_a + 1} R_a S_{dc} - \frac{\zeta}{R_a + 1}(1 - \langle s \rangle)S_m} \tag{4.22}$$

4.4 Verification of the Analytical Results

4.4.1 Stormwater Capture Efficiency

Eq. (4.22) can be used to conveniently estimate the stormwater capture efficiencies of PPSs. Several assumptions were made in its derivation. In applying the analytical probabilistic model to describe the hydrologic processes involved in the operation of a PPS, rainfall event characteristics (i.e., rainfall event volume, duration, and inter-event time) were assumed to be statistically independent and exponentially distributed. In adopting the stochastic approach to estimate the antecedent moisture content of a PPS, it was assumed that the rainfall event arrivals are Poisson-distributed, each rainfall event is virtually instantaneous, and individual rainfall event volumes follow the same exponential distribution as used in the analytical probabilistic model. To verify the accuracy of the derived analytical expressions and validate the simplifying assumptions, results calculated using the analytical equations are compared to those determined from continuous simulations. A set of continuous simulations using the United States Environmental Protection Agency's Storm Water Management Model Version 5.1 (SWMM) (Rossman, 2015), which does not require similar simplifying assumptions (Daubney, 2014; Zhang and Guo, 2014a), were conducted.

Some jurisdictions specified that the depth of the storage layer should be

limited in the range from 100 mm to 400 mm and the area ratio should be less than 1.5 (e.g., TRCA and CVCA, 2010; Schueler and Claytor, 2000). PPSs of Charlotte, NC in soils with different permeabilities, varying storage layer depth, and varying area ratios are modeled with results shown in Fig. 4.2. Some other jurisdictions, such as PDEP (2006), specified that the upper limit for storage layer depth can be expanded to 900 mm and the area ratio can be expanded to 5. To cover more possibilities, storage layer depths ranging from 100 mm to 900 mm and area ratios ranging from 0 to 5 were also simulated. Underlying soils usually have a hydraulic conductivity ranging from 2.54 mm/h to 254 mm/h (PDEP 2006). Thus, representative sand, sandy loam, and loam soils with infiltration rates of 36 mm/h, 10.9 mm/h, and 2.5 mm/h, respectively, are used as surrogates to represent highly

Table 4.3 Parameters Used in the LID-SWMM Simulations

Contributing Catchment	Area		0 – 0.5 ha
	Imperviousness		100%
	Depression Storage		2 mm
Permeable Pavement System	Area		0.1 ha
	Pavement Layer	Depression Storage	1 mm
		Thickness	100 mm
		Void Ratio	0.165
		Permeability	254 mm/h
	Storage Layer	Void Ratio	0.625
		Thickness	100 – 900 mm
	Drainage Layer	Drain Coefficient	1000
		Drain Exponent	0.5
		Drain Offset Height	0 - 450 mm

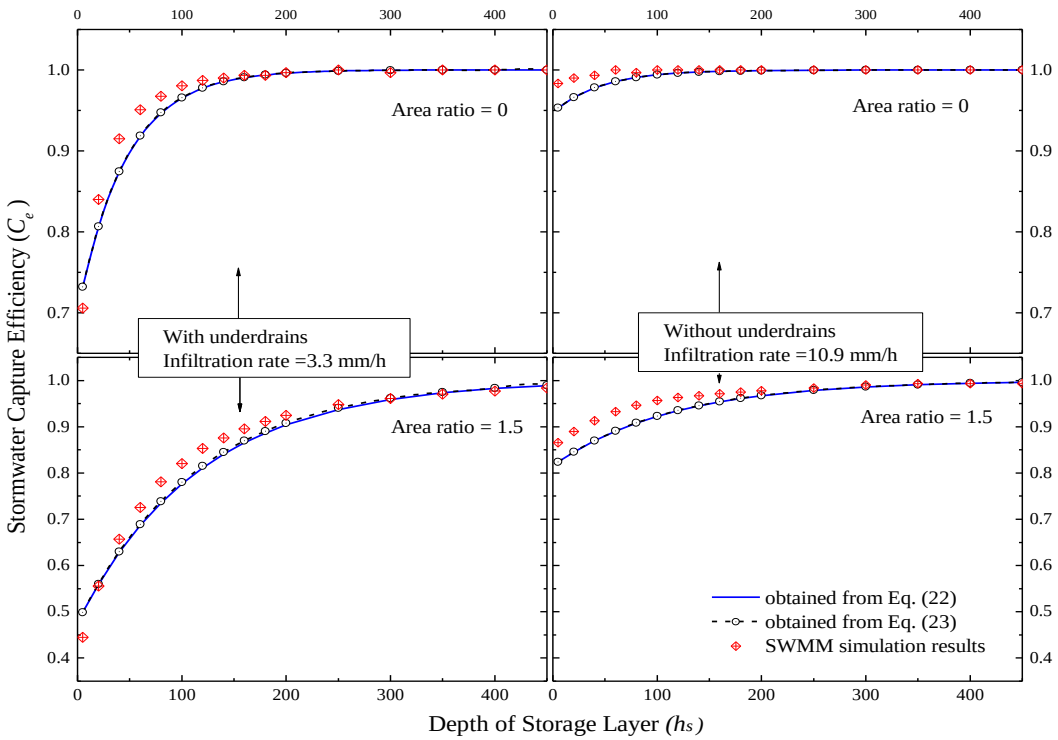

Fig 4.2 Stormwater capture efficiency of PPSs with varying area ratios and storage capacities in Charlotte, NC, USA

permeable, moderately permeable, and slightly permeable native soils. The depression storage depth of the contributing area is set to zero and all the other input parameter values for SWMM models are the same as shown in Table 4.3.

Atlanta, GA, New Durham, NH, and Flagstaff, AZ are selected as the test locations. These locations have different climates: e.g., Atlanta has a humid climate, New Durham has a less humid climate, and Flagstaff has a dry climate. Their rainfall statistics are summarized in Table 4.2. Hourly rainfall records are used as the rainfall inputs for continuous SWMM simulations. From the simulations, the

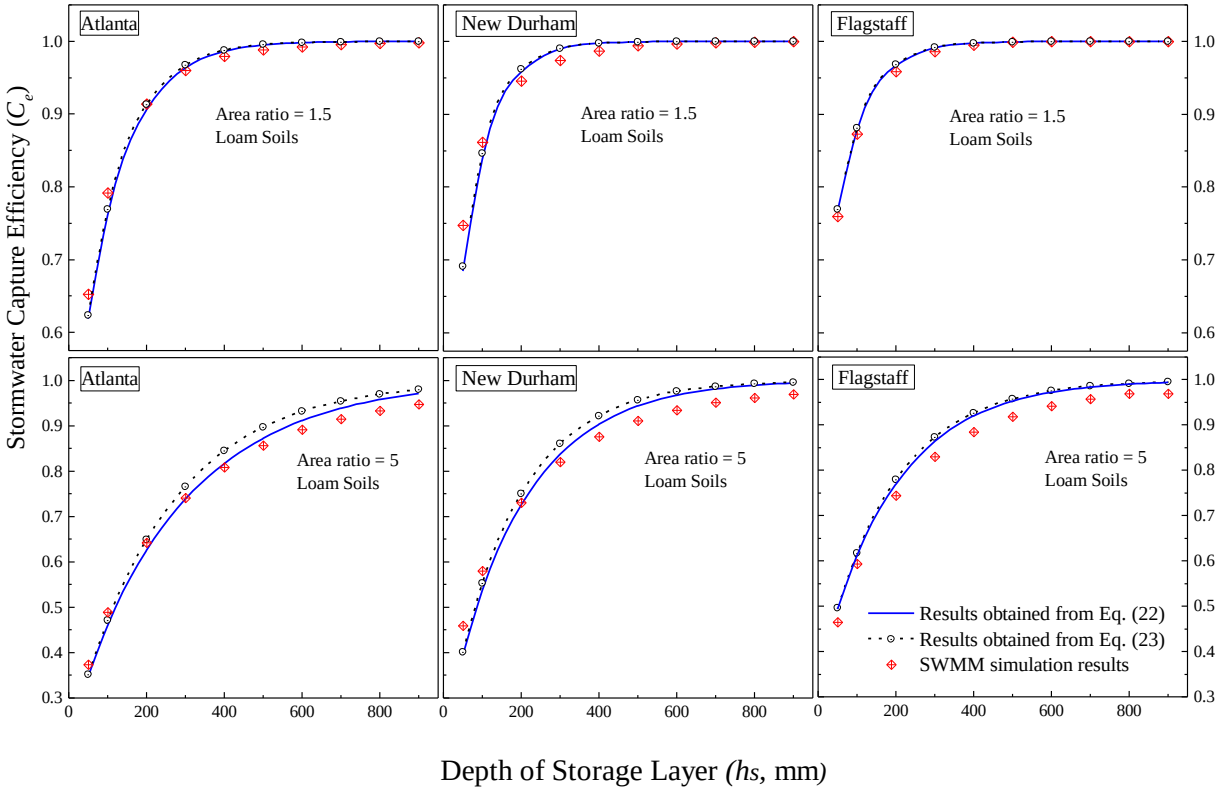

Fig 4.3. Stormwater capture efficiency of PPSs of different sizes located in areas with different climates

total inflow into a PPS (V_i, mm), surface outflow (i.e., overflow) (V_{os}, mm), and drain outflow (V_{od}, mm; when underdrains are installed) from the PPS can all be outputted. The long-term average stormwater capture efficiency as determined by a SWMM simulation can be calculated as $[(V_i - V_{os} - V_{od})/V_i]$. Stormwater capture efficiencies determined using Eq. (4.22) are compared to those estimated from SWMM simulation results. The results for cases with sand soils are all close to one,

that is why only cases with sandy loam and loam soils are presented in Fig. 4.3. Figs. 4.2 and 4.3 show close agreements between the analytical and SWMM results, which illustrates that the derived analytical equations can accurately estimate the stormwater capture efficiencies of PPSs.

4.4.2 Antecedent Moisture Content

Eqs. (4.17) and (4.18) can be used to determine respectively the probability distribution and the long-term average value of the antecedent moisture content of a PPS. From SWMM simulations, the water level stored in the storage layer on an hourly basis in response to the input rainfall series was obtained. As previously described, the input hourly rainfall series was divided into separate events, thus the water level stored inside a PPS at the start of each event can be collected, which generates a series of actual individual antecedent moisture contents. Analyzing this actual antecedent moisture content series, the histograms and the average value of the antecedent moisture contents can be calculated and plotted. Fig. 4.4 shows the histograms and the probability distributions determined from Eq. (4.17) for a design case of PPS located at different locations. Fig. 4.4 shows that the derived distribution fits reasonably well the frequency distribution determined based on SWMM simulation results.

In the planning and design of PPSs, the average antecedent moisture level should be kept as low as possible. To reveal the characteristics of $\langle s \rangle$ varying with climate, design capacity, and soil type, a series of calculations were performed using Eq. (4.18) and the results are presented in Figs. 4.5 and 4.6. Fig. 4.5 shows that, for a specific PPS with a fixed storage space and area ratio, a decrease in the permeability of the native soils always leads to an increase in $\langle s \rangle$. This is because for PPSs with less permeable soils, less water can be infiltrated from the PPS into the surrounding soils during dry periods, and more water remains in the PPS at the ends of dry periods (i.e., the starts of rainfall events).

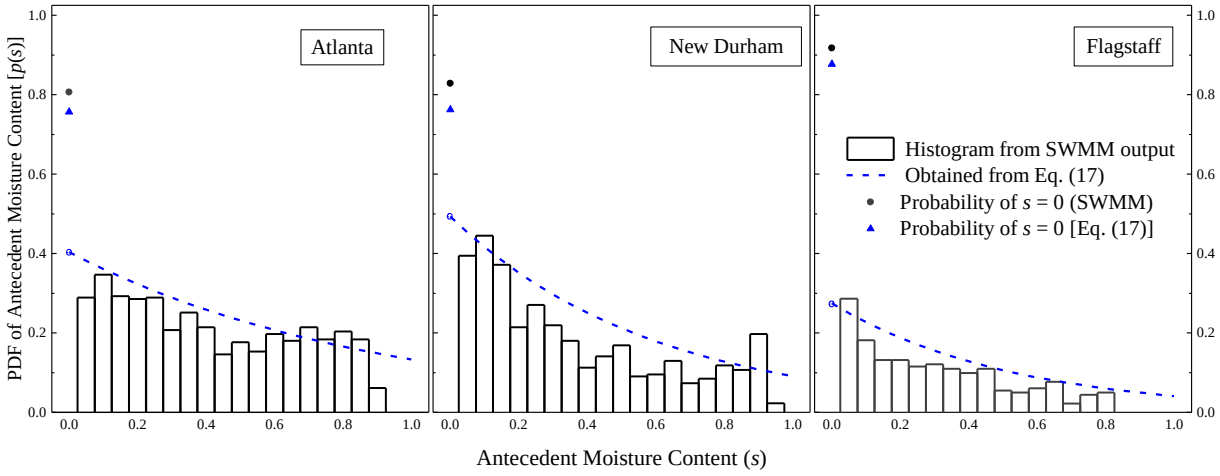

Fig 4.4. Histograms and probability distribution of the antecedent moisture content of a PPS (Area ratio: 5, storage layer depth: 400 mm, soils: loam)

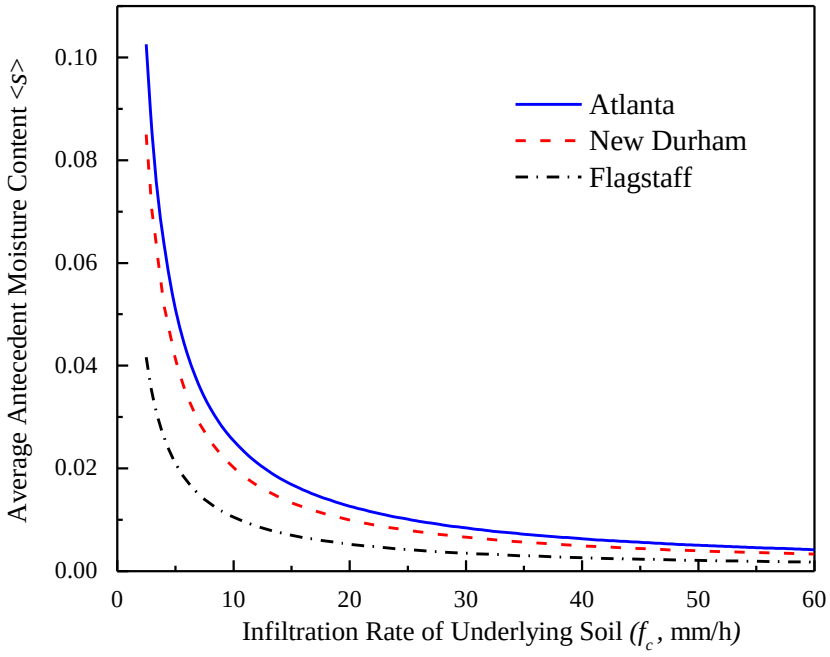

Fig 4.5. Average antecedent moisture content of PPSs in soils with varying permeabilities (Area ratio: 5, storage layer depth: 450 mm)

To find the upper limit of $\langle s \rangle$, PPSs in Atlanta, New Durham, and Flagstaff with least permeable soils were analyzed and the results are plotted in Fig. 4.6. A set of SWMM simulations with an area ratio of 5 was also conducted and results also plotted in Fig. 4.6. The average antecedent moisture contents determined from SWMM simulation results were found to be quite close to those calculated from Eq. (4.18). Fig. 4.6 shows that an increase in area ratio always leads to an increase in $\langle s \rangle$. This is because, as area ratio increases, more runoff is generated from the contributing area and therefore more or at least the same amount of water will be

captured by the PPS at the end of a rainfall event, whereas deep infiltration occurs over the same bottom area of the PPS. It can also be seen from Fig. 4.6 that an increase in storage depth would not always result in an increase of $\langle s \rangle$. Taking New Durham for example, $\langle s \rangle$ increases as the storage layer depth increases from 100 mm and reaches its highest level of 0.088 when the storage depth increases to 374 mm. However, further increase of the storage depth would not result in any further increase of $\langle s \rangle$. This can be explained by the fact that, although the additional storage space can hold some more stormwater, beyond a certain depth, this additional rainfall withheld by the PPS is just enough to keep the additional depth of the storage layer to be at the same $\langle s \rangle$ as the case with less storage space.

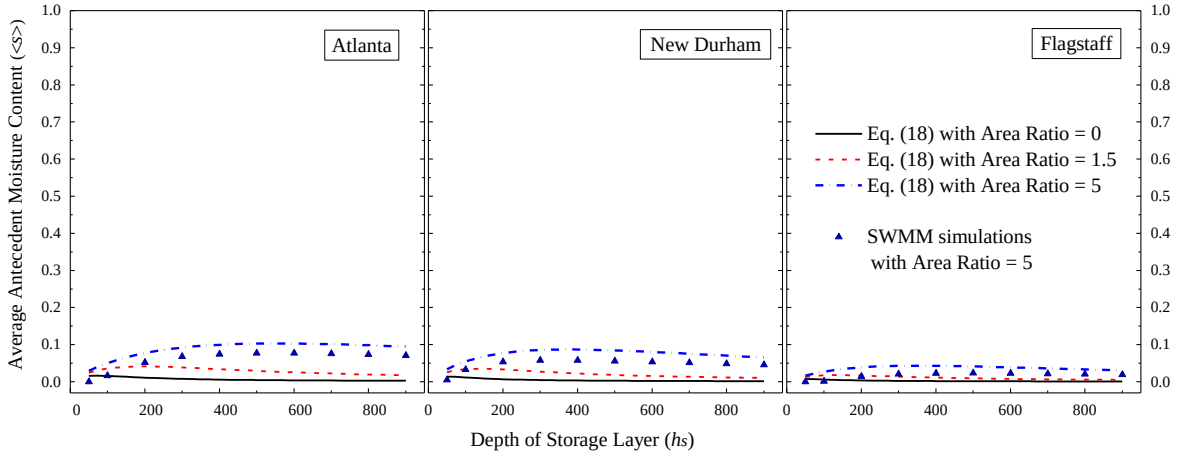

Fig 4.6. Average antecedent moisture content of PPSs of different sizes located in areas with different climates (soils: loam)

4.5 Simplification and Possible Applications of Analytical Results

For the tested locations and almost all possible PPS cases, the largest $\langle s \rangle$ is only about 0.1. Since $\langle s \rangle$ is always very small and close to zero, an assumption that $\langle s \rangle$ for any PPS case is equal to zero may be made. This is equivalent to assuming that a PPS is empty at the start of a random rainfall event and thus S_i in Eq. (4.1) can be treated as zero for any cases. With this simplification, stormwater capture efficiency can be calculated by replacing $\langle s \rangle$ in Eq. (4.22) with zero, and the revised equation becomes

$$C_e = 1 - \frac{(\alpha+1)\lambda}{(1+\alpha e^{-\zeta S_{dc}})(\lambda + \frac{\zeta}{\alpha+1} f_c)} e^{-\frac{\zeta}{\alpha+1}(\alpha S_{dc} + S_m)} \tag{4.23}$$

The estimates provided by Eq. (4.23) are added to Figs. 4.2 and 4.3 and compared with SWMM results. The close agreement illustrates that, at least for the tested locations and PPSs, the proposed assumption is acceptable and Eq. (4.23) can provide a relatively accurate estimation of stormwater capture efficiencies. The main reason that Eq. (4.23) can be used for the vast majority of PPSs is that PPSs are designed to receive runoff from very small urban areas and the initial water level in the storage layer at the beginning of a rainfall event is indeed most likely very low.

4.6 Summary and Conclusions

In this paper, the analytical probabilistic approach was used to analyze the hydrologic response of a permeable pavement system (PPS) to a random rainfall event. The antecedent moisture conditions of the PPS are quantified by solving the stochastic differential equation describing the dynamic water balance of the PPS at an instant of time. The analytical results for the long-term average antecedent moisture condition [Eq. (4.18)] and stormwater capture efficiency [Eq. (4.22) or (4.23)] are all in closed-form and easy to apply for the planning and design of PPSs or for estimating the equivalent curve-numbers and runoff coefficients of areas with permeable pavements. The reliability of the analytical equations was verified by comparing analytical results with continuous simulation results. Comparisons did show that for PPSs of a wide variety of characteristics located in four different states of the U.S., the analytical results are all fairly close to SWMM simulation results.

The analytical results also reveal that the antecedent moisture level of a PPS at the start of a random rainfall event is usually quite close to zero for all the four tested locations. Therefore, it may be assumed that a PPS is always empty (i.e., the full storage is available) when a rainfall event begins and based on this assumption, a more concise and simplified analytical equation was obtained for estimating the PPS' stormwater capture efficiency. The simplified equation was found to also

provide reliable estimates for the four tested locations. The quick and easy quantification of the important performance measures provided by the analytical results may help improve the planning and design of PPSs.

Acknowledgement

This work has been supported by the Natural Sciences and Engineering Research Council of Canada [RGPIN-5112-2016] and the China Scholarship Council [201306220046].

References

Adams, B., Bontje, J., 1984. Microcomputer applications of analytical models for urban stormwater management. Emerging Computer Techniques in Stormwater and Flood Management: 138-162.

Adams, B.J., Fraser, H.G., Howard, C.D., Sami Hanafy, M., 1986. Meteorological data analysis for drainage system design. Journal of Environmental Engineering, 112(5): 827-848.

Adams, B.J., Papa, F., 2000. Urban Stormwater Management Planning with Analytical Probabilistic Models. John Wiley & Sons, Inc., New York, USA.

Ahiablame, L.M., Engel, B.A., Chaubey, I., 2012. Effectiveness of low impact development practices: literature review and suggestions for future research. Water, Air, & Soil Pollution, 223(7): 4253-4273.

Bacchi, B., Balistrocchi, M., Grossi, G., 2008. Proposal of a semi-probabilistic approach for storage facility design. Urban Water Journal, 5(3): 195-208.

Balistrocchi, M., Grossi, G., Bacchi, B., 2009. An analytical probabilistic model of the quality efficiency of a sewer tank. Water Resources Research, 45(12).

Ball, J.E., Rankin, K., 2010. The hydrological performance of a permeable pavement. Urban Water Journal, 7(2): 79-90.

Bean, E.Z., 2005. A Field Study to Evaluate Permeable Pavement Surface Infiltration Rates, Runoff Quantity, Runoff Quality, and Exfiltrate Quality, North Carolina State University, Raleigh, North Carolina, USA.

Bean, E.Z., Hunt, W.F., Bidelspach, D.A., 2007a. Evaluation of four permeable pavement sites in eastern North Carolina for runoff reduction and water quality impacts. Journal of Irrigation and Drainage Engineering, 133(6): 583-592.

Bean, E.Z., Hunt, W.F., Bidelspach, D.A., 2007b. Field survey of permeable pavement surface infiltration rates. Journal of Irrigation and Drainage Engineering, 133(3): 249-255.

Benjamin, J.R., Cornell, C.A., 1970. Probability, Statistics, and Decision for Civil Engineers. McGraw-Hill, New York, USA.

Botter, G., Peratoner, F., Porporato, A., Rodriguez-Iturbe, I., Rinaldo, A., 2007. Signatures of large-scale soil moisture dynamics on streamflow statistics across US climate regimes. Water Resources Research, 43(11).

Collins, K.A., Hunt, W.F., Hathaway, J.M., 2008. Hydrologic comparison of four types of permeable pavement and standard asphalt in eastern North Carolina. Journal of Hydrologic Engineering, 13(12): 1146-1157.

Daubney, E., 2014. The Effect of Conventional Block Pavement (CBP) on Surface

Runoff, Chalmers University of Technology, Göteborg, Sweden.

Dietz, M.E., 2007. Low impact development practices: A review of current research and recommendations for future directions. Water, Air, & Soil Pollution, 186: 351-363.

Eagleson, P.S., 1978. Climate, soil and vegetation. 2. The distribution of annual precipitation derived from observed storm sequences. Water Resour. Res, 14(5): 713-721.

Fassman, E.A., Blackbourn, S., 2010. Urban runoff mitigation by a permeable pavement system over impermeable soils. Journal of Hydrologic Engineering, 15(6).

Gardiner, C., 2004. Handbook of Stochastic Methods for Physics, Chemistry and the Natural Sciences, 3rd Ed. Springer-Verlag, Berlin Heidelberg, Germany.

Guo, Y., 2001. Hydrologic design of urban flood control detention ponds. Journal of Hydrologic Engineering, 6(6): 472-479.

Guo, Y., Adams, B.J., 1998. Hydrologic analysis of urban catchments with event-based probabilistic models: 1. Runoff volume. Water Resources Research, 34(12): 3421-3431.

Guo, Y., Baetz, B.W., 2007. Sizing of rainwater storage units for green building

applications. Journal of Hydrologic Engineering, 12(2): 197-205.

Guo, Y., Zhang, S., Liu, S., 2014. Runoff reduction capabilities and irrigation requirements of green roofs. Water Resources Management, 28(5): 1363-1378.

Hassini, S., Guo, Y., 2016. Exponentiality test procedures for large samples of rainfall event characteristics. Journal of Hydrologic Engineering, ASCE: 04016003.

Holman-Dodds, J.K., Bradley, A.A., Potter, K.W., 2003. Evaluation of hydrologic benefits of infiltration based urban storm water management. Journal of the American Water Resources Association, 39(1): 205-215.

Howard, C.D.D., 1976. Theory of storage and treatment-plant overflows. Journal of the Environmental Engineering, 102(EE4): 709-722.

James, W., von Langsdorf, H., 2003. Computer-aided design of permeable concrete block pavement for reducing stressors and contaminants in an urban environment, Proceedings of the seventh international conference on concrete block paving (PAVE AFRICA), Sun City, South Africa, pp. 12-15.

Laio, F., Porporato, A., Ridolfi, L., Rodriguez-Iturbe, I., 2001. Plants in water-controlled ecosystems: active role in hydrologic processes and response to water stress: II. Probabilistic soil moisture dynamics. Advances in Water Resources,

24(7): 707-723.

Leming, M.L., Malcom, H.R., Tennis, P.D., 2007. Hydrologic Design of Pervious Concrete. Portland Cement Association and National Ready Mixed Concrete Association, Skokie, Ill. and Silver Spring, Md.

Loganathan, G.V., Delleur, J.W., 1984. Effects of urbanization on frequencies of overflows and pollutant loadings from storm sewer overflows: A derived distribution approach. Water Resources Research, 20(7): 857-865.

Martin, W.D., Kaye, N.B., 2014. Hydrologic characterization of undrained porous pavements. Journal of Hydrologic Engineering, 19(6): 1069-1079.

Nemirovsky, E.M., Welker, A.L., Lee, R., 2012. Quantifying evaporation from pervious concrete systems: methodology and hydrologic perspective. Journal of Irrigation and Drainage Engineering, 139(4): 271-277.

PDEP (Pennsylvania Department of Environmental Protection), 2006. Pennsylvania Stormwater Best Management Practices Manual. Bureau of Watershed management, Harrisburg, PA, USA.

Porporato, A., Daly, E., Rodriguez-Iturbe, I., 2004. Soil water balance and ecosystem response to climate change. The American Naturalist, 164(5): 625-632.

Rodríguez-Iturbe, I., Porporato, A., 2005. Ecohydrology of Water-controlled Ecosystems: Soil Moisture and Plant Dynamics. Cambridge University Press, Cambridge, U.K.

Rodriguez-Iturbe, I., Porporato, A., Ridolfi, L., Isham, V., Coxi, D., 1999. Probabilistic modelling of water balance at a point: the role of climate, soil and vegetation, Proceedings of the Royal Society of London A, pp. 3789-3805.

Rossman, L.A., 2015. Storm Water Management Model User's Manual, Version 5.1 (EPA- 600/R-14/413b). National Risk Management Research Laboratory, Office of Research and Development, US Environmental Protection Agency, Cincinnati, OH, U.S.

Schueler, T.R., Claytor, R.A., 2000. Maryland Stormwater Design Manual. Vols. I and II, Center for Watershed Protection and the Maryland Department of the Environment. Maryland Department of the Environment, Baltimore, MD, USA.

Schwartz, S.S., 2010. Effective curve number and hydrologic design of pervious concrete storm-water systems. Journal of Hydrologic Engineering, 15(6): 465-474.

TRCA and CVCA (Toronto and Region Conservation Authority and Credit Valley Conservation Authority), 2010. Low Impact Development Stormwater Management Planning and Design Guide, Ontario, Canada.

WEF and ASCE/EWRI (Water Environment Federation and American Society of Civil Engineers/Environmental & Water Resources Institute), 2012. Design of Urban Stormwater Controls. McGraw-Hill Companies, New York. USA.

Zhang, S., Guo, Y., 2012a. Analytical probabilistic model for evaluating the hydrologic performance of green roofs. Journal of Hydrologic Engineering, 18(1): 19-28.

Zhang, S., Guo, Y., 2012b. Explicit equation for estimating storm-water capture efficiency of rain gardens. Journal of Hydrologic Engineering, 18(12): 1739-1748.

Zhang, S., Guo, Y., 2014a. Analytical equation for estimating the stormwater capture efficiency of permeable pavement systems. Journal of Irrigation and Drainage Engineering, 141(4): 06014004.

Zhang, S., Guo, Y., 2014b. Stormwater capture efficiency of bioretention systems. Water Resources Management, 28(1): 149-168.

Chapter 5

Conclusions and Recommendations for Future Research

5.1 Conclusions

In this thesis, a set of analytical hydrologic models for LID practices including infiltration facilities, rainfall harvesting (RWH) systems, and permeable pavement systems (PPSs) are developed, and analytical equations for the evaluation of their important performance indicators are derived.

Taking non-vegetated infiltration trenches as an example type of infiltration facilities, event-based probabilistic models are developed employing the exponential probability distributions of rainfall characteristics and the mathematical representations of the hydrologic processes involved in the operation of infiltration facilities in Chapter 2. The antecedent moisture content is analytically expressed based on the simplifying assumption that the storage space of the infiltration trench is completely empty at the start of the rainfall event preceding the analyzed rainfall event and the analysis of the response of the infiltration trench to the previous rainfall event-dry period cycle. Two sets of analytical equations are derived for estimating the overflow frequency and the stormwater capture efficiency of infiltration facilities either applying the Horton

infiltration model or considering infiltration rates as constants.

In Chapter 3, stochastic differential water balance equations describing the water content dynamics of RWH systems are established and their equilibrium solutions are derived. Without making the previously adopted simplifying assumptions about the antecedent moisture conditions, analytical expressions of stormwater capture efficiency and water supply reliability of RWHs with two typical water use patterns are obtained; one type is RWH systems supplying water only during dry periods and the other type is RWH systems supplying water during both rainfall events and dry periods.

In Chapter 4, the probability distribution of the moisture contents of a PPS is analytically expressed by applying the analytical stochastic approach to model the moisture content dynamics inside the PPS. Treating its expected value as the long-term average antecedent moisture content, the analytical probabilistic model is developed to analyze the hydrologic response of a PPS to random rainfall events and analytical results for the stormwater capture efficiency of PPSs are obtained.

The derived analytical equations can be implemented in computer spreadsheets, and they enable the easy determination of the long-term average hydrologic performances of the three types of LID practices. The hydrologic performances of a wide range of cases with different contributing areas, site conditions, and system configurations located in different climate regions, for

example, infiltration trenches in Concord (New Hampshire), RWH systems in Atlanta (Georgia), Concord (New Hampshire), Detroit (Michigan), Flagstaff (Arizona), and Billings (Montana), PPSs in Charlotte (North Carolina) and New Durham (New Hampshire), are evaluated using the analytical expressions. The analytical results are compared with those determined from SWMM continuous simulation results. The comparisons show good agreement for the majority of cases. This illustrates that the simplifying assumptions made in the derivation processes are acceptable.

The major simplifying assumptions are described as follows. In describing the local rainfall characteristics to establish an analytical probabilistic model, it is assumed that exponential distributions can adequately represent the frequency of rainfall event volume, duration, and inter-event time; in describing the local rainfall conditions to establish an analytical stochastic model, rainfalls are assumed to occur instantaneously, the input rainfall series is represented as a marked Poisson process, and the rainfall event volumes are assumed to follow exponential distributions. To calculate the runoff generated from a drainage area that flows into an LID device, it is assumed that runoff from the catchment fills the LID practices as soon as it starts to rain and ends when it stops raining, i.e., the time of concentration of the contributing catchment area is negligible. In an analytical stochastic model, the process of inflow into an LID practice is the input rainfall process with events just

satisfying initial losses removed and the remaining events form a new marked Poisson process.

Based on the comparison studies, the application ranges of analytical equations developed in Chapters 3 and 4 are found to be wider when they are compared with those presented in Chapter 2. They can remove the systematic underestimation or overestimation of the performance of the facilities for some extreme cases, e.g., cases where the drainage area, storage space or the outflow rate from the LID device (i.e., infiltration or water use) is extremely large or small. This illustrates that removing the aforementioned simplifying assumptions about the antecedent moisture conditions or analytically quantifying its frequency do improve the accuracy of the derived analytical equations. These newly derived analytical equations can therefore be used as an alternative to continuous simulation in the planning and design of LID practices.

5.2 Recommendations for Future Research

5.2.1 Hydrologic performances of infiltration trenches considering side infiltration

Chapter 2 in this thesis only focused on providing planning and design tools for jurisdictions specifying that only infiltration through the bottom of an infiltration trench should be considered for design (TRCA and CVCA 2010, MDE

2000). Recently, some monitoring studies indicated that due to the deposition of sediments in the bottom of the storage space, clogging might occur and the infiltration rates through the bottom of the trenches could be greatly reduced during the lifespan of infiltration trenches and lateral exfiltration through the sides of infiltration trenches generally dominates (Browne et al. 2008; Chahar et al. 2011; Duchene et al. 1994; Lee et al. 2014; Sànchez-Marrè et al. 2008; Schuh 1988; Siriwardene et al. 2007). This is extremely evident for a long and narrow infiltration trench where the sidewall area is much greater than the bottom area. Consideration of lateral exfiltration in design calculations may make a big difference in the required trench dimensions and is therefore urgently needed.

5.2.2 Applications of the Proposed Approach to Other LID Practices

This thesis extended the analytical probabilistic approach, which requires simplifying assumptions about the antecedent moisture content, to the analysis of the stormwater management performance of infiltration trenches. With this extension, the previously developed analytical probabilistic approach can now be used for the most commonly used LID practices including RWH systems, green roofs, rain gardens, bioretentions, PPSs, and infiltration trenches. The newly proposed approaches, which are referred to as the analytical stochastic approach in Chapter 3 and the improved analytical probabilistic approach in Chapter 4, are currently only applied to RWH systems and PPSs. Further applications or

verifications of the newly developed approaches to the analysis of the hydrologic performances of other LID practices are required.

Currently, rainfalls are assumed to occur instantaneously in the analytical stochastic models for RWH systems and PPSs. This assumption leads to ignorance of the water used for supply or infiltrated during rainfall events. To alleviate the effects of this assumption, in establishing the model for RWH systems with water use during both rainfall events and dry periods, the effective storage capacity of a RWH system for a rainfall event impulse is extended by adding the average volume of water used during a rainfall event to the maximum physical storage volume of the system. In the model for PPSs, this adjustment is directly employed because the average antecedent moisture content is close to zero. Applying the newly developed approach to other LID practices, the limitation of the instantaneous rainfall event assumption needs to be investigated and improvements may still be required.

5.2.3 Analytical Models of LID Practices on a Large Scale

Different combinations of various types of LID practices are usually implemented widely in a community or on a basin scale, and they work together to manage stormwater in the urban catchment. At the preliminary planning and design stage, design configurations of individual LID practices and the large-scale development scenarios incorporating different LID strategies need to be modeled.

The commonly used continuous hydrologic models can provide quantitative assessment of the hydrologic performances of different scenarios; however, they may consume too much time. Therefore, based on the derived analytical equations for individual LID practices in this thesis, studies on analytical models for groups of LID practices implemented on a large scale need to be conducted in the future.

References

Browne, D., Deletic, A., Mudd, G. M., and Fletcher, T. D. (2008). A new saturated/unsaturated model for stormwater infiltration systems. *Hydrological Processes*, 22(25), 4838-4849.

Chahar, B. R., Graillot, D., and Gaur, S. (2011). Storm-water management through infiltration trenches. *Journal of Irrigation and Drainage Engineering*, 138(3), 274-281.

Duchene, M., McBean, E. A., and Thomson, N. R. (1994). Modeling of infiltration from trenches for storm-water control. *Journal of Water Resources Planning and Management*, 120(3), 276-293.

Lee, J. G., Borst, M., Brown, R. A., Rossman, L., and Simon, M. A. (2014). Modeling the hydrologic processes of a permeable pavement system. *Journal of Hydrologic Engineering*, 20(5), 04014070.

Sànchez-Marrè, M., Béjar, J., Comas, J., Rizzoli, A., and Guariso, G. (2008). Assessment of data availability influence on integrated urban drainage modelling uncertainty. *Environmental Modelling & Software*, 24(10), 1171-1181.

Schuh, W. M. (1988). In-situ method for monitoring layered hydraulic impedance

development during artificial recharge with turbid water. *Journal of Hydrology*, 101(1), 173-189.

Siriwardene, N. R., Deletic, A., and Fletcher, T. D. (2007). Clogging of stormwater gravel infiltration systems and filters: Insights from a laboratory study. *Water Research*, 41(7), 1433-1440.

TRCA and CVCA (Toronto and Region Conservation Authority and Credit Valley Conservation Authority) (2010). *Low Impact Development Stormwater Management Planning and Design Guide*, Ontario, Canada.

Appendix A (Thesis Related Paper)

Discussion of "Green Infrastructure Recovery: Analysis of the Influence of Back-to-Back Rainfall Events" by Bridget M. Wadzuk, Conor Lewellyn, Ryan Lee, and Robert G. Traver

Rui Guo and Yiping Guo

This paper argues that the design of green infrastructure (GI) systems cannot be performed properly using the conventional design storm approach. This is because the performance of a GI system is not only sensitive to the volume and duration of a single rainfall event (e.g., the specified design storm event), but also the duration of the dry period after the single rainfall event as well as the size of the subsequent event. The authors estimated the frequencies of occurrence of different back-to-back rainfall events and evaluated the performance of GI systems under those back-to-back event loadings. Simple numerical models were used for evaluating the performance of the GI systems. The discusser agrees well with the authors in that for GI design, it is necessary not to view storms as singular, isolated events, but as a series of events. However, we feel it is necessary to demonstrate an alternative way of characterizing and calculating the frequency of occurrence of different back-to-back storms and briefly introduce a more convenient method for evaluating the performance of GI systems under series of rainfall events.

A.1 Analytical Way of Characterizing the Frequency of Occurrence of Back-to-Back Storms

Based on the statistics of a series of rainfall events instead of on a single storm event, Guo and Baetz (2007) developed a so-called analytical probabilistic approach for sizing rainwater harvesting systems. To apply the analytical probabilistic approach, a statistical analysis of the rainfall event characteristics for a location of interest must be performed first. In this discussion, we applied this statistical analysis for the Philadelphia International Airport meteorological station, which is one of the seven stations analyzed by the authors of the paper. Hourly rainfall data covering 104 years from 1901 to 2005 and every year for the non-winter months from March through November recorded at that station (obtained also from the National Climatic Data Center of the USA) were analyzed. The period of rainfall data used here is not exactly the same as what was used in the paper. Since the record is already quite long and it is only for illustration purposes, we just used what we currently have and did not try to obtain the same period of data as used in the paper.

Using a minimum inter-event time of 6 h (rainfall episodes separated by dry periods shorter than 6 h are grouped into the same rainfall event) and a volume threshold of 0.26 cm (rainfall events with volumes less than 0.26 cm are ignored, which is the same as proposed in this paper), the continuous rainfall data were divided into

separate rainfall events. Each rainfall event is characterized by its rainfall volume (v) and duration (t), as well as the inter-event time (b) before the occurrence of the subsequent event. Since only v and b are needed in this discussion, only the histograms of v and b are shown in Fig. A.1. Visually from Fig. A.1, we can see that the theoretical exponential distributions fit the corresponding histograms reasonably well. It was noted here that if the volume threshold was set to be 0.1 cm instead of 0.26 cm, the goodness of fit of the theoretical distributions would be better, especially for the lower end of the event volumes. But to be consistent with what was used in the paper, we still used 0.26 cm as the volume threshold. The theoretical probability density functions (PDFs) for v, t, and b are given in Table A.1, where $\bar{v}$, $\bar{t}$ and $\bar{b}$ are the mean rainfall event volume (mm), mean rainfall event duration (h), and mean inter-event time (h), respectively, calculated based on a sample rainfall series. The values of $\bar{v}$, $\bar{t}$ and $\bar{b}$ for the Philadelphia station were found to be 16.4 mm, 9.5 h and 127.9 h, respectively.

In previous studies including the one conducted by Guo and Baetz (2007), consecutive rainfall events are assumed to be independent of one another. To test whether the separated events are indeed statistically independent, Poisson partial duration models may be formulated and tested. Since *b* is exponentially distributed and *t* is much smaller than *b* (this can be seen by comparing the $\bar{t}$ value of 9.5 h with the $\bar{b}$ value of 127.9 h for the Philadelphia station), the occurrence of storm

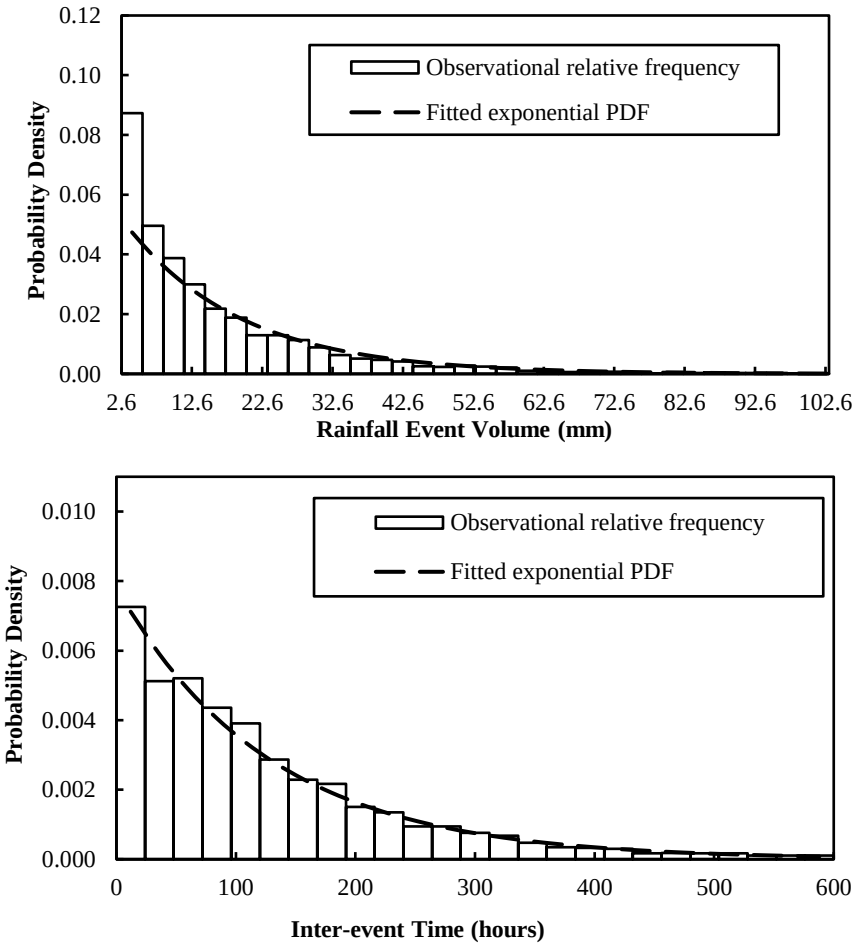

Figure A.1 Histogram and fitted exponential distribution of rainfall event volume and inter-event time - Philadelphia International Airport Meteorological Station

Table A.1 Probability Density Functions of Rainfall Characteristics

Rainfall Characteristic	Exponential PDF	Distribution parameter
Rainfall Event Volume v, mm	$f(v) = \zeta e^{-\zeta v}, \quad v \geq 0$	$\zeta = 1/\overline{v}$
Rainfall Event Duration t, h	$f(t) = \lambda e^{-\lambda t}, \quad t \geq 0$	$\lambda = 1/\overline{t}$
Rainfall Inter-event Time b, h	$f(b) = \psi e^{-\psi b}, \quad b \geq 0$	$\psi = 1/\overline{b}$

events can likely be approximated as a Poisson process. If the occurrence of these events can indeed be accepted as Poissonian, then the likelihood of correlation between them is greatly reduced and consecutive events can be considered as statistical independent. The test for the Poisson assumption is based on the well-known fact that the mean and variance of a Poisson distribution are equal to each other. The number of events occurred each year (n) was obtained for the Philadelphia station and the ratio between the variance and the mean of n was found to be 0.96. This ratio closely approaches unity and indicates that the occurrence of rainfall events follows approximately a Poison process. The separated rainfall events can therefore be considered as statistically independent. Details about this independence test can be found in Guo and Baetz (2007).

The individual v, t, and b values obtained from the above-described separation of an observed rainfall series are treated as realizations of the three corresponding random variables. These random variables are usually assumed to be statistically independent of one another. Since only v and b are used in this discussion, only the independence between v and b are verified. Using the sample v and b values from the Philadelphia station, the sample correlation coefficient between v and b was calculated and it was found to be 0.04, almost 0, indicating that v and b are not correlated and can be treated as statistically independent random variables.

Building upon this event-based statistical characterization of a rainfall series, the frequency of occurrence of different back-to-back storms can be calculated analytically. For example, the probability that an initial rainfall event occurs with a volume greater than or equal to v_1 followed by another rainfall event occurring b_1 h or less afterwards and having a volume no less than v_2 can be derived as follows. First, according to the PDF of rainfall event volume v as shown in Table A.1, the probability of occurrence of the initial rainfall event with a volume equaling to or exceeding a given magnitude v_1 can be calculated as

$$P(v \geq v_1) = \int_{v_1}^{+\infty} \zeta e^{-\zeta v} dv = e^{-\zeta v_1} \tag{A.1}$$

It should be noted here that v is treated as a continuous random variable, the probability of v equaling to a specific value is zero. That is why the initial and subsequent events are defined as events with volumes equaling to or exceeding a given value.

Since the occurrence and magnitude of the next rainfall event is statistically independent of the initial event, the probability of occurrence of the next, i.e., the subsequent event with a volume greater than or equal to v_2 can be calculated as

$$P(v \geq v_2) = \int_{v_2}^{+\infty} \zeta e^{-\zeta v} dv = e^{-\zeta v_2} \tag{A.2}$$

According to the PDF of inter-event time b as shown in Table A.1, the probability that the dry period (i.e., the inter-event time) between the initial and subsequent

events is less than or equal to a given value b_1 can be calculated as

$$P(b \le b_1) = \int_0^{b_1} \psi e^{-\psi b} db = 1 - e^{-\psi b_1} \tag{A.3}$$

The probability of occurrence of a back-to-back event (i.e., an event with volume larger than v_1 followed within b_1 hours by another event with volume larger than v_2) can be evaluated as $P[(v \ge v_1) \bigcap (b \le b_1) \bigcap (v \ge v_2)]$, which is the probability of the intersection of the three different random events. (The occurrence of an inter-event time less than or equal to b_1 is also regarded as the occurrence of an event in the terminology of probability and statistics.) The intersection, i.e., joint occurrence, of the three random events results in one back-to-back rainfall event as defined in the paper, its probability of occurrence is denoted here as $P(v_1, b_1, v_2)$ for simplicity. As explained earlier, the occurrence and magnitude of the first rainfall event is independent of the occurrence and magnitude of the second rainfall event, the volumes of the two events are both independent of the inter-event time, therefore the joint probability $P(v_1, b_1, v_2)$ can be calculated as follows:

$$P(v_1, b_1, v_2) = P(v \ge v_1) P(b \le b_1) P(v \ge v_2) = e^{-\zeta v_1} (1 - e^{-\psi b_1}) e^{-\zeta v_2} \tag{A.4}$$

With the values of v_1 set as 2.5 cm, 3.8 cm, and 8.1 cm, v_2 as $0.5v_1$ or v_1, and b_1 as 24 h, 48 h, 72 h, and 96 h, Eq. (A.4) can be used to estimate the frequencies of occurrence of the same back-to-back events as defined by the authors

of the paper. The average annual number of occurrence of a back-to-back event is simply the corresponding $P(v_1, b_1, v_2)$ multiplied by the average annual number of rainfall events (48 events per year for the Philadelphia station). For a location of interest, as shown in Table A.1, the ζ value needed in Eq. (A.4) is simply the inverse of the mean rainfall event volume and the ψ value is simply the inverse of the mean inter-event time. For the Philadelphia station and for all the back-to-back events defined in this paper, the discusser calculated their probabilities of occurrence using Eq. (A.4), the probability results presented in the form of average annual number of occurrences are summarized in Table A.2 of this discussion. In the paper, similar results for 7 stations in the mid-Atlantic region were obtained and were reported in Table A.2 there. It can be seen that the analytical results obtained by the discusser either falls into or are fairly close to the range of values reported in Table A.2 of the paper. This illustrates that Eq. (A.4) can provide an accurate estimation of the frequency of occurrence of all the back-to-back events defined in the paper. Obviously, Eq. (A.4) is much easier to use than the method used in the paper.

A.2 Analytical Probabilistic Approach for Estimating the Performance of GI Systems

In the paper, numerical models were used for the estimation of the performance of GI systems under different back-to-back storm loading conditions.

Table A.2 Analytically Estimated Average Annual Number of Occurrences of the Back-to-Back Events defined in the Paper - Philadelphia International Airport Meteorological Station

Design rainfall and subsequent event	Average annual occurrence	Design rainfall and subsequent event	Average annual occurrence	Design rainfall and subsequent event	Average annual occurrence
$v \geq 2.5$ cm		$v \geq 3.8$ cm		$v \geq 8.1$ cm	
$P_{2.5}$	10.4	$P_{3.8}$	4.7	$P_{8.1}$	0.3
$P_{24,1.25}$	0.8	$P_{24,1.9}$	0.3	$P_{24,4.05}$	<0.1
$P_{48,1.25}$	1.5	$P_{48,1.9}$	0.5	$P_{48,4.05}$	<0.1
$P_{72,1.25}$	2.1	$P_{72,1.9}$	0.6	$P_{72,4.05}$	<0.1
$P_{96,1.25}$	2.6	$P_{96,1.9}$	0.8	$P_{96,4.05}$	<0.1
$P_{24,2.5}$	0.4	$P_{24,3.8}$	0.1	$P_{24,8.1}$	<0.1
$P_{48,2.5}$	0.7	$P_{48,3.8}$	0.1	$P_{48,8.1}$	<0.1
$P_{72,2.5}$	1.0	$P_{72,3.8}$	0.2	$P_{72,8.1}$	<0.1
$P_{96,2.5}$	1.2	$P_{96,3.8}$	0.2	$P_{96,8.1}$	<0.1

Recent work has made use of the fitted exponential distributions of rainfall event volume, duration, and inter-event time and derived analytical equations for estimating the performance of GI systems under series of rainfall events, including all the naturally occurring back-to-back storms. For example, the statistics about the overflow and runoff capture efficiency of green roofs, rain gardens and infiltration trenches operating under different climate conditions were derived

analytically by Guo and Gao (2016) and Zhang and Guo (2012a, b). Since the same type of PDFs of rainfall characteristics were found to be applicable for the Philadelphia station, the derived analytical equations can be used for that location as well. These equations are more convenient to use than numerical models. As these equations are analytically derived based on the probability distributions of rainfall inputs and the hydrologic operation of GI systems, the overall approach used is referred to as the analytical probabilistic approach.

References

Guo, Y., and Baetz, B. W. (2007). "Sizing of rainwater storage units for green building applications." *Journal of Hydrologic Engineering, ASCE*, 12(2), 197-205.

Guo, Y., and Gao, T. (2016). "Analytical Equations for Estimating the Total Runoff Reduction Efficiency of Infiltration Trenches." *Journal of Sustainable Water in the Built Environment, ASCE*, 06016001.

Zhang, S., and Guo, Y. (2012a). "Analytical probabilistic model for evaluating the hydrologic performance of green roofs." *Journal of Hydrologic Engineering, ASCE*, 18(1), 19-28.

Zhang, S., and Guo, Y. (2012b). "Explicit equation for estimating storm-water capture efficiency of Rain Gardens." *Journal of Hydrologic Engineering, ASCE*, 18(12), 1739-1748.